TÉCNICO LISBOA

Simulation and Energy Management Strategy Development for a Fuel Cell Hybrid Electric Powertrain of a Zero-Emission Boat

Multi Disciplinary Optimization for Hybridization

Sevgi Can Erensoy

Thesis to obtain the Master of Science Degree in

Energy Engineering and Management

Supervisors: Prof. Paulo José da Costa Branco

Eng. Georg Wesolowski

Examination Committee

Chairperson: Prof. José Alberto Caiado Falcão de Campos

Supervisor: Prof. Paulo José da Costa Branco

Member of the Committee: Prof. João Filipe Pereira Fernandes

October 2018

Acknowledgement

Olá Dear Reader,

First of all, I would like to thank you for giving your time and interest for the clean energy technologies and this particular research. I have been in an interesting and colourful journey in the past two years of my studies. There are a few beautiful people and organisations to whom I want to express my appreciation for their support.

Da mir Humphry Marine vertraut hat, war es mir möglich für meine Wunsch Thesis zu arbeiten. Desweiteren, haben mir die Verantwortlichen die Freiheit für meine endlosen Anfragen und zahlreichen Entdeckungen gegeben.
Shotgun, Ich danke ihnen!

InnoEnergy has a great vision and perseverance for the clean energy transition and I am so happy to be a part of this effort. Being an ENTECH and the Open Space Studio experience have been life changing. I got the chance of understanding many different realities of the world and of myself.

There have been many inspiring research studies that I could dig in and I am so grateful to those amazing minds out there who shed light in front of me. Außerdem wäre diese Studie ohne die perfekten Bedingungen der Berliner Stadtbibliothek nicht möglich gewesen.

Eu sou amiga do Duarte Magalhães do qual me orgulho de ser. Um aspirante cientista e um amigo verdadeiro que sofreu com a minha capacidade linguistica de uma forma bondosa nos seus tempos atarefados.

Eu reconheço que o Tiago Mendes é uma alma bondosa e cativante neste planeta.

Benim güzel Hakimecim ve Erolum, bana her zaman ama her zaman verdiğiniz koşulsuz desteğiniz, sonsuz sevginiz ve emeğiniz için minnettarım. Çok özel iki insansınız. En güzel denizi gördük. Sizin çocuğunuz olmak en güzeli. En güzel günler sizinle. Ve size söylemek istediğim en güzel söz, henüz söylememiş olduğum sözdür.

Abstrato

Este estudo explora o potencial da implantação de um moto-propulsor híbrido eléctrico de célula de combustível para um barco de baixa potência e emissões nulas em termos tecnológicos e económicos. Uma arquitectura retrospectiva do moto-propulsor, consistindo de célula de combustível (500 W), bateria de iões lítio (5 kW), conversor amplificador e motor eléctrico foi construída em ambiente MatLAB-Simulink com vários níveis de abstracção de modelagem para adquirir um alto nível de coerência. Estratégias de gestão de energia de baixo nível e supervisão foram desenvolvidas para explorar vantagens da hibridação para extensão de autonomia, alta eficiência e longevidade e para reduzir desvantagens das fontes de energia como indivíduos. Para demonstrar as capacidades da abordagem desenvolvida em termos de desempenho dinâmico e distribuição de energia, o moto-propulsor empreendeu um ciclo de condução de cruzeiro terrestre e estímulos de carga transitória. O moto-propulsor mostrou respostas ágeis e precisas às cargas com máxima oscilação da tensão principal de $\mp$0,15 V e eficiência total do moto-propulsor de 74,6%. O balanço de carga alcançou operação ideal da célula de combustível com gasto de hidrogénio de 0,24 nmi/g no ciclo de cruzeiro escolhido. Finalmente, um algoritmo genético multi-objectivo foi desenvolvido para investigar soluções de hibridação optimizada e economicamente viável para os dois principais desafios perante esta tecnologia. Um conjunto pareto-óptimo hospedando 40 indivíduos mostrou que um estudo de optimização intuitivo baseado em modelagem retrospectiva antes do projecto moto-propulsor pode render uma redução até 10% dos custos e 70% do peso quando satisfeitas as restrições de desempenho.

Palavras-chave: algoritmo genético, barco de emissões nulas, célula de combustível, gestão de energia, moto-propulor eléctrico, simulação

Abstract

This research explores the potential of a fuel cell hybrid electric power-train deployment for a zero emission low-power boat application in terms of technological and economical merits. A backward looking power-train architecture consisting a 500 W fuel cell, a 5 kW Li-ion battery, a boost converter and an electric motor has been built in MatLAB-Simulink environment with various levels of modelling abstraction to acquire a high level of coherence. A low level and a supervisory energy management strategies have been developed to exploit the advantages of the hybridisation for range extension, high efficiency and longevity and to undermine the drawbacks of the power supplies as individuals. To demonstrate the capabilities of the developed approach in terms of the dynamic performance and energy distribution, the power-train undertook an in-land cruise drive cycle and transient load stimuli. The power-train has shown agile and precise responses to the loads with maximum ∓ 0.15 V bus voltage ripple and 74.6% overall power-train efficiency. The load balancing could reach optimal fuel cell operation and the hydrogen expenditure was 0.24 nmi/g on the chosen cruise cycle. Finally, a multi-objective genetic algorithm has been developed to investigate cost effective and lean hybridisation solutions for the two main challenges in front this technology. A pareto-optimal set hosting 40 individuals has shown that an intuitive optimization study based on backward modelling prior to the design of the power-train can yield up to 10% cost reduction and 70% leaner power-train whilst performance constraints are satisfied.

Keywords: electric power-train, fuel cell, genetic algorithm, power management, simulation, zero emission boat

Contents

List of Figures

List of Tables

Nomenclature

List of Abbreviations

BEP Battery Electric Power-train

BLDC Brushless Direct Current Motor

DDP Deterministic Dynamic Programming

ECA Emission Control Areas

ECMS Equivalent Consumption Minimization System

EMS Energy Management Strategy

ESS Energy Storage System

FC Fuel Cell

FCHEP Fuel Cell Hybrid Electric Power-train

FCP Fuel Cell Power-train

GA Genetic Algorithm

GHG Green-House Gas

HV High Voltage

ICE Internal Combustion Engine

IMO International Maritime Organization

LNG Liquefied Natural Gas

MPC Model Predictive Control

MSPC Multi Stage Power Conversion

PCU Power Control Unit

PEMFC Polymer Membrane Fuel Cell

SDP Stochastic Dynamic Programming

SMPS Switch mode power supplies

SSPC Single Stage Power Conversion

UC Ultra Capacitor

Nomenclature

α Charge transfer coefficient

ΔG Activation barrier

η_t Transmission system efficiency

γ Crouch specific constant

A Tafel slope

a_{cruise} Acceleration of the boat

$C(X_D, U(X_D))$ Constrain functions of optimization

D Duty cycle

E_0 Open circuit voltage

E_n Nernst voltage

E_{Bat} Open circuit battery voltage

F Faraday's constant

f Friction factor

f_t Frequency of the PWM

F_{cruise} Net force for the cruise

F_{prop} Propulsion force

F_{res} Hull resistance force

h Planck's constant

i_0 Exchange current

I_C Capacitor current

I_L Inductor current

I_{bat} Battery current

I_{fc} Fuel cell measured current

$J(X_D, U(X_D))$ Objective functions of optimization

k Boltzmann's constant

K_c Fuel cell voltage constant

L Length of the water line

m_{boat} Weight of the boat

N Rotational speed

n Froude variable

N_c Number of cells

P_{bat} Battery power

P_{ch} Battery charge power

P_{dis} Battery discharge power

P_{fc} Fuel cell power

P_i Partial pressure

P_{load} Electrical load on the power-train

P_{mload} Mechanical load on the power-train

P_{supply} Hybrid power-source supplied power

P_{tload} Load on the transmission system

R Gas constant

R_{int} Internal resistance

S Wetted surface area

SOC State of charge

T	Temperature
t_on	Turn-on time of the transistor
T_d	Dynamic response time
U_{f_i}	Utilization of the reactant
V_{Bat}	Battery voltage
v_{cruise}	Velocity of the boat
V_{dis}	Displaced water volume
V_{fc}	Fuel cell measured voltage
V_{lpmi}	Volumetric flow rate
$x\%$	Hydrogen purity
X_D	Vector of optimization variables
$y\%$	Oxygen purity
z	Number of moving electrons

Chapter 1

Introduction

1.1 On Philosophy of Science and Climate Change

Science is the most successful enterprise and a very expensive affair of the modern age of humanity. The ideologies are the ultimate source of funds of the scientific researches and in return, they shape the scientific agenda to determine what to do with the resulting discoveries. The alliance between science and politics may be a powerful tool of mass manipulation (Shaftesbury et al., 2011). Thus, philosophy of science is a dimension to understand the fuzzy linkages between the two. The study of scientific method is the attempt to discern the activities by which the success is achieved. The scientific theory follows a sequence of (i) systematic observation and experimentation, (ii) inductive and deductive reasoning, and (iii) the formation and testing of hypotheses and theories. Scientific goals and methods and the means by which those goals are achieved, should be distinguished to demarcate scientific activity from non-science (Harari, 1989). Meta-methodology is an intentional and coherent approach to analyse data across studies statistically and create a common ground which is always subjected to further scientific methods such as replication, external review and data sharing. A scientific theory is a ground for understanding and should be respected to use the power of the science for the society.

There is still not a consensus on the 'hot' topic of *Climate Change* among parties of the world leading agents. And it is totally legitimate to question the 'scientific theory' and efficient for the progress instead of ignorance.

Is climate change real? There are numerous scientific measurements and observable evidences pointing that the planet is in the regime of warming and experiencing extreme climate conditions. Such that, the surface average temperature has risen about 1.0 degree Celsius within the last 35 years. Ocean temperature increased by 0.17 degrees Celsius. The rate of Antarctica and Greenland ice mass loss has tripled. Global sea level rose 20 cm. The acidity of surface ocean waters has increased by about 30 percent. Extreme weather events are occurring much more frequently. Thus, climate change is a unequivocal scientific fact with changes unprecedented over decades to millennia (NASA, 2016).

Is it anthropogenic? Greenhouse gases have reached the highest concentration in the atmosphere of the last 800,000 years. Based on 11,944 research papers, a 97% consensus in published climate research, consistent with other surveys of climate scientists and peer-reviewed studies concluded that: *"Climate-warming trends over the past century are extremely likely due to human activities."* (Cook et al., 2016)

What are the consequences of climate change? The most influential consequences of last two decades were: extreme heat and cold related deaths, spreading of water-borne illnesses and disease vectors, flooding and erosion of coastal areas with increased sea levels, extreme weather events causing floods, decreasing water quality and availability of water resources, heat waves causing wild fires and droughts and reduced fertility of the earth. One of the most significant potential mechanisms is a shift in ocean circulation pattern known as thermohaline circulation resulting with abrupt change in local climates. Extreme weather conditions affected more than 5.5 million people and caused direct economic losses of more than €90 billion within past 20 years (Ciscar et al., 2011). Sectors that rely strongly on certain temperatures and precipitation levels such as agriculture, forestry, energy and tourism are particularly affected. On the other hand, living beings that are neither contributor of the anthropogenic climate change nor benefiter of economic development, are confronting the severest measures. Most of the human population, citizens of the developing countries, depends on natural environmental conditions and ill-equipped for tackling consequences and many of the plant and animal species are under risk of extinction since they are not capable of coping with these extreme changes in the environmental conditions. A recent study proves the accelerated human induced species loss, stating that vertebrates, amphibians and reptiles are disappearing 114 times faster than their precedents (Ceballos et al., 2015).

Can human innovation solve it? CO_2 concentration in the atmosphere was 408 ppm by July 2018, accompanied with many other greenhouse gases (GHG) in ppb levels. A commonly cited goal is to stabilize GHG concentrations around 450-550 ppm at which the most damaging impacts of climate change can be avoided. *Pacala and Socolow* suggested seven wedges of technology to reduce GHG emissions and hold the GHG concentration at current levels, rather than relying on an enormous change in a single area. Those wedges are energy efficiency, vehicle fuel economy (enables down-sized energy production), wind and solar power boost, usage of hydrogen as energy carrier, energy from biomass, natural gas, and nuclear power (Pacala and Socolow, 2004).

Observable, measurable and building-up evidences of the *Climate Change* theory renders the ignorance towards the issue dangerous for the well-being of world societies. There is a variety of reasons and options to put the planet on a path toward a sustainable climate, most of which are incremental rather than radical. In this thesis, the performance of a zero emission fuel cell hybrid power-train of a recreational boat is investigated. This study can be a powerful tool whose impact falls on multiple wedges for climate action such as:

- electric propulsion system that are increasingly energy efficient

- hybrid system enabling smart algorithms to achieve higher fuel economy

- hydrogen as a fuel empowering utilization of renewable energy whilst solving intermittency and storage issues

- fuel cell powered by hydrogen working with zero emission

An overview of the topic in terms of economic, social and technological aspects will be introduced in the following sections.

1.2 Motivation For Zero Emission Boats and Policies

The transport sector contributes to 19% of the global energy consumption and 23% of the energy related carbon emissions. EU has announced the energy transcript of the union in form of a Sankey Diagram shown in Figure 1.1. 2% of the primary energy resources are spent in maritime transport for maritime bunkers and inland navigation activities which displays quite modest statistics in comparison to the backbone of $ 8.1 billion of global market volume of water-borne trade (Transparency Market Research, 2015). However, as visible in Figure 1.1, the transport industry is the highest polluted among all others. Maritime transport is relatively a benign option in terms of CO_2 emission with approximately 3% contribution to global GHG emission, yet is responsible of the global contaminations in combustion-born SOx by 8%, NOx by 15% and particulate matter by 15%.

More than 80% of global trade is based on maritime transportation since transportation of goods and materials in bulk is possible, hence the potential of the industry to subdue climate change is significant. Internal combustion engines powered by heavy fuel oil or marine diesel oil have an undeniable monarchy in the commercial maritime transport. International Maritime Organization (IMO) is a global standard setting authority under United Nations to create a regulatory framework for the safety, security and environmental performance of the shipping in the international waters. Measures of IMO covers all aspects of international shipping from ship design and construction to operation and disposal. IMO established legally binding international standards with ANNEX VI of MARPOL (International Convention for the Prevention of Pollution from Ships), first adopted in 1997, on local and global scales for regulation of exhaust gases and prohibition of ozone depleting substances and volatile organic compounds. This agreement is the first legally binding international climate change treaty since Kyoto Protocol (IMO, 2018b).

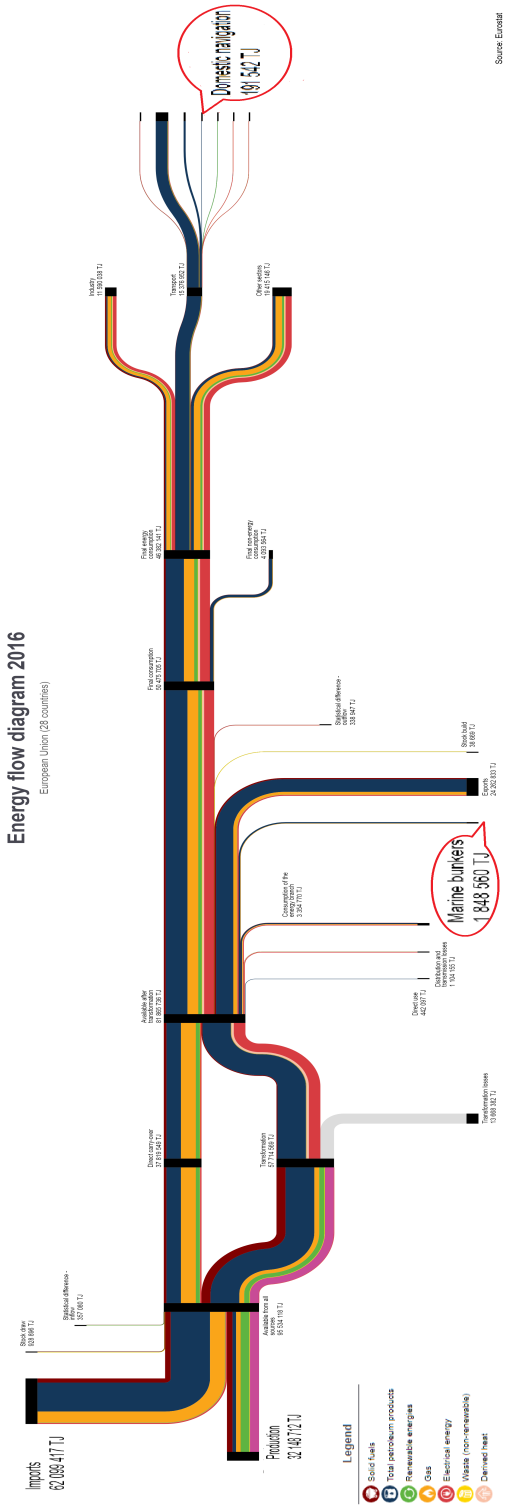

Figure 1.1: Energy flow of European Union, (European Commission, 2018)

The initial idea of European Emission Trading System was to include sea and air transport in the scheme,

yet due to opposition of non-EU countries EU has stepped back with a condition that an international organization puts an effective measure for climate solution. To meet the headline goal of the Paris Agreement, limiting global temperature rise to 1.5 degree Celsius by 2050, shipping emissions needs to be cut by minimum 70%. Despite the inertia exerted by the countries with huge fleets which based their system on bunker fuels, in April 2018, 170 member countries of IMO have reached to a revolutionary consensus to de-carbonize the maritime industry.

"Shipping emissions will be halved by 2050, compared to 2008." (IMO, 2018a).

While 2050 may seem like a long way, most of the new ships built in the 2030s will have to run on zero carbon renewable fuels which requires compelling technological changes in the global industry, which has a fleet of over 50,000 ships trading internationally. Quality of the air on the coastal regions has been severely affected by the concentrated emissions of the maritime traffic, since about 70% of ship emissions occur within 400 km range of land. According to the joint report of Norwegian non-profit organizations, air pollution caused by boat emissions of SOx, NOx and particulate matter accounts approximately for 50,000 premature deaths per year in Europe to which adds on an annual cost to society of more than €58 billion (AirClim and European Environmental Bureau, 2011).

Emission Control Areas (ECAs), shown in Figure 1.2, defining allowable emission levels of SOx, NOx, Ozone Depleting Substances and Volatile Organic Compounds from the ships in certain zones, has been introduced by IMO in 2005. According to latest revision of MARPOL-Annex VI, the global sulphur cap needs to fall below 0.5% which corresponds to one sixth of of the current limits until 2020 to meet the amendments of ECA limits. Furthermore, IMO has empowered mandatory energy efficiency measures in 2011, The Energy Efficiency Design Index, which will support the reduction of CO_2 emissions by limiting the emissions of each individual design for a multitude of boats and ships.

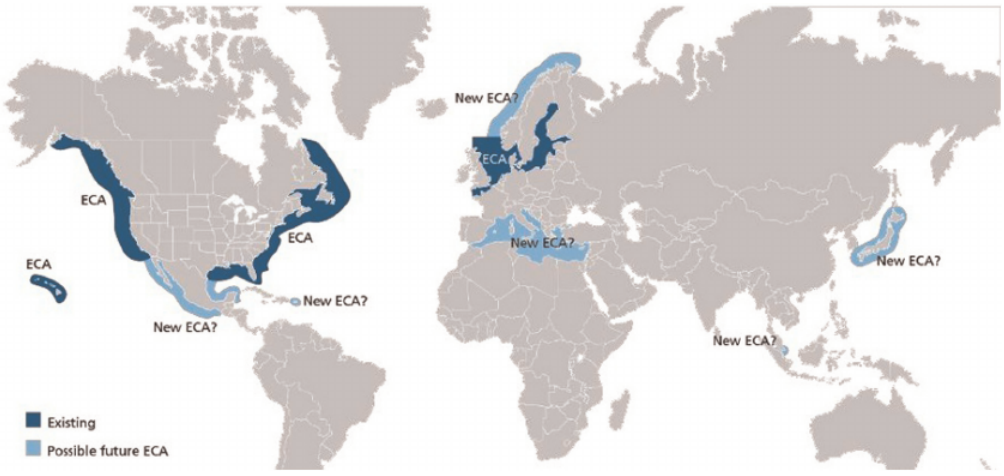

Figure 1.2: Existing and potential ECAs around the world (Elhogary and Seediek, 2015)

Marine transportation load characteristics show low acceleration and high cruising loads in comparison to terrestrial vehicles with high acceleration and low cruising loads. In addition to technical challenge of increased power demands and highly varying loads, the shipping companies are under growing pressure to comply with emission regulations which are stringent in ECA. Mentioned developments are forcing a revolution in the transport market to reduce fuel consumption. The smaller marine segment below 120 ft is yet conservative and usually follows the trends in the vehicle industry. Some straight forward methods to reduce fuel consumption in vessels are reducing the hull resistance, increasing the propeller efficiency, reducing the auxiliary power and eco-driving. The current trend is towards retrofitting for hybridization or integration of scrubbers for exhaust gas treatment, yet these solutions are rather band-aid to preserve the businesses and far from compensating the initial investment for them.

Large international companies and certification bodies have started to invest in development of all-electric and hybrid-electric propulsion technologies. Three alternative solutions under investigation are: battery, liquefied natural gas (LNG) and fuel cell to power drive trains. Battery sourced power-trains are strong candidates with some shortcomings which will be discussed in detail in the literature review.

LNG is a preferred solution for the fleet owners and heavy duty applications with compatibility to internal combustion engine and opportunity for dual set-up that they can shift between LNG and diesel according to ECAs. According to *Cruise Industry News*, LNG powered cruise ships will have 20% market share by 2026. On the other hand, beyond lack of refuelling infrastructure and costly liquefaction process of LNG requiring temperatures below -160 degree Celsius, hydrocarbon and CO emissions caused by LNG are higher than some conventional fuels. Although it seems that LNG can provide a fitting to current legislation with significant reductions in NOx and CO_2, LNG cannot be the solution in the long term.

In what respects the third aforementioned solution, the first fuel cell implementation in a power-train was a 15 kW fuel cell in Allis-Chalmers tractor at 1959. Further on, the space race between USA and the USSR has lead to significant progress in fuel cell application, specifically alkaline fuel cells, for propulsion systems. Current system efficiencies are reaching beyond 60% with average life time of 10 to 15 years. Hence, utilization of fuel cell powered drive-trains to maritime applications started raising attention which will be discussed in detail in the following chapter.

As hydrogen makes its way through the electrolyte, electricity is generated and hydrogen mixes with the oxygen present in air to produce the sole by-product, water. There is a variety of fuels, such as methanol, methane or natural gas, to power different types of fuel cells, yet those are disregarded in the scope of the thesis and only pure hydrogen supplied fuel cells have been considered. Hydrogen is the most abundant element in nature, however the most applied hydrogen production techniques are fossil fuel based. Current annual hydrogen production is about 8000PJ corresponding to 2% world primary energy supply. The energy sources of hydrogen production are; 48% by natural gas, 30% by oil, 18% coal and remaining 4% by water electrolysis. On the other hand, the overall contamination of fuel cell using entirely fossil fuel based hydrogen is 50% less than a conventional internal combustion engine (ICE) (Codina, 2017).

Furthermore, hydrogen is a fundamental energy carrier to leverage renewable energy and energy security. Hydrogen can be produced through electrolysis of water almost anywhere in the world regardless of the electricity resource which gives chance of freeing from reliance of politically unstable oil-rich countries. Moreover, remote communities can produce their own hydrogen which cuts off the financial and environmental costs of fossil fuel transportation and puts a stepping stone on renewable energy transition for cleaner, more reliable, more resilient micro-grids. Fossil fuel powered engines might cause severe local air-pollutions due to geographical reasons and hydrogen is totally environmental friendly fuel even it is combusted. The common argument is that if the electricity source of batteries and hydrogen production is harvested through the generators powered by fossil fuels, technologies are not emission free. Despite the validity of the argument, the large scale generators of the grids usually benefit combined cycle technologies and reaches efficiencies up to 61% (Ibrahim et al., 2017). Moreover, diffusion of the hybrid electric technology establishes the conditions for off grid and renewable energy production compatibility. On the other hand, hydrogen technologies need improvement of the refuelling infrastructure for a noticeable diffusion. 2014/94/EU is the Directive of the deployment alternative fuels infrastructure putting deadline of 2025 to EU member states to provide appropriate number of refuelling stations.

1.3 Zero Emission Boat Market

In general, manufacturers only offer all-electric propulsion on a custom design basis with a very small number of productions showing that there is an interest in the market, but it is very sensitive to concerns around cost and performance. Electric propulsion for marine applications are attractive for many reasons; fuel saving, lower maintenance cost, environmental regulations, improved manoeuvrability, reduced noise and vibration are some to be mentioned. Electric propulsion systems has already attracted attention in several ship applications: supply vessels, drill-ships, shuttle tankers, ice breakers and cruise liners. Currently, there is limited market acceptance for electric propulsion technology for small vessels, but the interest of recreational and commercial boat industry has already arisen. The early adopters of the technology will likely drive further developments in integrated system controlling which can significantly increase market acceptance and viability of the wider applications (NSBA, 2015). The electro-mobility is young and even a newborn technical field in terms of particular relation with computer control systems and has large amount of possibilities to be explored.

For smaller vessels below 40 m, there has not been much improvement until recently when few boat manufacturers introduced their "green model" to meet the demands set by environmentally concious customers. Powerboat of the year 2010 in Germany was 33 ft Greenline Hybrid by Segway and the recent 39 ft model has been nominated as Powerboat of the year 2018. HyMar, *High Efficiency HYbrid Drive Trains for Small and Medium Sized MARine Craft*, is a EU supported collaborative research and development project to improve hybrid systems' fuel economy by minimum 30% for displacement vessels up to 23 m. Low speed operations, below 7 knots, are about 30-50% of the coastal region operating vessels which are highly interested in hybrid applications to reduce their emission and noise in the harbours and restricted areas. (CORDIS, 2013)

Mattsson and Thordsson have conducted a market scanning for marine hybrid activity for vessels smaller than 90 ft and taxonomy of the study is as listed below and each sub-segment includes three different kinds of system configuration; Battery Electric, Parallel Hybrid, Series Hybrid. Approximately 50 producers of electric or hybridized vessels have been identified. To provide an overview of the zero emission market niche which fuel cell powered boats addresses, zero emission boats have been trimmed to present in the listing (Mattsson and Thordsson, 2010).

1. **Sailing Boats:** African Cat and Elco Electric Launch are two producers. Batteries are charged with shore power and renewable energy sources, such as regenerative breaking, wind and solar energy. Regenerative energy produced during sailing by propeller rotation left to spin free. This "free" energy source impacts the customer attention, yet the batteries become the cost driver (NSBA, 2015) .

2. **Commercial Motor Boats:** Segment is addressing passenger transportation, military, near shore fishing and sea rescue applications. Czech company Grove Boats has a solar empowered passenger

vessels in 8-15 m range. The power-train deploys 8 kW DC motors that can propel vessels up to a displacement of 10 tons.

3. **Leisure Motor Boats:** There is a large market competition with more than 15 serious producers. The first common vessel type is used primary for rental and pleasure rides at tourist attractions. The power-train technology is generally adopted from golf-cars, powered with simple DC motors and often 36 V bus systems. The second vessel type category is day cruiser in 5-7 m range serving mainly in South Europe coast or Europe in-land waters. The vessels usually go on 1-8 h cruises and recharge of the batteries takes 4-28 h depending on the available shore power. Electric motor sizes are varying 25-75 kW, the system voltages are from 96 V to 640 V. The market leaders of day cruisers are Frauscher and Austrian Marian Boats. In Sweden, Nimbus N-27 was given a lot of media coverage at boat exhibitions.

Active and credible producers of the zero-emission boats are only producing Battery Electric propulsion systems, thus there is no commercial competitor of fuel cell hybrid zero-emission boats yet. Companies and their associated partners have been listed in Table A.1.

Players who are interested in hybrid zero emission technologies are defined as Boat and Yacht Manufacturers and end-users. Needs of the market segment have been identified after review of literature and oral discussions with users, system manufacturers and authorities. The needs of customer have been dissected as follows:

- **Unspoken Basics:** Those needs to be met for sure. Equivalent driving characteristics as the conventional vessel (easy to control and safe convey at all circumstances) and robust design.
- **Spoken Features:** These are included in the specification of the product and customer wishes those to be fulfilled. Reduced fuel consumption, reduced emission, performance improvement thanks to electric motor boost for acceleration, environmental awareness, safety (twice as many power sources, fail-safe protection of HV system), cost efficiency (pay-off of the capital investment), increased life time, plausible maintenance interval, legislative competence
- **Unspoken Features:** These are not expected by the customer and hold the potential drastically increase customer value. Reduced NVH (Noise, Vibration, Harshness), improved manoeuvrability and increased robustness with faster torque reaction of EM

For some recreational boaters, lifestyle priorities takes a big share in choice of the power-train, the virtual elimination of the noise, vibration and smell might be simply worth the cost increment of the electric propulsion. Early adopters of the electric leisure boat market can create a €3 billion size market within the next ten years (Grapentin, 2017). There is not a commercial attempt for a long-range recreational boat production, since the other few zero-emission producers are focused exclusively on battery technologies and their application area is relatively restrained. Neither conventional nor electric manufacturers seem to move into the higher performance electric market in the near future.

There are few successful projects in which fuel cells empowered electric drive trains of marine applications,

yet none of them has achieved mass commercialization and remained rather as proof of concept. Pleasure crafts and passenger vessels are two common application segments for low temperature fuel cells (60-80 degree Celsius) providing fast start up in the range of milliseconds with high power density, low power requirement and hence smaller fuel storage. The chronological progress of the market is as follows:

1. **2003**: Concept project of L'Institut d'Énergie et Systèmes Électriques (IESE) has proved the feasibility of PEMFC driven boats with a catamaran equipped with 3 kW fuel cell.

2. **2008**: The first fuel cell powered passenger vessels, Zemship and Nemo-H_2 have started to serve in German and Dutch in-land waters. Zemship was operating with 100 kW PEM fuel cell with 50 kg compressed H_2 on board which was able to deliver maximum power for 6 h. The project has been withdrawn due to economic infeasibility of the refuelling.

3. **2009**:For Germany originated project e4ships, Thyssenkrupp and Meyer Werft have been developing fuel cell systems for ocean-going vessels since 2009.

4. **2009**:Another actor was Frauscher who announced their capability for serial production of fuel cell powered boats in 2009. However, the mass production has never taken place due to high cost and infrastructure problems with refuelling.

5. **2016**: Another marine segment of fuel cell application is sub-marines. In the fall 2016, German navy has included six fuel-cell and diesel generator hybrid submarines type U212-A in the the fleet. The total worth of the vessels is €2.6 billion and manufactured by ThyssenKrupp Marine Systems.

6. **2017**: In June, multi-million dollar worth signature boat of CEA-Liten that powers itself without any fuel has set off to begin a 6-year trip around the world. The Energy Observer will use a combination of a hydrogen fuel cell system, solar panels and wind turbines to sail throughout its voyage spanning 50 countries and 101 stopovers.

7. **2018**: 60 kW fuel cell powered Shimpo has successfully launched in Japan by last June. The project is product of collaboration of Yanmar and Toyota with modules of Ballard Power Systems of Canada.

8. **2018**: Humphry Marine has announced the launch of their first prototype with 0.5 kW fuel cell for recreational maritime to be sailed in German in-land waters in September 2018.

9. **2019**: Golden Gate Zero Emission Marine will launch US's first fuel cell powered boat, Water-Go-Around, in mid-2019. Water-Go-Around will serve up to 84 passenger and be capable of 2 full days of operation with high capacity composite hydrogen tanks.

Introduction of fuel cell powered boats into European market will not encounter with legislative inertia. The regulatory framework of EU, 2013/53/EU, to develop pleasure boat from 2.5-24 m is not proclaiming any specific requirement for fuel cell applications and only requirement is declaration of conformity which is

fulfilment of standards defined by European Standardization Organization common for all recreational crafts (European Commission, 2017).

1.4 Computer Aided Engineering

Model based design is replacing the traditional design in the industries working with complex embedded systems. Sequential path of the traditional design is as follows: requirement setting, design, implementation and testing which is prone to fail when specification needs to be communicated between different engineers, application requires rewriting of design algorithm or problem is not detected until test phase. Model based design uses models early in the process to create executable specifications allowing engineers to immediately verify specification and requirement competency. Computer Aided Engineering is enabling more accurate and efficient designs, hence gaining more interest and appreciation among scholars and industry professionals. With the computational capacity increase of the processors, engineers use computer simulations to design a power-train, analyse the performance and optimize the system all prior to manufacture. The art of system design is to acquire efficient performance of the components whilst incorporating other fields to optimize the whole system which requires inter disciplinary approach. There are multidisciplinary optimization software to assist power-train design such as Hyperworks with topology focus and MSC combining dynamic and finite element analysis.

Power-train simulation software use different methodologies depending on model detail level. SIMPLORER and Saber are network oriented, whereas MATLAB-Simulink is block oriented, which is suitable for reflecting dynamic behaviour, is of particular interest. MATLAB is ideal for complex numerical computations and a multi-paradigm programming language providing an interface between other programming languages such as C and Java. Simulink is a graphical programming tool providing block diagrams for various mathematical operations associating with Matlab to drive the results. It has been widely used by researchers and developers for various applications such as to simulate and test dynamics systems, analyse multi-objective complex non-linear systems or test hard-ware for real time. Simulink eases communication between different teams of a project, such that engineers may share models demonstrating performance of the specific system of interest, generate codes in other languages with Real Time and Embedded Coder to facilitate Hardware In Loop (HIL) testing.

Setting up experimental test platforms for different configurations, component dimension and parameters to achieve optimum design is time and cost inefficient and a weak tool in comparison with variation creation and computational capacity of simulations. The dynamic behaviour of the designed system under optimization and control strategy can be predicted prior to decision of the power-train architecture to be built for the experiment. As design process evolves engineers can perform Model-In-Loop, Software-In-Loop and Hardware-In-Loop to improve model competency. Hardware In Loop methodology provides embedding a hardware into constructed simulation and evaluation of the performance of the component within the system. Such approach is often preferred in industry application for component identification, modification of already established well performing systems or by-pass of modelling for complex sub-systems.

ADVISOR (Advanced Vehicle Simulator) is a highly preferred visual programming based simulation in which it is easy to modify parameters, architectures and graphically examine the outputs for vehicle applications.

1.5 Objectives of the Study

The performance, lifetime and cost of fuel cells and batteries are demonstrating a complex and interactive behaviour, thus the non-linear nature of their operation makes the large scale system analysis dependent on simplifications which cannot always be applicable. This thesis aims to capture the interface between the fundamental science of system operations and practical applications. A mathematical framework has been developed to understand the physics of operations, communicate them with system level control and evaluate the performance of the fuel cell hybrid electric power-train configuration (FCHEP). This research aims to contribute to literature in the field of system level analysis of power-trains defined with physics driven models.

A conventional power-train with internal combustion engine (ICE) manages the load with direct command from the driver through the acceleration pedal determining the operational state of the engine to produce required power. In a hybrid vehicle, addition of an another energy source provides an extra degree of freedom to manage the demand of the driver. The overall operating efficiency of the system will be a function of how the load has been distributed over time. Energy Management Strategy (EMS) is a supervisory control mechanism to decide that load balancing. Power management logic dissects the operation into sub-segments to manage components of the system to maximize the system efficiency. Successful EMS can reach up to 20% fuel saving in hybrid applications (Opila et al., 2012). On the other hand, utilizability of such supervisory mechanism enables to accommodate complex concerns and play with trade-off. Although EMS has not any direct effect on component costs when it coupled with the optimization, downsizing and longevity of the components can be controlled. For example, avoidance of transient load on the fuel cell can be possible with battery coupling, which might both down-size the fuel cell stack and reduce the maintenance cost with increase in the investment cost.

Hybrid energy supply and storage systems under dynamic loads have been explored extensively by automotive, power system and control engineering communities. There is a noticeable knowledge gap in the hybrid and electric power-train applications for maritime vehicles which performs under high fluctuations in voltage and frequency that occur in transient conditions of frequent and large amount of load changes. Although this problem has been widely investigated for mechanically driven systems, the hybrid systems can provide a more complex and flexible solution with multiple mode of operation which are to be explored.

The goal of this research is to analyse performance of a FCHEP of a low-power pleasure boat propulsion, develop a power management logic and embed multidisciplinary optimization for component sizing to realize an optimal solution across engineering and business fields. Since the designed power-train targets commercial use, the objective function seeks for cost concious solution in the frame of acceptable performance indicators. On the other hand, the objective of the optimization can significantly change the outcome of the design, and can be prioritized accordingly, e.g. for a boat to take part in a prestige race, the performance objective takes the top priority.

1.5.1 Research Questions and Outline of the Thesis

This thesis has been structured with the aim of building an understanding of the need and the feasibility of the zero-emission fuel cell powered hybrid electric boats in terms of technological and economical conditions. In the following chapters, the content will be answering the listed questions as below.

- ***"What are the state of art FCHEP architectures, applications, system simulations and energy management strategies in the literature?"***
  This question has been comprehensively answered in the literature review, in section 2.1, section 2.2 and section 2.3.

- ***What are the developed optimization techniques for FCHEP?***
  Multi-disciplinary design optimization for hybrid electric power-trains has been introduced in section 2.4.

- ***What is the load profile of a common drive cycle for a low power leisure boat?***
  Derivation of a load profile of a low-power boat from a GPS record has been modelled and explained in section 3.1 and section 3.2.

- ***Which methodology should be followed for modelling of commercial components?***
  chapter 3 analyses the approaches for the power-train component modellings and explains the taken decisions for the modelling of designed FCHEP elaborately.

- ***How to acquire coherent performance of a post-united power-train modelling and simulate dynamic behaviour of a fuel cell hybrid electric power-train?***
  Interface building strategies have been explained in chapter 3 as complementary to component modelling studies.

- ***What is the design framework for an efficient energy management strategy?***
  EMS requirements have been introduced in section 2.3 and a power-assist control based energy management strategy development has been presented in chapter 4.

- ***What are the performance limits of the designed FCHEP under supervision of developed energy management strategy over high transient load conditions ?***
  The most compelling requirement for a power-train deployed for a maritime application is high transients. The designed system performance is simulated for two extreme cases in section 5.1.

- ***What is the performance of the designed FCHEP over a common drive cycle?***
  Designed FCHEP has been subjected to the developed load profile of in-land cruise drive cycle. Detailed analysis based on each component and system level have been presented in section 5.2.

- ***What are the cost and down-size trade off for FCHEP hybridization and the benefit of conducting an optimization study prior to the design of power-train?***

Multi-disciplinary genetic algorithm based on multi-objectives of cost minimization and lean power-supply has been presented in chapter 6 and comparative analysis for design alternatives were provided.

1.5.2 Limitations

Within the realm of this thesis, not every control system possibility could have been explored. Rather, few methodologies and tools have been utilized to construct a robust basis for the power-train simulation to be built on with further studies. Similarly, development of the detailed thermal models reflecting degradation of electrochemical components and efficiency reduction of electro-mechanic components is an elaborate task and beyond the scope of a single master project. Instead, the efficiency reductions were approximated and EMS has been designed with the awareness of degradation mechanisms and operational states set to maximize the lifetime in a wide range quantitative manner.

For marine applications, predictability of the dynamic load torque is highly unlikely due to natural conditions, which creates a significant knowledge gap for accurate design of EMS. Propulsion load fluctuations at the propeller were not considered which might interfere with the performance of all electric network.

Computational expense of certain simulations such as high resolution analysis of the power-train for a long simulation and con-current optimization of the power-train embodying the EMS algorithm cannot be possible with limited CPU.

Chapter 2

Literature Review

In this chapter, analysed literature has been summarized to provide a broad understanding of the state of art and the recent developments in the field. Firstly, feasibility of fuel cell hybrid electric power-trains has been analysed and the developed power-train architectures have been introduced with a coherent classification which is used to navigate in the rest of the literature review. Main aim and challenges of energy management strategies of the classified power-train topologies have been explained as an introduction to the similar studies in the field. Finally, hybrid power-train optimization methodologies and the respective studies were provided.

2.1 Feasibility of Fuel Cell Hybrid Electric Power-trains

Hybridization of power sources creates a wide opportunity window to design engineers for creating a superior offspring which benefits good 'genes' of the sources, such that coupling a source with high specific energy (Wh/kg) with high specific power (W/kg) , getting advantage of the source which has fast response time, utilizing the source which has higher power density (W/L) for average load and even storing the excess energy in one another. It is significantly inefficient to balance the power load with turning the fuel cell on and off due to inherent properties (Ceballos et al., 2015). In a hybrid power supply, a battery with high specific power and fast response can back-up the power-train for fuel cell with a high specific energy to operate in an efficient region and not follow the abrupt changes in the load. Moreover, integration of new family of storage devices, advanced electronic drives and semiconductors, sophisticated fabrication materials have played an important role to bring the whole hybrid system cost down and compensate for expensive components (Hou, 2017).

Fuel cell utilization of hydrogen is much more efficient than combustion of it. ICE has complete dependence on a single fuel source and can only reach 40% efficiency at best which corresponds to very limited range of RPM and within usual performance range with drive-line inefficiencies, it reduces to 25%. Whereas fuel cell powered electric drive line is reaching to 60%, twice as hydrogen powered ICE drive-line (Hosseinzadeh, 2012). Increase and instability in the oil prices and observable effects of climate change have driven governments to undergo

legislative adjustments. Power-train designs are improving in terms of efficiency and reduced emissions thanks to consumer awareness and taxation pressure on the industry. On the other hand, the main performance drain of internal combustion engine run power-trains is the thermal efficiency of the engines which is ultimately bounded by physical laws to Carnot Efficiency which defined by the temperature rise of combustion gases. Downsizing of ICE is the most preferred emission reduction solution which requires advanced modifications, such as supercharging which increases the mechanical complexity and failure tendency of the power-train (Leikarnes, 2017). As the ICE technology reaches saturation, the incremental efficiency of ICE is getting lower, more complicated and expensive. Thus, research and development efforts have started to discover alternative power-train solutions.

Battery run systems depend on the recharging electricity rate to be supplied and converted into chemical energy which takes considerable amount of time even with the most advanced technology in the market. Unless there is a technological breakthrough in battery technologies, battery powered power-trains will be hindered by range and refuel timing in the foreseeable future. There is even a newly established term in English; range anxiety to describe discomfort of the driver to rely on BEV to reach final destination. For example, a frontrunner model of Frauscher is 740 Mirage which is equipped with a 30.5 kWh battery storage provides a 55 km range at 5 knots and can only run 35 minutes at full speed of 15 knots (Frauscher, 2018). On the other hand, an immense research effort has been devoted in battery technology and investment in wide network of charging infrastructure. Northvolt of Europe and Gigafactory of Tesla are two mass production enterprises with billions Euro worth of investments to reduce the market price of high quality Li-ion battery prices which is €1000/kWh at the moment. Moreover, new field of nano-batteries is promising tremendous performance advantages in terms of charging and discharging, if scientists can achieve nano-coating of electrodes. The state of the art in battery technology and fast-charging infrastructures matches are capable of 85% charging 30.5 kWh battery in 20 minutes. While the marine market is not a primary driver of the activity in battery development, it would surely be one of the secondary markets to benefit, yet shore charging infrastructures are not likely to benefit from the investments. In a usual scenario, electric drive owner has access only to single phase charger with maximum 3680 W (260V*16A) and it will take more than 8 h to recharge 30.5 kWh battery. Battery mass already constitutes significant portion of the over-all weight and increasing the size of the pack to extend the range will only cause increase in energy need to propel the boat. As a result, increasing the size of battery will cancel out the results as return of range. Using the batteries as only source of energy does not answer the need for longer cruises. In addition, batteries are storage devices rather than a generating device like a fuel cell which will continuously deliver electric power as long as fuel is supplied.

Integration of fuel cell as energy source enables the power-train to meet the comfort of conventional refuel timing and range, whilst preserving all the benefits of an electric power-train. Hydrogen is a power dense fuel allowing more energy storage without significant increase in the power-train mass and volume. Fuel cell systems can be tailored in terms of energy and power requirements individually thanks to completely

decoupled energy storage and conversion systems. Moreover, independent storage system makes fuel cell totally competitive with conventional fuels with reduced refuel timing. Development of smaller fuel cell systems and high energy storage devices introduce the hybrid power trains for small vehicular applications. On the other hand, high power fuel cell systems, up to 250 kW, are becoming attractive as back-up power generators with high efficiency. Higher partial load performance of fuel cell in comparison to ICE making it desirable for transport applications mostly work at part-load conditions (Hoogers, 2003). Fuel cells have no moving parts which reduces maintenance need and noise which improves the cruise comfort. Polymer Membrane Fuel Cells (PEMFC) are highly preferred for transport applications due to faster response time, low temperature operation and high efficiency.

Besides all the inherent advantageous of fuel cell systems and hydrogen as a strong alternative for transportation industry, the technology suffers from few economical and scientific challenges:

- **Cost**

  The foremost drawback is cost of the system because of the immaturity of the technology and manufacturing processes, the low production volumes and the singular production of hydrogen tanks and the cost of the catalyst (Shulock and Pike, 2011). There are many research projects to reduce the amount of platinum and the system cost is expected to halved by 2020. Fuel cells cost 3,000$/kW to 5,000$/kW, compared to 35$/kW for an internal combustion engine, about 100-fold price differential (Fuchs and Reuter, 2017). The theoretical price of a system under mass production in 2017 was an average of 46.9$/kW which is still almost the double amount of US Department of Energy feasibility limits, Figure 2.1.

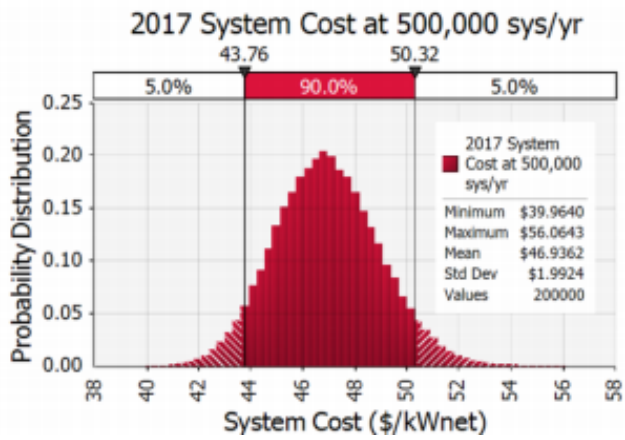

Figure 2.1: Mass production estimates of 2017, (Wilson and Kleen, 2017)

In the past 5 years, a cost reduction more than 20% in fuel cell system fabrication was achieved, yet it is still not enough for commercialization (James, 2017). On the other hand, industry investments and cooperation of strong companies are expected to give the boost that the technology needs. In January

2017, the Hydrogen Council announced a $ 10.7 billion investment to be allocated in hydrogen related product development (Bloomberg, 2017). In July 2017, Honda and General Motors has initiated the first manufacturing joint venture to mass produce an advanced hydrogen fuel cell system that will be used in future products from each company from 2020 on. Fuel cell systems can be manufactured at the same cost of ICE systems, once they are in mass production (Honda, 2017).

- **Degradation**

  Degradation is measured as reduction in the performance with respect to certain time of use. Although there are no set standard for marine applications, vehicular applications needs to meet 5000 hours based on a 250,000 km lifetime with 60% efficiency, whereas the the lifetime of a well performing PEMFC is about 2500h (Hosseinzadeh, 2012), (Dresselhaus and Crabtree, 2004). The issues of cost and durability are making fuel cells unfavourable in terms of purchase and maintenance. Moreover, the solution of the issues are interdependent and counter forcing. The capital cost of the fuel cell can be reduced with lowered amount of Platinum in the catalyst or smaller stacks running at higher relative powers which will affect the long term performance and reduce the lifetime and outweigh the gain from the manufacture costs.

- **Storage**

  Despite higher stack efficiency, better performance and lower cost in comparison to reformate fuel, the storage of hydrogen requires eloquent processing. Despite hydrogen being a three times more power dense carrier with 33kWh/kg in comparison to fossil fuels, the volumetric density needs to be increased with pressurizing, liquefaction or capturing into solid state storage. In practical terms, when conventional 3600 psi natural gas storage technology for vehicular applications has been utilized for hydrogen, there will be a 20 fold energy density penalty in comparison to gasoline. High pressure storage needs to be accompanied with high insulation and safety mechanisms, whereas a solid state storage might cause lag in the power-train due to slow rate of reaction limiting the hydrogen release.

- **Infrastructure**

  Lack of infrastructure for re-fuelling hinders mass production and use of the hydrogen and locks the relation to a chicken and egg scenario. On the other hand, it should be noted that the development of entirely new propulsion system requiring a new fuel choice needs to balance off the societal costs in terms of financial and environmental sustainability. Fuels needs to be evaluated from well to tail(wheel) basis, such that the fuel efficiency, system total cost, environmental impact of extraction, refining, distribution and on-vehicle usage should be considered.

2.2 FCHEP Architectures and Applications

Battery Electric Power-trains (BEP) use only Energy Storage Systems (ESS) and Fuel Cell Power-trains (FCP) is powered by a fuel cell only, whereas FCHEP is the result of hybridization of ESS and fuel cell. As explained in section 2.1, a fuel cell is not capable of responding abrupt changes in the power load. Thus, slow speed and relatively monotonous power delivering applications such as forklifts, trams and submarines utilize FCP. In order to a fuel cell to deliver high speed under varying load conditions, modifications need to be made to the basic power-train which leads to new configuration of FCHEP. Basic power-train architectures of FCP and FCHEP are shown in Figure 2.2. FCHEP adopts another ESS, which can be a battery or ultra-capacitor, to be charged or discharged based on power demand and supply. Deployment of power converters are varying according to the design and power control schemes, thus flexibility has been indicated with dashed lines in the drawing.

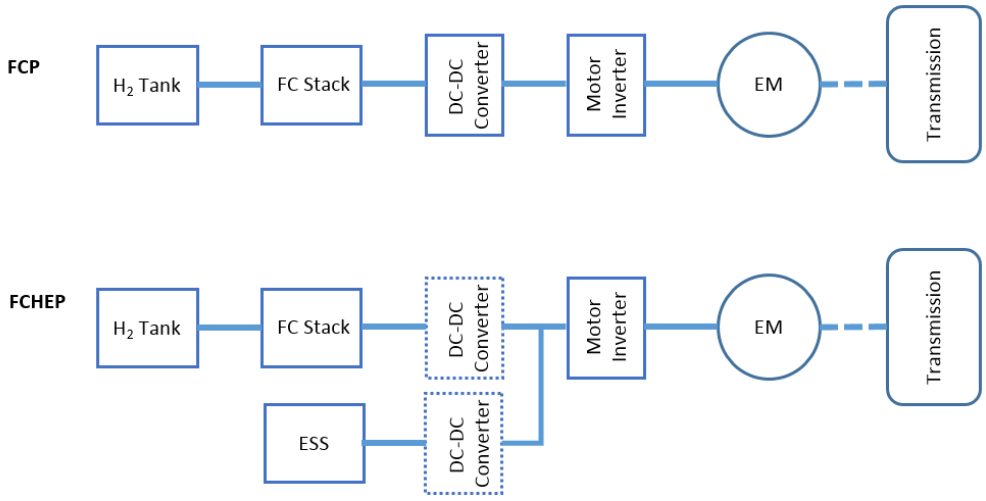

Figure 2.2: Basic FCP and FCHEP configurations

Typical considerations of the FCHEP configurations to be taken care of for a smooth performance are sizing of the power converters, weight and resilience of the power-train, converter efficiency, electromagnetic interference, bus voltage and current ripples(Das et al., 2017).

Hybrid electric power-train configurations typically are categorized in two system classes; series and parallel. Series hybrid power-trains are similar to an electric power-train with an on-board generator. The power-train runs on the main ESS until it reaches a predetermined discharge level and at that point the auxiliary power unit is activated by the control system to recharge the main ESS. (Xcellsis and Ballard, 2001) Parallel system architecture allows both of the power supplies to be directly connected to the bus and feed the load at the same time. However, such a classification is not meaningful for FCHEP, since the main point of the hybridization is to benefit ESSs for managing with abrupt load changes in the bus. Hence, FCHEP are always in parallel configuration according to classical categorization and it is more intuitive to define the

FCHEP architectures depending on the power conversion stages: multiple stage power conversion and single stage power conversion.

2.2.1 Multiple Stage Power Conversion FCHEPs

Power conversion in a hybrid electric power-train usually takes place in two stages; initially low DC voltage from power sources is converted into high voltage DC and then inverted into AC to run the electric motor. The topologies of such multi stage power conversion (MPSC) have been discussed by *Tazelaar and Veenhuizen* and classified under six types, as displayed in Figure 2.3 and are explained below (Tazelaar and Veenhuizen, 2013).

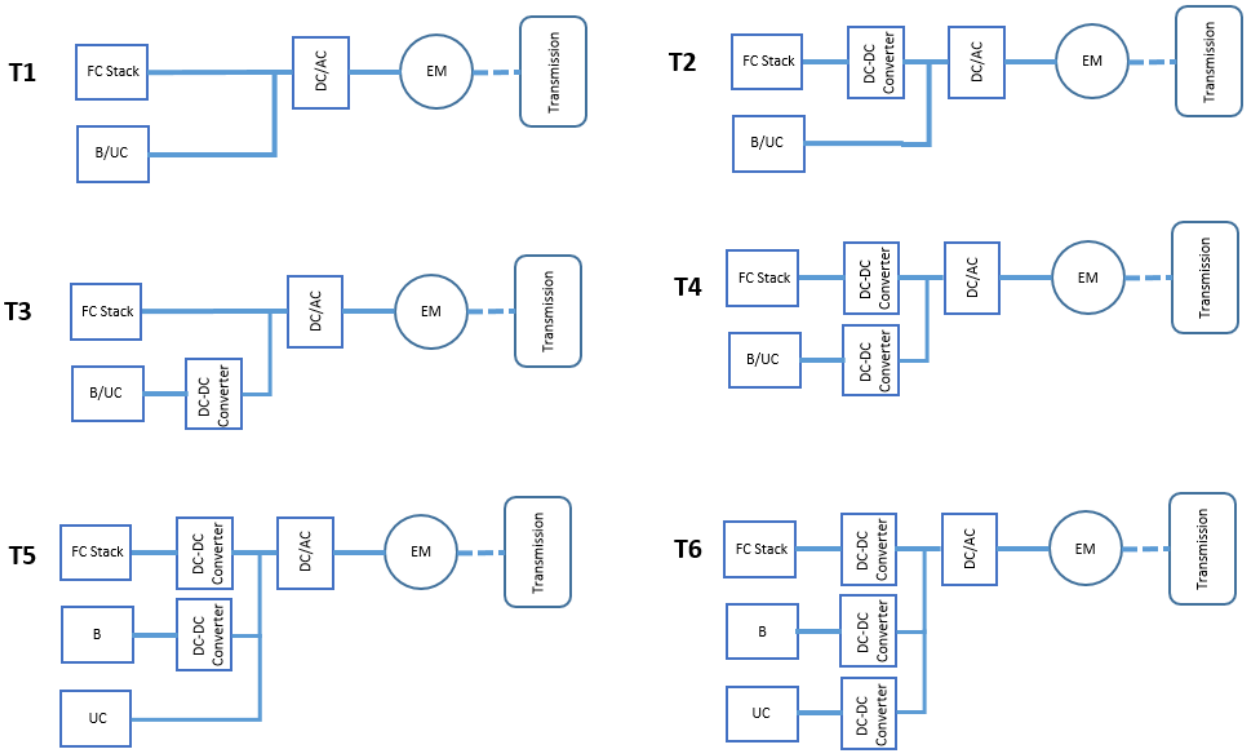

Figure 2.3: FCHEP Topologies

- **T1** is floating DC Bus, application of such architecture is rare and more suitable for single stage power conversion. *Wu* has studied on passive hybridization of FCHEP through allocating super-capacitor (Wu, 2014). In detriment of losing active control over load management, high cost DC converters and associated losses can be cut off from the system off. The passive system achieves this by direct coupling to match operating voltages of the sources which in addition makes system component sizing highly crucial. Power split between the devices is achieved by the thermodynamic potential difference or impedance change. A 2010 study deploys the topology and control is based on power decoupling through charge controller of ultracapacitor (UC)(Azib et al., 2010). In another passive system designed

by *Zhao*, UC is coupled directly in parallel with the fuel cell (FC) with a power diode to avoid reverse flow and the power sharing is determined by the current-voltage characteristics of the FC and UC.(Zhao and Burke, 2010)

- **T2** is a preferred topology with power split control between sources via controlled FC with floating ESS (Jingang and Charpentier, 2014),(Li et al., 2012), (Tazelaar and Veenhuizen, 2013), (Ogburn, 2000), (Gao and Zhenhua, 2016), (Smith, 2009), (Codina, 2017), (Hosseinzadeh, 2012). *Offer and Howey* have concluded that the greatest benefits of fuel cell power-trains are realized when hybridised with batteries and the system capital cost, hydrogen cost and electricity cost are determinants of the feasibility. In the battery-fuel cell hybrid configuration, fuel cell is serving as a range extender and allowing for the downsize of the batteries in comparison to same range BEP and FCP (Offer and Howey, 2010). *Hosseinzedah* utilized battery and ultra-capacitors to downsize fuel cell stack and reduce the transient load on the stack which lead to a lower capital cost and volume savings, as well as longer operational life and simpler system control (Hosseinzadeh, 2012). Analysed power-train of this study is T2 type as well and different load management strategies in the literature will be explained in detail in the following section.

- **T3** provides floating FC with storage system of battery or UC interfaced via bidirectional DC converter. This configuration has higher losses in comparison to T2 due to bi-directionality of the DC converter. There are few studies worked on it and *Zhao and Burke* argues that in comparison with FCP, T1 and T2 architectures, load levelling strategy accommodated T3 architecture provides the most fuel efficient performance if employed with a UC (Zhao and Burke, 2010) (Bell, 2016).

- **T4** allows a high level of control on the bus with complex control strategies and is the most preferred topology among researchers to exploit the real potential of the power-trains. DC converters restricts large voltage swings and the inverter requirement is flexible. Typical strategy for load management is deploying the Power Control Unit (PCU) which sets the duty cycle of the converters according to the comparison between load and FC power handled by PCU. In a 2018 study 96.8% power efficiency was reached around the rated power with highly accurate DC voltage regulation in the experimental set-up (Fathabadi, 2018). A predictive control model, Equivalent consumption minimization strategy (ECMS) aimed to obtain minimum fuel consumption and the results of the system have been compared by rule based PCU embedded system (Zheng et al., 2012). *Bernard and Delprat* aimed to identify effect of FC and ESSs sizes on fuel consumption. Global optimization algorithm respecting charge sustaining in ESSs has been used to eliminate the influence of control strategy to focus on the power source sizing (Bernard and Delprat, 2010). *Fletcher* has developed a novel Stochastic dynamic programming control to reduce overall running cost including degradation of the fuel cell. His study has shown that optimizing solely the fuel efficiency is not the most cost efficient solution, moreover compromise of fuel efficiency up to 3.7% increases the life time of fuel cell significantly and reduces overall running costs by 9% (Fletcher,

2017). Another widely investigated control mechanism is fuzzy logic which attempts to keep DC bus voltage level stable around the nominal value. Deterministic dynamic programming,anticipatory power splitting, neural network optimization algorithm, wavelet-based frequency decoupling and adaptive neuro-fuzzy inference are some advanced techniques for load balance which have been tried by researchers (Sulaiman et al., 2015).

- **T5** consists of a controlled FC and battery with floating UC. The main advantage of this topology is that it benefits hybridization of battery and UC that delivers high power and energy density, yet it suffers from system complexity. *Goyal* has developed a closed loop feed back with fuel cell Hardware-In-Loop system with two level control system, base-line and load following (Goyal, 2014). A recent study had single level yet complex PCU operation requiring strategy suggested. The current distribution on the bus is dictated by the internal impedance of each component any given time. PCU strategy is based on a State Machine Map has high resemblance with study of (Jingang and Charpentier, 2014) which has been applied for T2 configuration (Aschilean and Varlam, 2018). The topology proposed by *Li et al.* has a battery connected to a DC bus directly and UC with DC converter interface. The system is a fuzzy controlled architecture, whereas almost the same system with slight modification has been achieved to control with simple PI by *Odeim*. (Li et al., 2012), (Odeim and Roes, 2015) Study of *Bubna* examines different hybridizations for fuel cell power-trains, such as Fuel Cell-Battery, Fuel Cell-Ultra Capacitor, Fuel Cell-Ultra Capacitor-Battery which can impact the tractive performance and fuel consumption and should be customized according to load characteristics. He concluded that T5 configuration yields best fuel economy with prediction- based power management strategy (Bubna et al., 2012). Ultra-capacitors and flywheels are good candidates to mitigate pulse power effects, that are high in power and short in duration. Ultra-capacitors have higher power density than batteries, yet for long duration loads, batteries which have higher energy density, are preferred. Still, battery has shorter life time and limited recharge rate in comparison to ultra-capacitor. Super-capacitors theoretically appeared to be a good alternative for Li-ion batteries, yet laboratory performance of them barely acquired few kWh(Hu et al., 2015). Thus, hybridization of the power-train has many parameters for design dependent on objectives of the performance.

- **T6** configuration has the most control over the DC bus voltage with DC converter interfaced connection of all the energy sources. Moreover, existence of UC and battery as secondary power sources provides high power density and high energy density, essential for good acceleration. When a UC handles power, battery stores energy more efficiently compared to other topologies. In a study, researchers managed to use a single DC converter with multiple input run by fuzzy logic control (Melero-Pérez and Gao, 2009). *Garcia et al.* reported on performance of applicable control strategies for T6, including operation mode control, cascade control, fuzzy logic control, ECMS control and predictive control. ECMS has shown the greatest fuel economy which is relatively simpler control strategy as well. Meanwhile, the fuzzy logic and predictive control have been the most complex systems to design (Garcia et al., 2013).

2.2.2 Single Stage Power Conversion FCHEPs

Recent research focused on single stage power conversion (SSPC), since the converters of the multi-stage power conversion is relatively bulkier, less efficient and more expensive. SSPCs are capable of levelling bus voltage and inverting current to be ready for electric motors. The basic topology of FCHEP deploying SSPC is given in Figure 2.4.

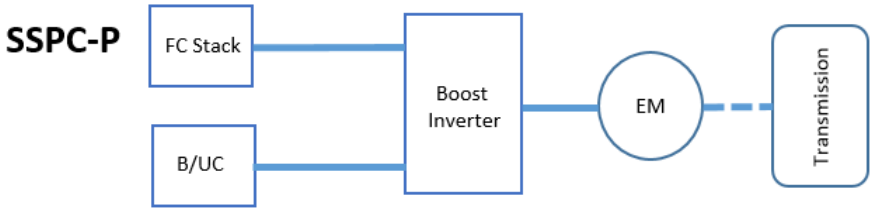

Figure 2.4: Basic SSPC power-train architecture

Researchers have investigated switched boost inverters, Z-source inverters and differential boost inverters. For fuel cell applications where low input voltage and high boost ratio is required, the differential boost inverters are preferable with the highest boost ratio available among others. Besides, the converter needs special modification in the topology to connect with multiple inputs. There are three management strategies developed in the literature for the differential boost inverters; PWM control, sliding mode control and dual loop control (Jang and Agelidis, 2011). Dual loop is the only control mechanism capable of coping with dynamic load changes. However, this control system does not allow the break energy recovery (Das et al., 2017). The auxiliary energy unit is only charged by FC when the load current is low. FCHEPs are attractive for the regenerative breaking and corresponding energy saving through assistance of reversible energy storage systems, such as battery or ultra-capacitor. Typically battery absorbs energy during regenerative breaking and meets the transient loads, when fuel cell continues to charge the battery and extends the range of the vehicle. This system becomes unattractive for vehicular applications, yet regenerative breaking is not possible for power boats by nature which uses the viscous forces on the hull to slow down, rather than "break". There are applications for implementation of the reverse reaction energy conversion for sailing boats, such as *Opal* project of Nordic Innovation for whale watching tourism, yet that application is not focus of this study (Gunnarsson and Skúlason, 2016). Hence, differential boost inverter with dual loop control system has a strong potential to be a good solution for FCHEP maritime boat applications and further investigation is beneficial.

In the following section, EMS developed for FCHEPs and elaborate literature survey devoted particularly for T2 architecture is delivered, since this architecture is the focus in this research. In the same section, an outlook of the FC deployment and management in electric power-trains with respect to architecture classification are given with the aim of keeping the review diverse and comprehensive. There are many

specific and cross-field working research groups which are giving new approaches and solutions to the field. In addition to specifically given studies in the review, few initiatives to be followed to remain updated with the developments in the FCHEP projects are: Hy-Mar, IEEE electric ship technologies initiative, Marinelive -the initiative of European Commission for All Electric Ships (AES) by Naval Architecture University of Athens-, International Conference on Marine Science and Technology for Environmental Sustainability run by University of Newcastle.

2.3 Energy Management Strategies

The optimal running points of individual components do not necessarily coincide with one another, meaning that a global compromise is required to avoid undesired operating points within the system (Staffell, 2011). The key role of EMS is to manage multiple energy storage devices to meet the load required by the driver. Understanding of the system design of FCHEP is obligatory to control the EMS. In a FCHEP, each power source can be directly or indirectly connected to high voltage DC Bus. *Gao* argues that a significant reduction in cost of the power-train and complexity of the energy management strategy achieved when a minimum of one power source is used to make up power difference between loads and other sources (Gao and Zhenhua, 2016). *Shagar* states that multiple power sources and existence of energy storage elements is an opportunity to reduce transients to a great extend in the power system with an effective control (Shagar, 2017).
T2 topology hybridises fuel cell with floating battery or ultra-capacitor for two main reasons; to absorb regenerative braking energy, which will not be investigated in this study, and to balance the load to operate the system efficiently and reliably. Most of the EMS related research aims to go beyond just delivering the required performance. Cost, degradation and storage of hydrogen the three main challenge areas of FCHEPs and can be improved with successfully designed EMS. Battery provides additional power to downsize fuel cell and reduce initial cost. Secondly, battery balances transient loads and operation of the fuel cell within its optimum region will limit its degradation. Finally, fuel economy can be significantly improved by EMS easing the job of storage system.

2.3.1 EMS Requirements

Global focus of control strategies to provide an efficient and reliable operation, loss minimization and reduced fuel consumption and system cost. Those superior objectives can be achieved by sub-objectives dictated to sub-systems. There are different sub-objectives for EMS development of MSPC power-trains and the broadly explored ones in the literature are listed below (Fletcher, 2017).

- **Fuel Economy**

  The majority of research has been devoted solely to improve fuel efficiency which reduces the running costs and improves the range without increasing ESSs. Efficiency of the fuel cell depends on the load, such that at low loads the ratio of the current supplies to ancillaries becomes higher compared to

useful power output which reduces efficiency, at low loads ohmic losses dominates ancillary current draw and at very high loads the mass transfer of the species across fuel cell becomes limiting factor. The phenomena has been explained and compared with ICE by *Rousseau* as shown in the Figure 2.5 (Rousseau and Sharer, 2004).

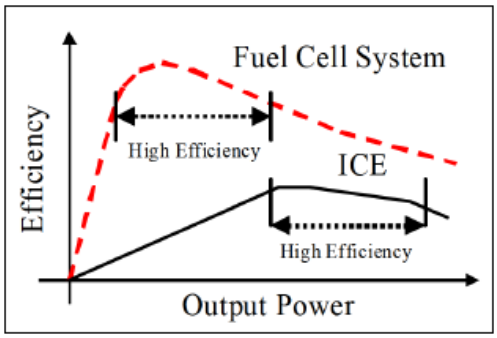

Figure 2.5: Fuel cell and ICE efficiency comparison (Rousseau and Sharer, 2004)

Staffell and *Gao* have shown in their studies on fuel economy for FCHEPs that the main focus of attention should be fuel cell to keep the overall system efficiency at optimum. Other components of the power-train such as auxiliaries, converters, battery and motor have relatively more consistent efficiencies in average and causing less power losses (Gao et al., 2016), (Staffell, 2011).

- **Fuel Cell Degradation**

  Fuel cell degradation is taken into account to identify achievable targets for supervisory control. EMS can improve the lifetime of the fuel cell and reduce the required minimum number of hours of operation of fuel cell by running it less and still be competitive with conventional ICE (Wu, 2014). Reliable and efficient performance of the fuel cell depends on many factor such as material properties, operating conditions, impurities of the reactants and environmental conditions. Even though EMS cannot have affect on many parameters, it can avoid the degradation due to operating conditions.

- **Battery degradation**

  EMS controls the state of charge and the current loading of the battery which have direct effect on degradation mechanisms. Batteries degrade due to number of chemistry depending reasons, but the most profound mechanisms are operations outside of temperature and voltage limits. Voltage limit is respected by not charging an already fully charged battery, avoiding deep-discharge and not exceeding the safe charging-discharging battery current (Skender, 2017). Finally, charge-discharge cycles cause incremental damage to the battery and therefore the EMS should avoid cycling the battery more than necessary.

- **Reliability**

  Power-train should be able to deliver a predictable and consistent performance. Reliability covers many

aspects of performance, such as acceleration, noise, breaking, mode shifting (Goyal, 2014). For example, performance in the acceleration should not be detracted by a lower state of charge in the battery. Thus, reliability concerns should take part in the EMS when a globally optimized solution is searched.

2.3.2 EMS Methodologies

The topologies introduced in the previous section can be run by various control strategies based on the configuration and focus of the optimization. In this section, acquainted EMS throughout the literature review were introduced, yet only EMS devoted for control of T2 architected FCHEP applications was elaborated. Applied control approaches on multiple stage conversion deploying hybrid electric power-trains in the literature has been classified as shown in Figure 2.6.

In the ***passive control***, the linear feed-back and feed-forward controllers are adopted to control the duty cycle of DC converters and to set the current of the fuel cell according to the voltage of the bus.

Heuristic strategy is inspired by the expected behaviour of the propulsion system and uses predetermined sets of "rules" to determine operation states of the system. Deterministic rule-based methods are usually based on analysis of power flow in the drive-train, efficiency/fuel maps of components and human experiences, generally implemented in the form of lookup tables and by splitting powers between power sources. The number of states may vary according to designer choice and those states can be optimized to achieve minimum fuel consumption. The simplicity and real time operation made this approach popular. Power-assist based on operational state and load levelling are two of the deterministic rule based strategies applied in the literature.

Power assist control is the most widely investigated and the classical approach for T2 FCHEP energy management strategy for various applications. This control mechanism splits the current demand of the motor based on the fuel cell power, energy storage and state of charge. One study has developed power assist control for mid-power pleasure boat propulsion. In order to maximize the system efficiency, EMS determines the operation point of the components based 11 operational intervals mapped according to the comparison of load with power sources' efficient operation ranges. Load levelling of FC was managed by PI and low pass filter controlled DC converter was used to avoid abrupt fluctuations, whereas the reference current of FC was determined by the EMS. The performance of the power-train evaluated under real driving cycle of a boat and EMS achieved higher efficiency compared with load command tracking control. (Jingang and Charpentier, 2014) A NREL supported project for development of a concept car for Virginia Tech used a power assist strategy to comply with fuel economy restrictions by running the fuel cell at efficiency range and avoiding losses due to battery charge/discharge inefficiencies. The operational modes of the power-train enabled discard of the fuel cell and when hybrid modes was activated the boost converter the boost converter transferred power to the bus from the fuel cell whenever the state of charge is below a pre-set level. The fuel saving was nearly twice of the stock vehicle. The performance of the simulated power-train in ADVISOR has been validated with

experimentally measured values and the predicted fuel economy only deviated by 1% (Ogburn, 2000). *Gao* has conducted a research to develop a hybrid fuel cell/battery bus for public transportation in urban areas. EMS aimed to improve fuel economy, maintain the battery operation for long duties and avoiding degradation of fuel cell whilst delivering reliable performance. The performance requirements of such applications include frequent start and stop, load transients which exacerbate the fuel cell performance in long term and storage of the regenerative energy. Thus, state based power assisting strategy is realized using look-up tables built with fuel cell target power with respect to SOC of the battery and load power. EMS has not been shared explicitly other than 3-D graph, yet the it has been reported that devoted strategy has performed 3.5% less in terms of fuel economy than another study has achieved with another EMS based on power-assisting for the same architecture (Gao et al., 2016). Another study uses this strategy to control a forklift power-train with fuel consumption minimization, prevention of fluctuations in the load of fuel cell and state of charge maintenance in the battery objective. The strategy is quite simple, such that the fuel cell supplies power only if the state of charge falls below 65% and the supplied power is a constant and corresponds to the maximum efficiency zone of the fuel cell. The fuel cell stops operation above 90% to allow the battery to absorb regenerative breaking energy (Hosseinzadeh, 2012).

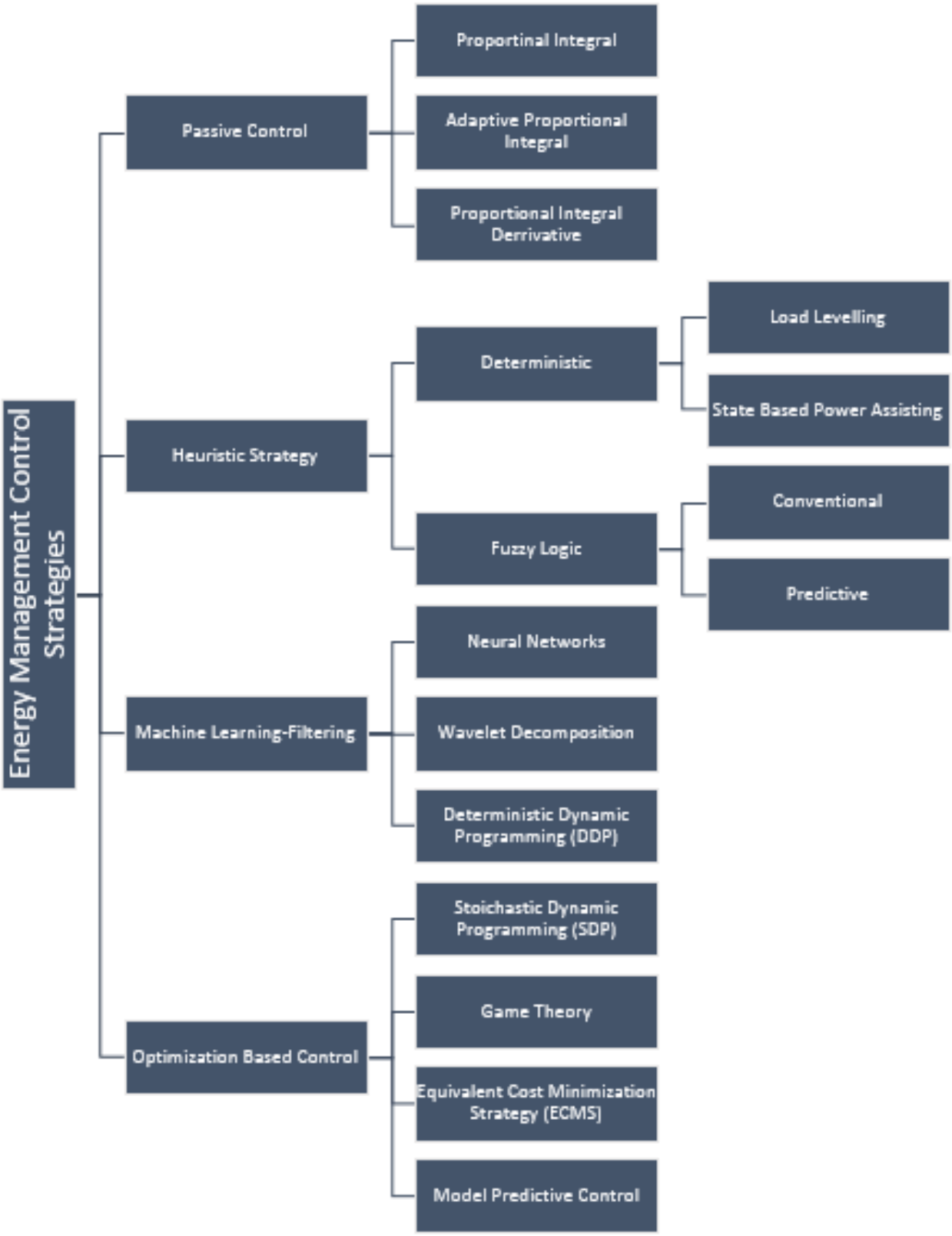

Figure 2.6: Energy management control strategies for MSPC power-trains

Load levelling is another preferred strategy that makes the fuel cell power supply relatively steady and the ESS device backs-up whole system for storage and management of transient loads. *Virginia Tech* research group has designed a boost converter of the fuel cell sourced power-train to assist the EMS and take the complex task of power transfer control away from the on board computer whilst preserving the root power transfer strategy. Two layer control strategy balances the load with just control of a buck converter. Low-level controller, using fuzzy logic, strictly controls the inductor current to track a reference, whereas high-level strategy is used to calculate the reference value for the inductor current based on load-levelling to maximize fuel cell performance even under most dynamic loads. The passive battery inherits all the load dynamic behaviour, and is therefore used for peaking power delivery, while the fuel cell delivers base or average power (Smith, 2009). In a study, power assisting and load-levelling strategies have been compared for the same topology under same dynamic load conditions of US06 driving cycle. Compared to power-assisting, load levelling is much better to mitigate load transient on the fuel cell which results less stress on the fuel cell stack. However, with load levelling significant amount of power flow/energy passes on the DC converter to be charged or discharged which causes high losses due to power electronics. It has concluded that power-assist strategy results in larger improvements in the fuel economy due to less loss in power electronics and energy storage units. On the other hand, the same study shows that the best performance is obtained with T3 topology deploying ultra-capacitor with simple load-levelling strategy as indicated before in the explanation of architectures and applications (Zhao and Burke, 2010).

Instead of using deterministic rules, the decision making property of ***fuzzy logic control*** can be adopted to realize a real-time power-split controller. The fuzzy logic gives more freedom of system design. It works on a set of if and then rules which basically sets the boundary conditions of the member functions and produce output with respect to satisfaction of the condition. However, freedom arising in the range of conditions is prone to relax the control goal and hence cause dis-function of the control. Efficient rule allocation can reduce the member functions and produce plausible results. As mentioned before, *Smith* has implemented fuzzy logic to track the reference value of buck converter's inductor current with minimal error and to avoid disturbances in the dynamic load (Smith, 2009). ***Fuzzy predictive strategy*** seeks for the optimal solution based on minimizing an appropriate cost function over a drive cycle, attainable by knowing the entire trip information beforehand (Brian Su-Ming Fan, 2011).

Machine learning provides output control that can be optimised automatically, thus it tends to give much better performance without the complexity of a large number of "rules" as defined by Heuristic approach. Moreover, the re-optimization of the controller for different power-train topologies is considerably less extensive than that of rule-based approaches. Most of the applications use this strategy off-line and subsequent results are applied on the power-train. ***Neural network*** algorithm with three layer with inputs

of load power, interval time for change of the load and state of charge for the DC output power has been developed and provided 7.23% fuel saving in comparison to the fuzzy logic ruled EMS (Xie and Quan, 2008). ***Wavelet-based*** frequency decoupling strategy is load sharing algorithm through filtering. ***Deterministic dynamic programming*** (DDP) is a method for solving complex problems by breaking them down into smaller sub-problems and a combination of the solutions can then be used in order to reach the optimal overall solution. DDP for off-line optimization of PI controller based on Pontryagin's Minimum Principle, in which system is represented by space state dynamics with three parameters was compared with a fuzzy control with 10 parameters to minimize hydrogen consumption of a FCHEP when the complete load is known in advance. The results have shown that PI controller outperform the fuzzy logic, even though it had fewer parameters (Odeim and Roes, 2015).

Optimization-based control are used to mathematically define the control goals in a cost function and typically utilizes global optimization when determining the control strategy which is non-causal since the global solution has been found for a fixed drive cycle which suggests the past and future demands are already known. Hence, the draw-back of this approach using global optimization is infeasibility for the real-time applications most of the time, yet it is a powerful tool for designing rules and evaluating other control strategies. The cost function can be defined for many objectives such as fuel consumption, system cost, system loss. ***Stochastic dynamic programming*** (SDP) is the optimization based method producing time-invariant causal solutions with respect to the state of the vehicle and the probability of transitioning to another state. SDP allows multiple drive-cycles to be optimized and is suitable for direct implementation on board and real world data to be examined concurrently by Markov Chain (Fletcher, 2017). Jaguar Land-Rover power-train load manager uses ***Game theory*** to penalize the fuel consumption, NOx emissions, operating condition deviations and battery SOC deviations in a non-cooperative game between the driver and the power-train. ***Equivalent consumption minimization strategy*** regulates SOC while delivering the load and minimizing the fuel consumption. ECMS creates a local optimum instantaneously by considering the total energy consumption, while maintaining a certain level of SOC. ***Model predictive control*** (MPC) optimizes the present strategy, while keeping the future timeslots in account, therefore it needs a future input. MPC can be coupled with a global positioning system to provide real-time optimization.

There is a variety of approaches and objectives for selection of an EMS. Undeniably, few strategies are much sophisticated and complex to develop, yet the complexity does not necessarily offer the best solution or pay-off the effort for the insignificant incremental improvement. *Sulaiman* draws attention to the unimpressive performance of complex EMS when tested on the hardware(Sulaiman et al., 2015). Thus, EMS developers should pay attention not only to power-train dynamics, but also drive-train dynamics in terms of application area and consider the feasibility of the algorithm. For example, load fluctuations of the transport applications are mostly multi-frequency and deployment of filter based control strategy is strongly suggested in addition to a high level EMS (Gao and Zhenhua, 2016). Electric power-train application for maritime transport faces

with the challenge of propulsion load fluctuations from the propeller which are not isolated in the integrated power system. Three type of fluctuations are studied in the literature: the first impact of the first order wave at the encounter wave frequency, in-and-out-of-water effect, propeller rotation at the propeller-blade frequency. In this study, these effects were not taken into account due to time limitations. *Chanda* makes a point that the performance of the electric drive system needs to be validated under real world dynamic load conditions reflecting fluctuations in the usual driving cycle. Such testing is generally performed with dynamo-meters that are capable of motoring and generation (Chanda and Snyder, 2012). *Yang* has also preferred to verify his model of electric power-train under AC electric dynamo-meter test to conduct driving cycle simulation and the error of the model to predict energy consumption per kilometre was 15% (Yang, 2012). *Hou* proved that hybrid power-train might yield to undesirable interactions and poorer performance than of a single source power-train, when the controls are not coordinated properly. Unpredictability of the propulsion-load torque of marine applications was given as a limitation for success of the EMS (Hou, 2017).

2.4 Multi-disciplinary Design Optimization

Determination of a power-train architecture is the initiation step for the design of a power-train capable of delivering the desired performance. Besides EMS optimization, optimization of the components needs to be investigated to understand the cost-performance trade-off. As a result of literature survey, it was apparent that FCHEP architecture optimization literature has not developed yet. There is only one study for FCHEP that includes hybridization of super-capacitor and fuel cell in a topology T4 and focusing on cost minimization of the system with a basic EMS which is so called "thermostatic strategy". In the corresponding strategy, the fuel cell has only one operational mode providing maximum efficiency or else is in the turned-off state. For a defined driving cycle, the size and cost of the fuel cell and super-capacitor are minimized by identification of the best number of units subjected to various design and control constrains. ***Particle swarm optimization*** has achieved the optimum design. This study is valuable since it constitutes an example for further research. However, it does not contribute to neither fuel economy nor durability (Hegazy and Van Mierlo, 2010).

Research in the optimization of hybrid power-trains has predominately focused on either component sizing or EMS, yet these two important factors are coupled, such that different selection of component sizing requires another design of EMS for optimum performance due to their interdependent relation. Hence, application of con-current optimization incorporating optimizations of the power-train sizing and the power management logic simultaneously, can provide satisfying results. *Xiaofen* defines the concurrent optimization as decomposing the complex design into a number of small sub-systems and tackles each of them simultaneously (Xiaofen, 2014). In this methodology, the design engineer approaches the optimal system solution with a global objective function and subsequently finalizes the detailed design.

Usually researches use conventional methods tends to convert multi-objective optimization into a single-objective, by allocating weights to objective functions and unifying them. However, the appropriate

weights, i.e. capable of indicating the actual situation, are not easily defined to objective functions of FCHEP and can be misleading, since the system is complex. When the power-train component sizes are optimized, various design constraints should be met simultaneously. Hence, the problem can be treated as multi-objective constrained non-linear optimization. Optimization of the overall control design can be conjuncted through problem function variables which will be evaluated by objective functions and needs to meet constraints. *Desai* has developed a ***multi-objective genetic algorithm*** to optimize power-train components as well as fuel economy and emissions for an ICE hybrid electric vehicle. The algorithm alters the values of the fitness function and ADVISOR simulations evaluates objective function and constraints (Desai, 2009). *Kim* studied how to maximize fuel economy for FCHEP though con-current optimization of EMS and component sizing. EMS was developed from stochastic dynamic programming motivated basis functions to be run by ***gradient based optimization***. It was reported that 17% extra fuel saving was achieved with con-current optimization in comparison to only EMS optimization (Kim, 2007). Gradient based optimizations are incapable of obtaining global optimization and objective function needs to be continuous and differentiable, which may not be always the case for power-train optimization. In addition, for multi-disciplinary optimizations, calculation of derivatives for each point is required which is computationally quite expensive. Genetic algorithms are global optimization focused, derivative free and efficient to solve the design optimization (Jain, 2009). Therefore, *Jain* has preferred to use genetic algorithm based optimization with objectives of higher fuel efficiency and minimum power-train cost through simultaneous component sizing of FCHEP and EMS optimization. The author has outlined the structure of power-assist EMS with parameters which are also the parameters of fitness function of the optimization problem.

Brian optimized internal combustion engine hybrid electric vehicle with multi-disciplinary optimization methods, such as genetic algorithm, simulated annealing, pattern search and Nelder-Mead. Multi-disciplinary optimization problem and progress mechanism can be formulated as shown in Figure 2.7 (Brian Su-Ming Fan, 2011).

In the figure, X_D is the vector of variables which are provided to disciplines to be analysed and produce the output function $U(X_D)$ which will be used to evaluate objective function $J(X_D, U(X_D))$ and constraints $C(X_D, U(X_D))$

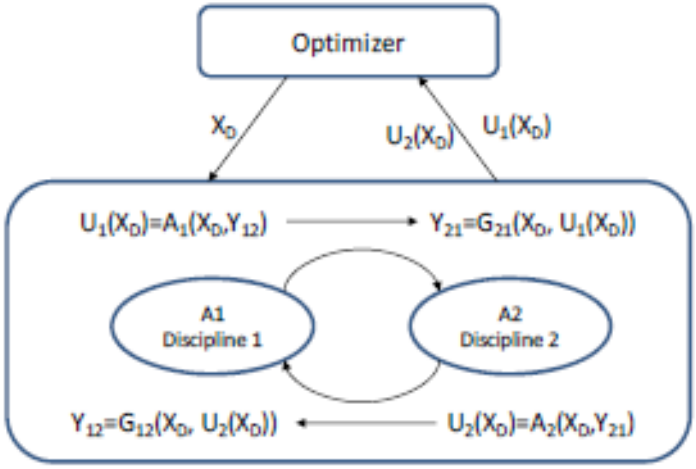

Figure 2.7: Multi-disciplinary optimization formulation

- Vector of variables X_D is assigned by optimizer for each optimization loop for analysis $A1, A2$ of the two disciplines to produce respective outputs, $U_1(X_D), U_2(X_D)$.
- The output functions are evaluated for their fitness with respect to objective function $J(X_D, U_1(X_D), U_2(X_D))$ and $C(X_D, U_1(X_D), U_2(X_D))$
- G_{ij} is the inter-disciplinary relation function of discipline j output, U_j to provide suitable input variable Y_{ij} for discipline i.

Chapter 3

Fuel Cell Hybrid Electric Drive-train Modelling

A successful model leads to a good compromise among flexibility, simplicity, computational load and detailed representation of the components. Development of a model consists 4 phases; (*1*) identification of model expectations, (*2*) determination of the key equations, parameters and assumptions, (*3*) building and refining the model and (*4*) the actual model application and evaluation (McDonald, 2012). There are three approaches when building a model of a system/component:

- **White-Box Method: Deriving a model from the first principles**

  When a system is simple enough to identify equations that governs the behaviour, this methodology referred as white-box is applied. The system resembles a box on which a flash light is shone, such that all the information making up the system is available. Therefore, the developer can prefer whatever technique she prefers to derive the model, such as free body diagrams, Lagrangian mechanics or building a system from individual components. The model is developed on the fundamental physical concepts and assumptions. This technique is widely applied for research studies since it gives total understanding of intricacies of the system to be controlled and identifies the important components to be focused and what can be left out. For example, the static friction modelling of a DC motor does not necessarily benefit the system model and even make the model over-complicated and slow, if the system is operating at non-zero speeds. SIMSCAPE tool of Matlab/Simulink essentially lets the developer avoid writing the ordinary differential equations out and instead enables drawing the mechanical and electrical circuits of the system directly which are inherently embodying those equations. Instead of using gain and integration blocks, block representation of the physical components such as resistor, inductor and voltage source can be used to create model from first principles. If the model is a good representation of the real physical system, the gains of the control system can be transferred over real hardware and work there as well.

- **Gray-Box Method: System parameter exploit**

  This approach is used when the the system structure is known, yet some specific parameters are missing for the differential equations defining the system. For instance, the value of inertia of a DC motor is not known. This is a common situation for industry based researches and the problem is handled by either testing the component and measuring the value missing or fitting the component already functioning system model to utilize software to estimate the optimal values for the parameter. Gray-box modelling has been preferred by *Skender* to complete models of the test bench components whose performance data could be measured in parallel (Skender, 2017).

- **Black-box Method: System identification**

  If the system is too complex to derive a model with differential equations or mechanical and electrical components, the system identification method needs to be applied. In black-box method, the developer does not have information about the fundamental physics and insight into specifics of the system, yet he has access to the input and output signals to infer a model of the system. For example, a water stream inlet leaves a system with higher temperature which implies that the system supplies heat. By understanding the thermal properties of the water, a heating model can be developed although the physics of the heating is not known. This model is useful since the developer can avoid the details and lumped into general behaviour of interest. However, this method should not be run with complete ignorance and developer still needs to know the system well enough to be sure the generated model structure is right. Heating of metal containing water needs to be avoided, if the heating is done by microwaves and a sole modelling of water heating does not provide this information. System identification is widely applied for the commercial system modelling, when most of a time the details of the individual components are not known, yet the system needs to function harmoniously and the control system to be established. Individual components can be treated as black-boxes in testing conditions and input signals and responses can be measured to fit a model to measured data. System identification can be much faster than slugging through a model with first principles and it is much easier to develop a control system for a transfer function identifying the black-box (Douglas, 2017).

Even though the non-linear systems based on fundamental physics are the most accurate representation of the actual systems, they are not the easiest to work with for system control. Hence, linearisation of the non-linear systems is preferred whenever the system behaviour is applicable. There is no truly linear real system, all have some non-linear behaviour but there is still a margin to approach a real system with a linear model. There are many tools to design and tune control system with linear systems, such as loop shaping, pole placement or some other classical linear control techniques.

For modelling of the system, generic system structure was developed as explained in the following section and modelling of individual components were explained in the subsequent sections. Aforementioned approaches of modelling were applied on various levels to include as much detail required and available for the dynamic simulation with heuristic EMS which is capable of real-time control to reflect the actual behaviour as accurate

as possible. Besides,the optimization study can only be done with a modular and flexible modelling, since the optimizer needs to scale the components for seeking the optimum solution. Thus, abstraction has been applied on a grant level to the system for optimization which will be explained in detail in the multi-disciplinary optimization chapter.

3.1 Generic System Structure

There are two approaches to model a drive-train: forward-looking and backward-looking.
Forward-looking structure, shown in Figure 3.1, has more realistic approach, since it reflects the actual interface between the driver and the drive-train. The simulation begins with the driver's demand and the power-train produces torque which propagates through the transmission before ending up as a torque applied on the propellers. This is exerted to the drive-train mass via thrust force and the resultant speed propagates back to the drive-train and returns to the motor as angular velocity. There is inevitably margin of error between the actual speed and the speed trace which is minimized by the driver control model. Hardware-In-Loop applications can be implemented in the model for development purposes. The model requires high fidelity from each component and therefore, it is complex and computationally expensive.

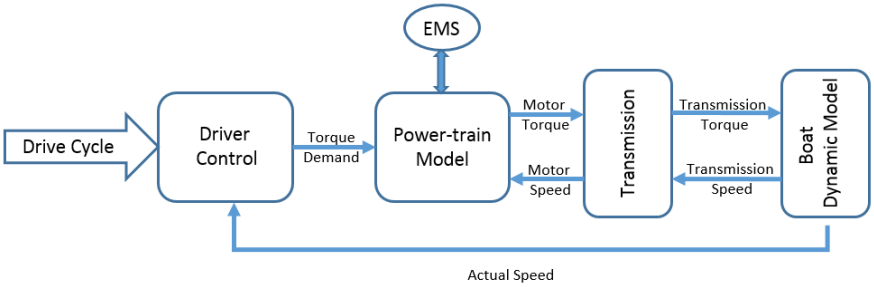

Figure 3.1: Forward looking generic system structure

Backward-looking power-train model, as in Figure 3.2, incorporates scalable power-train components, thus widely used for optimization researches. However, due to their quasi- static nature, the speed trace is imposed onto the drive-train model and they give very limited information about the limits of the system (Assadian et al., 2013). The model begins with determining the required vehicle power using a known drive cycle and the power-demand from the sources is computed in consideration of respective efficiencies and performances. This approach cuts off the computational effort at a great extend and enables most of the optimization methods.

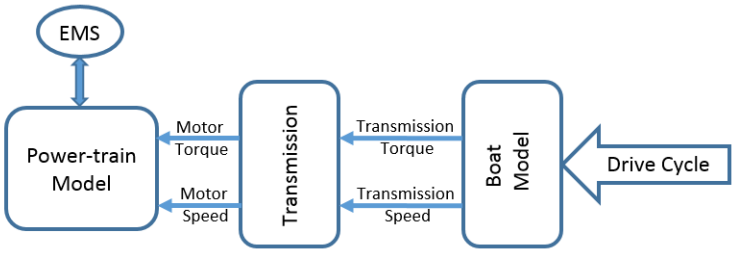

Figure 3.2: Backward looking generic system structure

The generic vehicle structure can be used to simulate any possible combination of power-sources and electronics in the power-train and any desired FCHEP configurations can be created. In this study, backward-looking structure will be used to reduce computational effort and complexity, since power-train optimization study is desired to be conducted in addition to heuristic EMS based power-train simulation. Therefore, boat model including transmission system is performed to calculate the load on the power-train.

3.2 In-land Cruise Drive Cycle Load Modelling

Boat and Transmission System Modelling

For calculation of the thrust of the propulsion and hull resistance, basic theories have been deployed and hence the quasi-steady model cannot reflect the real dynamics accurately. However, even simple modelling of the drive-train dynamics enables power-train to be evaluated under simulation of realistic load conditions. In the usual sense the boat dynamics can be modelled according to Newton's second law, as shown in Figure 3.3.

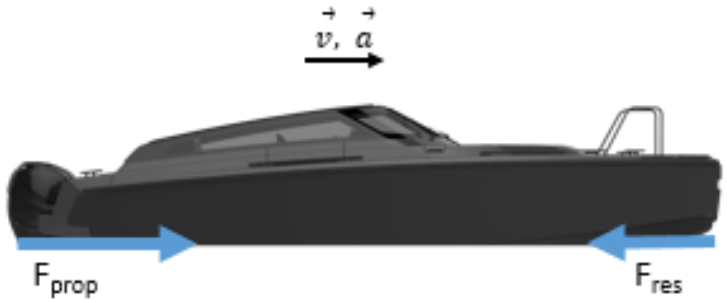

Figure 3.3: Diagram of propulsion dynamics

The backward-looking structure approaches the problem from the demand side, as explained in the Equation (3.1). Propulsion force needs to overcome resistance of the hull and provide the force for cruise at the desired velocity and acceleration.

$$F_{cruise}(t) = F_{prop}(t) - F_{res}(t), \quad \text{where} \quad F_{cruise}(t) = m_{boat} a_{cruise}(t) \tag{3.1}$$

The desired drive cycle is known and used as input to the boat model in the form of cruise speed and acceleration to find the load on the transmission system, modelled in the (3.2).

$$P_{tload}(t) = [F_{cruise}(t) + F_{res}(t)]v_{cruise}(t) \tag{3.2}$$

The mechanical load on the power-train has been calculated, with (3.3), through considering the inefficiencies of the propeller and shaft losses, total efficiency of the transmission system was approximated as 70% (US Naval Academy). This assumption should be considered as rough since the efficiency of the transmission system changes according to the load. Although this assumptions serves for the purpose of developing a load profile for the power-train which is the main concern of this step for this study, for more reliable and accurate analysis, this section of the modelling should be developed with knowledge of naval architecture.

$$P_{mload}(t) = \frac{P_{tload}(t)}{\eta_t} \tag{3.3}$$

Components of the hull resistance are drawn in Figure 3.4; at low speeds viscous resistance dominates, and at high speeds the total resistance curve turns upward dramatically as wave making resistance begins to dominate. Total hull resistance is a function of hull form, ship speed, and water properties.

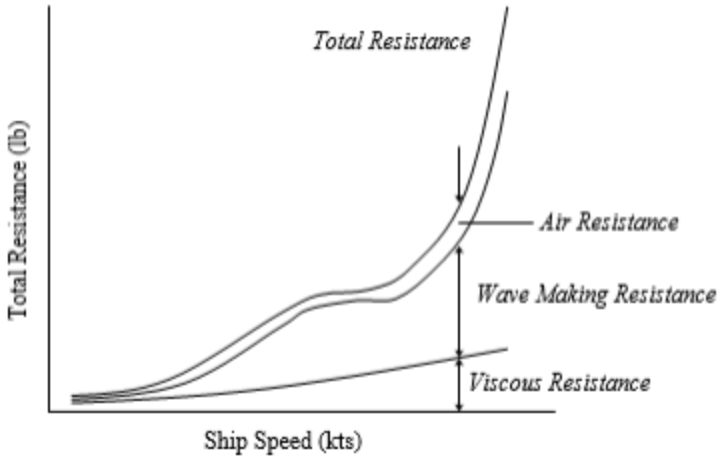

Figure 3.4: Components of hull resistance, (Molland, 2008)

In this study, air resistance was ignored and wave making resistance has not been included under the assumption that the boat will serve at low speeds where the viscous forces are prominent. However, it is a significant assumption which needs to be refined for an elaborate design study. The viscous hull resistance was based on experimental relation developed by *Froude* as (3.4) (Copisarow, 1945).

$$F_{res} = fSv^n \tag{3.4}$$

Frictional factor is f, S is the wetted surface, v is the velocity of the hull and n is the experimental variant

depending on hull properties are given in Figure B.1. The wetted surface area has been approximated with the (3.5). (Copisarow, 1945)

$$S = V_{dis}^{0.66}[0.75 + \frac{L}{2V_{dis}^{0.33}}] \tag{3.5}$$

The properties of boat to apply the modelling equations are listed in Table 3.1

Table 3.1: **Properties of the boat**

Boat weight, m_{boat}	1400 kg
Length of the water line, L	20 ft
Hull treatment	Varnished
Friction factor, f	0.0107
Froude variable, n	1.85

A possible increase of the weight by change in the passenger count was not taken into account in the resistance curve whereas the average passenger number was assumed as 3. Increased weight affects overall dynamic calculations and the center of the gravity, hence the trim angle of vessel. However, these considerations are too intricate for the scope of this thesis.

Power Map Generation

Drive cycle consists the vehicle velocity time history. For the terrestrial transport applications, there are pre-defined drive cycles by the standardization and control authorities to test the performance of the vehicles, such as drive cycle EPA US06 or FTP-45. However, there are no defined drive cycles for the performance analysis of marine power-trains. The ISO 8178 is an international standard for exhaust emission measurement from a number of non-road engine applications (International Organization for Standardization). For marine applications with propeller law commuting internal combustion engines which are serving for the targeted market are evaluated under E-type performance conditions. The emissions of the engines have been measured for some power and speed load conditions. However, a FCHEP operates with a zero emission and hence there is no regulatory evaluation criteria for the power-train. In order to acquire a realistic drive cycle for this application, the maritime data-bank Marine Traffic, (AIS Marine Traffic) data has been exploit for a vessel of interest displaying similar performance and activity characteristics of a boat in the target market. Since the GPS connection of the boat does not always have a perfect connection, the missing data points have been estimated through spline fitting to acquire a coherent and continuous drive cycle. The corresponding data is a drive cycle of in-land cruise taken place in 2018, July 21st between 06:15 and 08:10, the processed drive cycle is shown Figure 3.5.

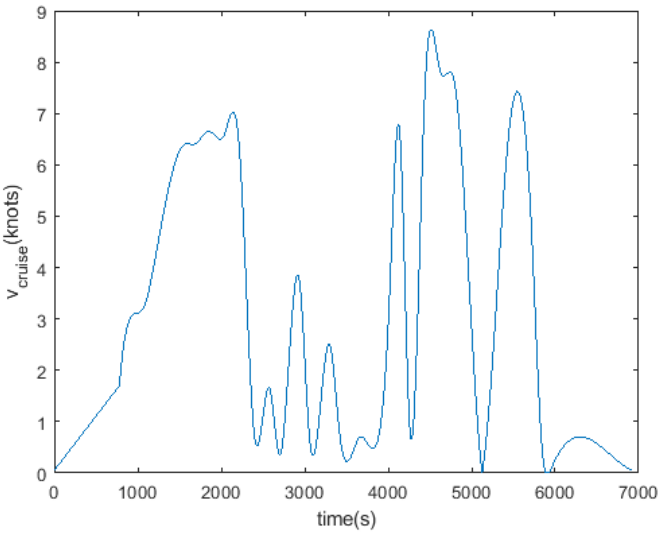

Figure 3.5: Drive cycle of in-land cruise

3D histogram has been used to analyse the drive cycle. As seen in Figure 3.6, the range of velocity and acceleration have been identified and an occurrence count based on defined interval has been generated. A bin is a combination of specific velocity and acceleration and each bin contains the number of occurrence of that combination over entire drive cycle. Since it is a cruise boat, most of the time the velocity was at lowest range and acceleration trends were mild. However, there is a wide range of acceleration demand which suggests the high transient load on the power-train as expected.

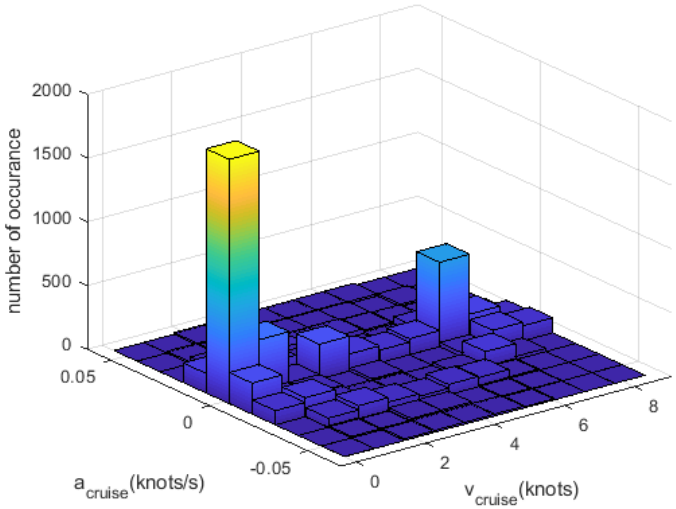

Figure 3.6: 3D histogram of the in-land cruise drive cycle

The power map of the drive cycle, shown in Figure 3.7 has been exploited after conducting the computations

for the boat dynamics and the transmission system. The contour color bar indicates the mechanical load which was scaled commonly with y-axis of the right-hand side plot. It should be noted that negative acceleration denotes slowing down, namely 'braking' and subsequently 'negative power' demand has been produced for regenerative energy storage. Since the power-boat does not have the system to store this energy, those intervals are taken as zero load on the power-train. The created power map is used as dynamic mechanic load of the power-train for simulations and optimization.

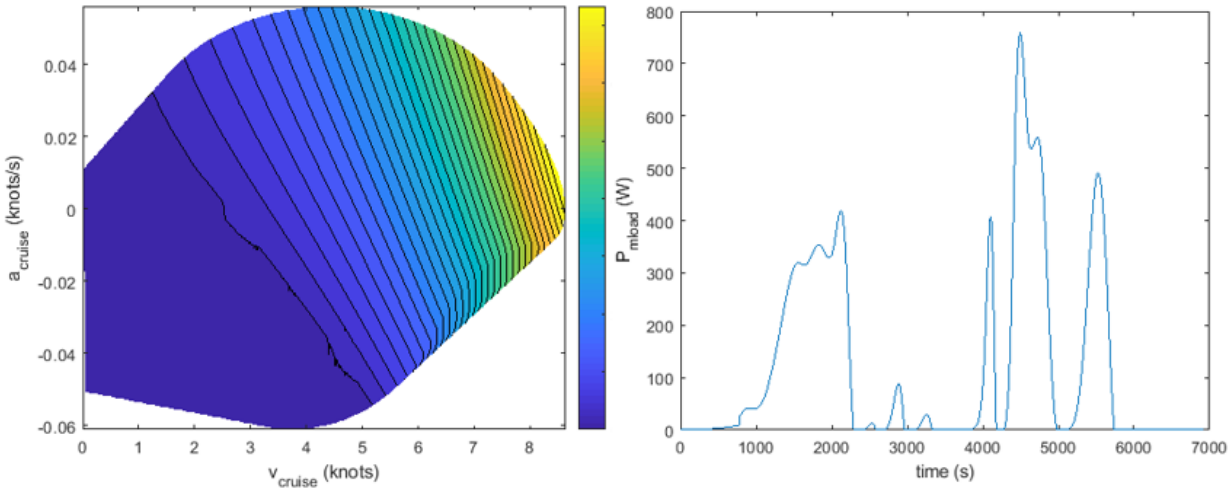

Figure 3.7: Map of the mechanical power load on the power-train

3.3 Modelling of Power-train Components

3.3.1 Fuel Cell System

Proton-Exchange Membrane Fuel Cells operating at relatively high efficiencies (up to 58%) under low operating pressures (1-3 bar) and temperatures (20-100 °C). One of the essential terms in choosing the fuel cell type for transport application is the low operating temperature that enables the quick start-up. PEMFC is the far best alternative with high power generation capacity and operational features in comparison to other alternatives, such as Phosphoric Acid FC, Solid Oxide FC, Molten Carbonate FC capable of reaching over 5 kW (Hosseinzadeh, 2012).

The electrolyte of the PEMFC is an organic polymer which is a good proton carrier operating in a water solution which also minimizes the corrosion related degradation and limits the cell operation temperature to the water evaporation temperature to avoid membrane dryness. Operation mechanism of PEMFC can be seen in Figure 3.8. Membrane serves for electron separation, the released electrons should not pass directly through the electrolyte which causes a short circuit. The catalyst layers speed up the reactions and typically consists platinum and is directly applied to membrane surface. Gas Diffusion Layers transport the reactant gases from the gas supply channels to the reaction site and the produced water to the sides.

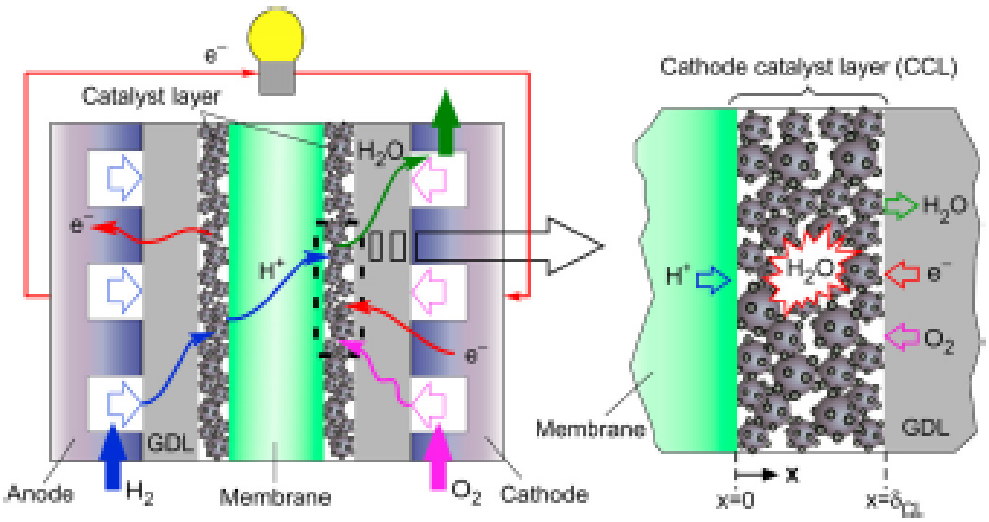

Figure 3.8: Operation schematic of PEMFC, (Das et al., 2010)

The redox reactions occuring in the PEMFC are given below:

Oxidation at anode: $H_2 \longrightarrow 2\,H^+ + 2\,e^-$

Reduction at cathode: $2\,e^- + 0.5\,O_2 \longrightarrow O^{2-}$

Overall reaction: $H_2 + 0.5\,O_2 \longrightarrow H_2O$

FC stack can only operate if the conditions have been provided by the auxiliaries, such as fuel processor, thermal management units, air compressor and humidifier to process inlet air which are to be fully regulated with electrical and control techniques. Moreover, the overall system efficiency and power consumption changes are beyond ignorable. Hence, the modelling of the auxiliary is beneficial for accurate modelling.

In this study, modelling of the fuel cell system only describes the basic electrochemical performance of an FC stack excluding the auxiliary operations due to complexity and the time limitations. On the other hand, the fuel delivery system and the control system have been modelled with consideration of the utilization ratio, fuel supply pressure, fuel composition and volumetric flow rate. Fuel cell stack modelling has been created through customizing the generic Simulink PEMFC model, which is significantly accurate modelling through white-box methodology thanks to complex non-linear model reflecting the physical behaviour of the system based on first principles (Souleman et al., 2009). The equivalent circuit of the model is given in Figure 3.9, open circuit voltage (E_0), exchange current (i_0) and Tafel slope (A) are the dynamic parameters depending on flow rates, pressure, compositions and temperature to determine voltage (V_{fc}) and current (I_{fc}) of the fuel cell. The chemical dynamic of the system has been expressed with a transfer function embodying Tafel slope and exchange current. Dynamic response time (T_d) of the system has been included with delay function for the error calculation.

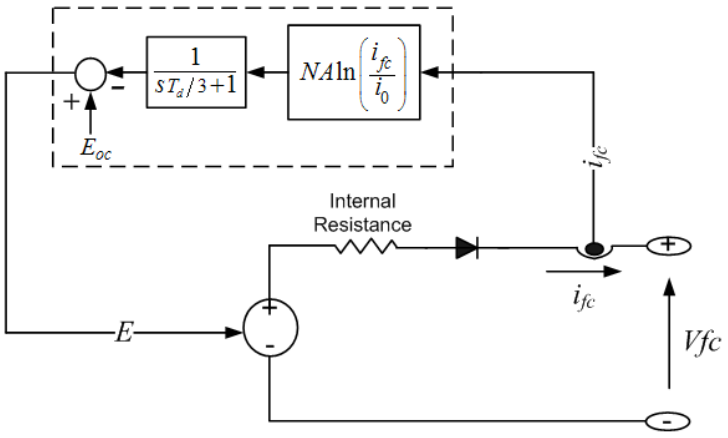

Figure 3.9: Equivalent circuit model of the PEMFC

Mathematical framework of the model is described as following.

- ***Open Circuit Voltage***, where K_c is voltage constant depending on exchange current and Tafel slope.

$$E_{oc} = K_c E_n \tag{3.6}$$

  - ***Nernst Voltage***

$$E_n = 1.229 + (T - 298)\frac{-44.43}{zF} + \frac{RTln(P_{H_2}P_{O_2}^{0.5})}{zF} \quad \text{when} \quad T \leq 100C \tag{3.7}$$

  - ***Partial Pressures***

$$P_{H_2} = (1 - U_{f_{H_2}})x\%P_{fuel} \tag{3.8}$$

$$P_{O_2} = (1 - U_{f_{O_2}})y\%P_{air} \tag{3.9}$$

  - ***Utilizations***

$$U_{f_{H_2}} = \frac{60000RTN_c i_{fc}}{2Fx\%P_{fuel}V_{lpmf}} \tag{3.10}$$

$$U_{f_{O_2}} = \frac{60000RTN_c i_{fc}}{4Fy\%P_{air}V_{lpma}} \tag{3.11}$$

- ***Exchange Current***

$$i_0 = \frac{zFke^{-\Delta G/RT}(P_{H_2} + P_{O_2})}{Rh} \tag{3.12}$$

- ***Tafel Slope***

$$A = \frac{RT}{zF\alpha} \tag{3.13}$$

- ***Fuel Cell Voltage***

$$V_{fc} = E - i_{fc}R_{int} \tag{3.14}$$

Few assumptions made for the model development. The gases were treated as ideal, where as uniform temperature distribution across the stack was considered. Humidification of the membrane was thought to be managed under any load condition. Mass transport related voltage drops were treated as reaction kinetics driven and the internal resistance of the stack was always constant. The fuel and air supply have been assumed to be always available and at desired condition, hence the tank system was not modelled as well which can bring other dynamic considerations, such as weight, conditioning and piping.

White-box methodology describing the complex physical and chemical phenomena with mathematical relations requires many specifications, as seen from the equations, which needs to be extracted from a data-sheet which can be daunting, if experimentation is not possible. In this project, SuSy500 PEMFC providing 500 W maximum power, has been preferred by the design engineer of the analysed power-train. The data-sheet of the PEMFC is given in Table C.1 with the processed information for modelling, Figure C.1. The performance curve of the component has been shared by the manufacturer which significantly matches with the polarization curve generated through simulation of the fuel cell, as shown in Figure 3.10. The deviation of the experimental curves from the model driven curves are increasing at the partial loads, which can be improved via more accurate modelling of likely to be caused by the change in the internal resistance.

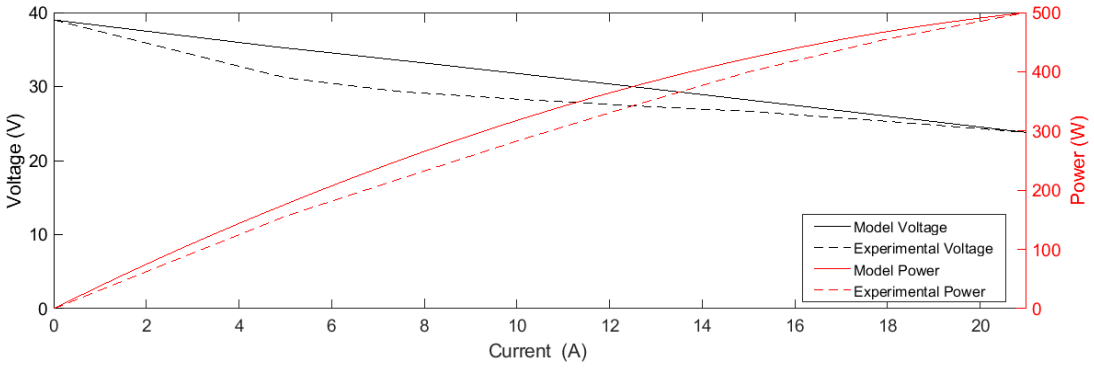

Figure 3.10: Comparison of the experimental polarization curves (dashed lines) and model driven polarization curves of the PEMFC (lines)

Finally, it should be noted that despite the successful modelling of the fuel cell, this model does not reflect the performance of the fuel cell in long term, in other words degradation was ignored which is one of the significant challenges of the fuel cell systems. On the other hand, this study focuses on the capital cost and performance delivery at the initial design stage. Moreover, the fuel expenditure of the power-train can still be estimated, which is one of the major operational cost.

Fuel Delivery System

The power management system sets the fuel cell current for the desired operational performance. The load of the system is directly connected through physical connection ports and the fuel cell is designed to supply

whatever load is on the equivalent electric circuit of the bus due to model assumptions. Hence, the fuel flow to the fuel cell stack has been controlled to achieve management decisions for current production. The fuel delivery has been modelled, as described in (3.15) with assumption of constant utilization ratio of Hydrogen, which is indicated as 4.5 slpm at 500W production in the data-sheet, corresponding to 0.8 utilization ratio for 2 bar fuel supply. This assumption suggests that the fuel consumption will be estimated greater than the actual performance, since the efficiency of the stack is lower at maximum generation point.

$$V_{lpmf} = \frac{60000RTN_c i_{fc}}{2Fx\%P_{fuel}U_{f_{H_2}}} \tag{3.15}$$

Although the fuel cell has a very agile response rate of just a second, it is not realistic to consider the fuel delivery system can adjust itself that sharply, hence the fuel cell stack. Coupling the Susy500 fuel cell with considerably large battery, neeoRACK to be explained in the following sections, utilizes a fast dynamic response of the battery on the order of milliseconds to compensate fuel delivery system and fuel cell reacting in few seconds to a minute and slow warm-up time of fuel cell. Therefore, the modelling of the fuel delivery system is acceptable for this configuration.

3.3.2 DC-DC Converter

Designed bus voltage for the power-train is 48 V with a fluctuation contingency of 20% thanks to wide range battery and design of electric motor controllers to regulate the pulse width modulation for the motors. However, the output voltage of the fuel cell system needs to be brought to 48 V level which provides 39 V under no load conditions as a highest voltage. Hence, the converter is essential for implementation of the fuel cell to the power-train and also protecting the fuel cell from the voltage and current ripples due to transient loads. The voltage regulation can be managed either with linear regulators or switch mode power supplies, SMPS. Linear regulators controls the output voltage through dissipating excess power in Ohmic losses. Hence, the linear regulators are applicable for voltage drops, whereas SMPS uses a switching regulator which has a power transistor, such as MOSFET, IGBT, operating in its switching mode at a high frequency between on and off which can serve for increase and decrease of the voltage according to the topology. Thus, deployment of a SMPS is mandatory for the specific operation in the analysed power-train to boost the fuel cell voltage to the bus voltage. Moreover, SMPS are replacing linear regulators in almost all modern applications with their higher efficiency thanks to the reduced power dissipation, smaller size and weight. Frequently used taxonomy for SMPS is based on the electrical insulation of the inlet and the outlet of the converter, as listed in Table 3.2 with heuristic power application range. An isolated DC-DC converter has a high frequency transformer providing a barrier withstanding anything from a few hundred volts to several thousand volts and the ability to provide multiple outputs. However, isolated systems are significantly much complex and expensive than non-isolated systems.

The preferred PEMFC, SuSy500, has been coupled with a 1500 W SM5567, wide range DC-DC Converter with ohmic insulation at both ends, in other words a full bridge SMPS, due to the business partnership of

the companies. Full bridge converter uses 4 switches and spreads the stress across them which is useful at high power but it is an unnecessary complication at a low power.

Table 3.2: **SMPS Topologies**, (Billings and Morey, 2011)

Non-Isolated	
Buck Converter	$V_{inlet} > V_{outlet}$
Boost Converter	$V_{inlet} < V_{outlet}$
Buck-Boost Converter	$V_{inlet} < (or >) V_{outlet}$
Isolated	
Fly Back	$< 200W$
Forward	$< 300W$
Push-Pull	$< 500W$
Half Bridge	$< 1kW$
Full Bridge	$< 2kW$

For low voltage inputs, such as 48 V in this case, full bridge is not optimum as limiting switch stress to 48 V is unnecessary. The most important advantage of the full bridge converter is possibility to operate at four quadrants with the motor, i.e. forward and reverse driving with regenerative braking. However, the design purpose of the power-train, which is only at first quadrant, does not align with such a complex operation. Hence, SM5567 is always operated at first quadrant with a low average load profile according to the analysed drive cycle which can be plausibly modelled as a simple boost converter. Moreover, the high capacity battery enables safe allocation of a non-insulated boost converter, since the battery is fast responding to any transient load which has been foreseen by the simulation and never gets to a point for power break by the transformers. Due to redundantly complex structure of the desired full bridge converter SM5567, shown in Figure D.1, which requires much more time and expertise, in this study fully elaborated boost converter and it's closed loop dynamic control have been designed which can simulate the performance of SM5567 for the design purposes.

When designing a converter, typically design criteria favours a SMPS over linear regulator. However, selecting the right topology for a SMPS can be difficult to meet cost, efficiency and performance targets. For the matter of interest hybrid power-train, initial design decision has been made as a DC-DC boost converter, the model configuration is shown in Figure 3.11, under the explained conditions of the power-train and its operation. The available information for the design of the converter is the polarization curve of PEMFC stack and nominal voltage of the bus. The converter should be able to provide a stable voltage in range of $48 \pm 9.6V$ with floating DC source of PEMFC to a bus under dynamic load. Too low and too high frequency current ripples limit the operational life and the general efficiency of the fuel cell, hence sizing of the components of the converter and efficient control is essential. Low output voltage ripple is hoped to improve converter

operation in a continuous conduction mode, hence an inductor is placed to suppress current ripples and a capacitor to filter out voltage ripples at the outlet. Reaching high efficiencies, over 90% allows smaller and lighter converters with a low temperature rise and a greater system reliability.

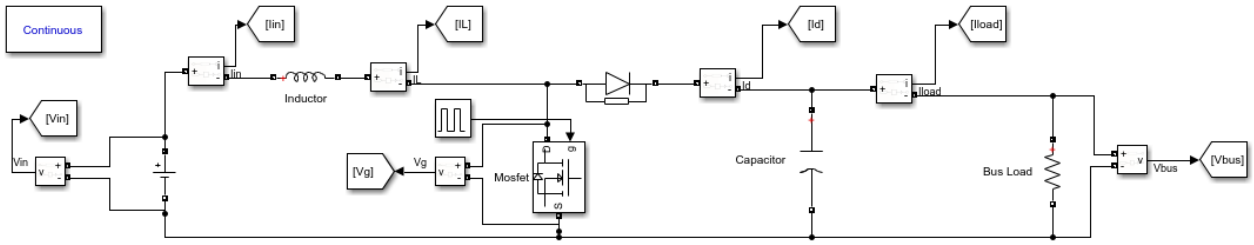

Figure 3.11: DC-DC boost converter configuration under open loop control

Despite the fuel cell being not an ideal DC source with varying voltage output according to the load, EMS, sizing of the converter components and the capacity of the power-train components have been utilized to obtain plausible performance and handle fluctuations. The converter was designed to be always in the continuous conduction mode, in other words the inductor current will never reach zero in the period of time. For nominal input current and voltage of the fuel cell has been used for the calculations and the efficiency of the converter, η_c has been assumed as 90% and the maximum input voltage is the no load condition of the polarization curve of the fuel cell, $V_{in,max}$. The high limit of the duty cycle, as in(3.22), has been set as 0.7 in line with the suggestion of heuristics to preserve the converter efficiency.

- **Resistor implementation to simulate the bus load**

$$P_{in} = V_{in} I_{in} \tag{3.16}$$

$$P_{out} = P_{in} \eta_c \tag{3.17}$$

$$I_{out} = P_{out} / V_{out} \tag{3.18}$$

$$R = (V_{out})^2 / P_{out} \tag{3.19}$$

- **Duty cycle limits**

$$D = 1 - V_{in} / V_{out} \tag{3.20}$$

$$D_{min} = 1 - V_{in,max} / V_{out} \tag{3.21}$$

$$D_{max} = 0.7 \tag{3.22}$$

Operation at high frequencies causes higher loss in the switches, on the other hand the size of the inductor can be reduced to achieve desired range for the current ripple. A real inductor functions as an inductor with a resistance, hence as the loss of the circuit decreases at a greater extend with high frequencies. The switching frequency, f_c, has been determined as 10 kHz for SM5567, hence it has taken same for the boost converter design without search for optimum frequency.

- **Turn-on time of the transistor**

$$T_t = 1/f_t = 100\mu s \tag{3.23}$$

$$t_{on} = D_t \tag{3.24}$$

Inductance limits the rate of the current increase and decrease, thus larger the inductor smaller the ripple. Yet, the larger inductor causes higher cost and power loss at the same time. It was assumed that current ripple has to be less than 10% to protect the fuel cell and 20% design contingency devoted to the inductor.(Targoński, 2006)

- **Inductor design**

$$< i_L >= I_{out}/(1-D) \tag{3.25}$$

$$\Delta I_L = 0.1 I_{in} \tag{3.26}$$

$$L = 1.2(V_{in} t_{on}/\delta I_L) \tag{3.27}$$

$$I_{L,max} = I_L + \delta I_L/2 \tag{3.28}$$

$$I_{L,min} = I_L - \delta I_L/2 \tag{3.29}$$

The power transistor enables high switching speed, therefore helps to reduce the size of the circuit. MOSFET has been chosen, due to nanosecond switching capability, large gate resistance, low conduction losses and simple design. The information of peak current, peak voltage and the switching frequency are needed to choose right MOSFET, hence the rms current has been calculated.

- **Power switch constraint**

$$I_{s,RMS} = \sqrt{(1/T)\int_0^T i_{fc,max}^2(t)dt} = \sqrt{\frac{1-D}{2}} i_{fc,max} \tag{3.30}$$

The diode needed is a middle power device, because the current through it will be only some amperes. The diode chosen has very low inner resistance and assumed to have fast recovery time.
Capacitor is a voltage buffer, a larger capacitor is deployed for smaller voltage ripple at the outlet. When the switch is open, part of the inductor current charges the capacitor. The voltage ripple at the outlet restrained to be 1% for this design assumptions, since the ripple will be higher for sure with the floating load and input.

- **Capacitor design**

$$I_c = C\Delta V_c/DT \tag{3.31}$$

$$\Delta V_c = 0.01 V_{out} \tag{3.32}$$

$$C = I_{Load} t_{on}/\Delta V_c \tag{3.33}$$

The gate driver for the MOSFET has not been physically modelled, rather the gate control has been managed with boolean signals from the converter controller. In order to analyse performance of the converter, shown in Figure 3.11 in terms of open loop control, based on a constant duty cycle calculated through (3.20), and validity of the continuous conduction mode assumption, the converter has been simulated under maximum and minimum constant load conditions. The maximum load simulation results are given in Figure 3.12. The converter was tested at nominal fuel cell voltage of 26 V, hence the duty cycle was 0.46 for bus voltage of 48 V.

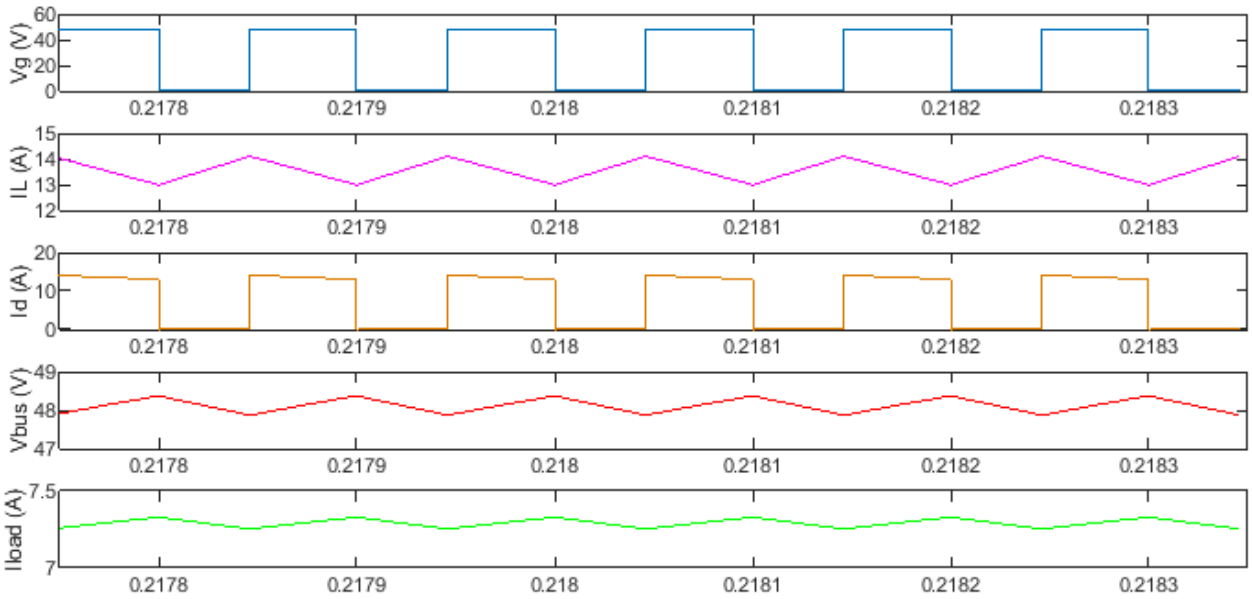

Figure 3.12: Steady state waveforms at high output power

The simulation results proves that the design of the converter was adequate and the operation was in continuous conduction mode, since the inductor has never experienced zero current. The simulations demonstrate the well selection of the circuit parameters. Moreover, the inductor current ripple was even lower than 10%. The simulation has been conducted in continuous mode powergui which takes significantly high computational effort, which needs to be eliminated for complete power-train simulations which includes much more complex physical and digital systems. On the other hand, the competence of the system should be proven for sudden and strong long changes. For that purpose transient load simulation with step pulse has been implemented to the load with a circuit breaker, as shown in Figure 3.13 and the performance of the converter, shown in Figure 3.14. The step pulse suddenly doubles the load on the converter and reaches to the peak load with adding parallel resistance.

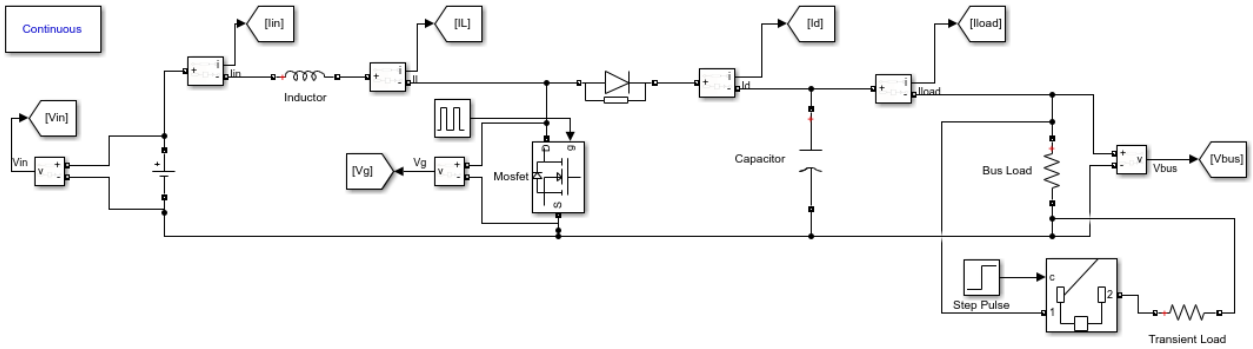

Figure 3.13: Configuration of the boost converter under transient load

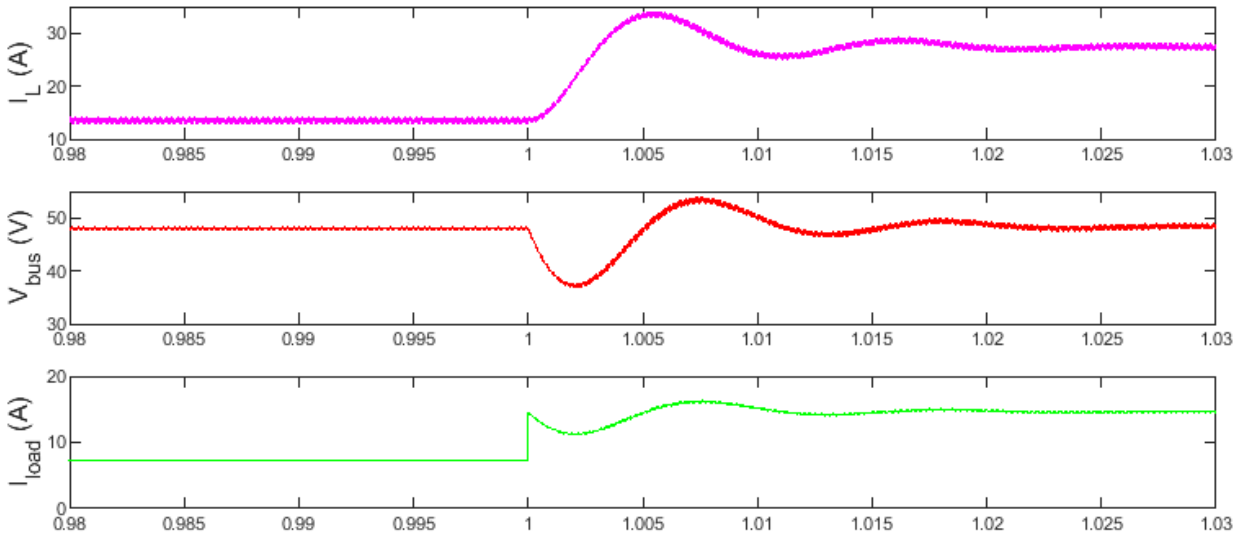

Figure 3.14: Performance of the boost converter with open loop control under transient load

The open loop control fails to pertain desired performance under extreme conditions, such that the bus voltage ripple should be further suppressed. Hence it has been concluded that design of a closed loop control with varying duty cycle is beneficial.

Closed Loop Control Design for DC-DC Converter

The converter must be regulated to provide the desired output voltage which is acquired via actuating the converter switch according to the duty cycle. Depending on the control configuration, the controller might have the reference of fuel cell current, the output current, the output voltage and the bus reference voltage. The control system has to protect power components such as switches which are sensible to over-current, hence the fuel cell current should be controlled. Moreover, under load transients with fast responding power train, over-voltages and over-currents could appear. Since the power-train has a high level supervisory control

through EMS regulating the FC current, the control of the converter is based on voltage mode which only controls the output voltage. The need for a closed loop control system capable of dynamically adjusting the duty cycle has been proven for the FCHEP under transient loads. The control system has been chosen as PI due successful applications seen in the literature review. Differential component of PID control systems is useful to obtain future based control, such that it improves stability and decreases overshoot. However, in this specific application differential component needs to be avoided, otherwise system will be demonstrating extreme noise, since the differential component takes action according to the trend of the variable which is pulse width modulation and it is highly steep and dynamic. Proportional and Integral components of the control system focus to adjust errors of the system with respect to present and past behaviours. Designed control system is shown in Figure 3.15, basically the system compares the reference voltage and measured voltage of the bus and compensates the difference through adjustment in the duty cycle. Saturation block has been used for duty cycle results to protect the circuit components and maintain the safe operation, as decided in (3.21) and (3.22). The gate pulses have been created according to comparison between repeating sequence of 0-1 pulses with 10 kHz frequency and control pulses from the PI controller.

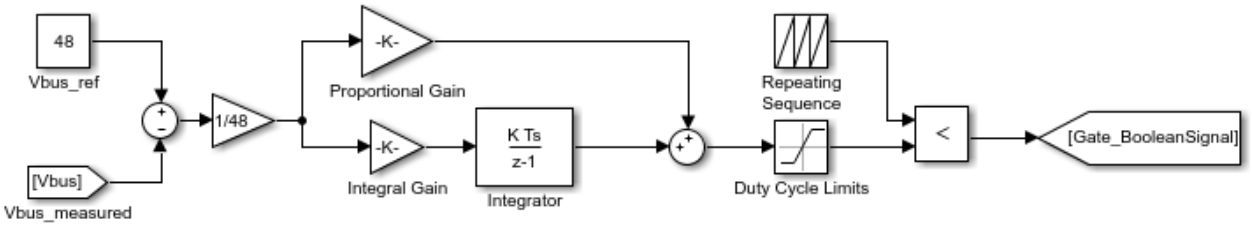

Figure 3.15: PI control system of DC-DC converter

For tuning the control system two different methods have been applied. Firstly *Ziegler-Nichols* ultimate gain method has been tried for a control system directly connected to the equivalent electric circuit of the converter. The gain for the proportional controller is increased to reach stability limit for the closed loop system. Although this method was able to reach 48 V mean bus voltage under the transient load, the response ripple margin was too high that it was not preferable over open loop control of the converter. Hence, Simulink PI Tuning module has been utilized and for that reason, firstly the *system identification* was made to obtain the transfer function of the closed loop system. The system identification is based on a step response of the system which has offset of the mean duty cycle. The identification has been tweaked for an under-damped pair of complex-conjugate poles, $\frac{K}{(T_\omega)^2 s^2 + 2\xi T_\omega s + 1}$ as shown in Figure D.2. The transfer function of the designed DC-DC converter operating with ideal DC voltage source to maintain 48 V output was approximated as (3.34).

$$G_{converter}(s) = \frac{(2)10^6}{9s^2 + 1920s + 10^6} \tag{3.34}$$

Tuning of the proportional and integral gain parameters have been done through dynamic simulation for optimized results, reference tracking and control effort comparison of the system response with and without

tuned control have been shown in Figure D.3. In order to test the capability of the tuned PI controlled DC-DC converter, the same transient load conditions have been applied with a circuit breaker and the load on the bus has been doubled at 1 second with an added parallel resistance. The response of the system is shown in Figure 3.16 which has more robust control after first over-shoot which is slightly less than of open loop control for the bus voltage. Elaborate measurement of the step response of the system for the transient load has been shown in Figure D.4 and the mean system voltage has been detected as 47.8 V which is significantly precise.

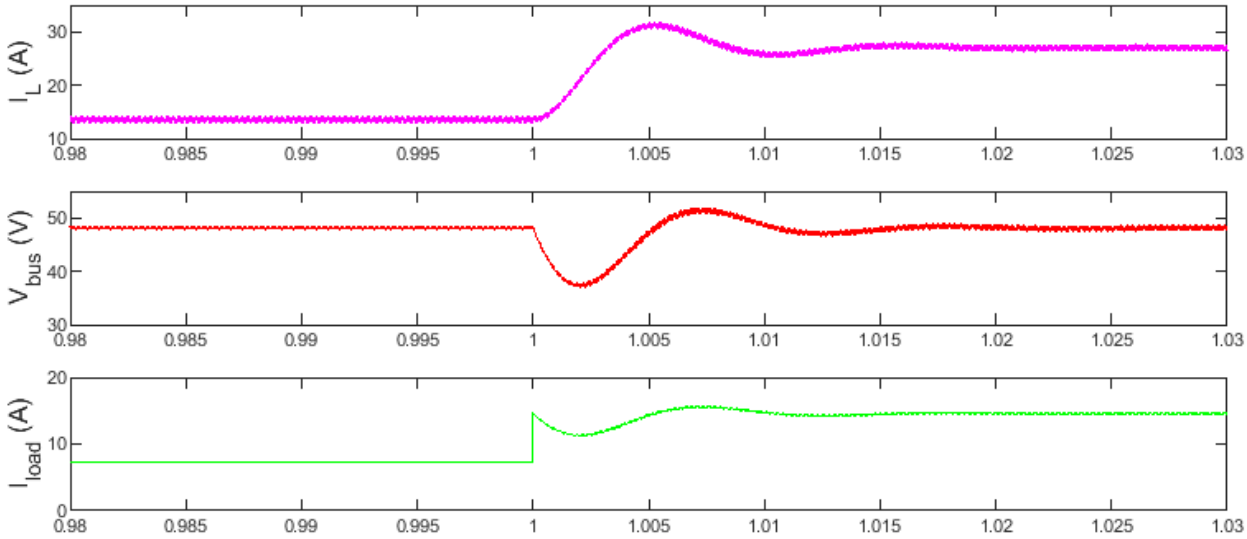

Figure 3.16: Performance of the boost converter with closed loop control under transient load

Determination of Simulation Solver and Powergui

As mentioned earlier, the computational effort for continuous simulation is too high and takes significant amount of time. Hence, discretization is compulsory to get the results for a drive cycle with high transient load in reasonable amount of time for computation, specially for the complete hybrid energy supply unit modelled with equivalent circuits. Powergui is an environmental block for Simscape electrical specialized power system models and mandatory to deploy. It stores the equivalent Simulink circuit that represents the state-space equations of the model. When setting the sample time for discretized powergui, the frequency of the pulse width modulation is the main parameter to set the resolution of the simulation. For the simulation, 0.5% resolution has been preferred to preserve model accuracy which corresponds to 2 MHz sampling frequency for 10 kHz pulses. Three different discrete solver option of powergui has been evaluated based on standard Tustin method; interpolation, time-stamping and base. Even though interpolation method reaches significantly accurate results at much lower sampling frequencies, it requires continuous simulation solver at supervisory level. Therefore, it has not been chosen. Whereas time-stamping requires allocation of time-stamping system before the gate to compute delays on and delays off for the pulse signal. However, time-stamping system

overcomplicates the process for system identification and does not improve the model resolution considerably in comparison to base Tustin discretized method.

The responses of the closed loop PI controlled DC-DC converter under step disturbance with continuous and 2 MHz discretized powergui have been given in Figure 3.17. It is clear that the discretization has been successful in terms of resolution with almost identical matching with continuous computation and decreased computational effort, approximately 20 times faster. Therefore, the simulation has been decided to run with a fixed-step discrete simulation solver and a discrete powergui with base Tustin method at 2 MHz.

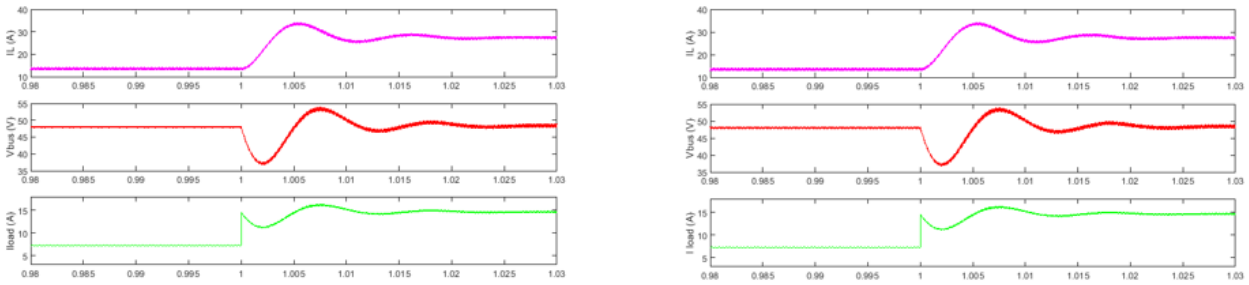

Figure 3.17: Step response of the converter with Continuous Powergui (left) and Discrete Powergui (right)

3.3.3 Battery

Designed FCHEP deploys 5 kW battery which has 10 times more power supply capacity in comparison to the fuel cell. Such choice has been made to secure performance delivery, to obtain more flexibility with a powerful floating energy supply and to extend the error margin, since this project is the first work of the group and will be proof of the concept. The battery specifications are given in Table 3.3 and the detailed data-sheet is given in Figure E.1.

Table 3.3: **Battery specifications**

Model	neeoRack
Chemistry	Li-ion
Nominal Power	5 kW
Nominal Voltage	48 V
Maximum Power	16.5 kW
Voltage Operation Limits	37.8 V-58.8 V
Nominal Capacity	106 Ah
Response Time	1 s
Operation Temperature	0-40 °C

Lithium-ion battery provides a high energy density and reliable charge-discharge performance without the

memory effect which makes them highly preferable for transport applications. On the other hand, there are disadvantages of the Li-ion batteries as well and from EMS point of view, fidelity for the battery limits for charging and discharging are the most important for safety reasons. Main working principle is based on transfer of lithium ions in between positive (lithium-cobalt oxide) and negative (graphite) electrodes to produce or store energy. In both cases, electrons flow in the opposite direction to the ions, moving in the electrolyte which is an effective insulating barrier for electrons, around the outer circuit. It is important to notice that the battery is not a power generation device, it only releases the energy which has been stored in advance. The battery has been modelled as a controlled voltage source with a constant internal resistance, as shown in Figure 3.18. The voltage control is based on the charge and discharge dynamics of the pack. In order to prevent algebraic loops in the model, delay simulation has been made with low pass filter for output voltage calculation. The internal resistance was assumed as 1% of the nominal power and kept constant for charge and discharge operations. The self discharge could have been included as parallel resistance, however lack of empirical data could have resulted with misguiding model, hence the phenomena has been neglected. Although temperature and ageing effects may have important effects on the performance, they have been ignored to avoid model complexity and high computational effort. However, this model is still detailed enough to demonstrate relation between current and voltage in wide range of state of charge which satisfactorily serves for the purpose of the thesis.

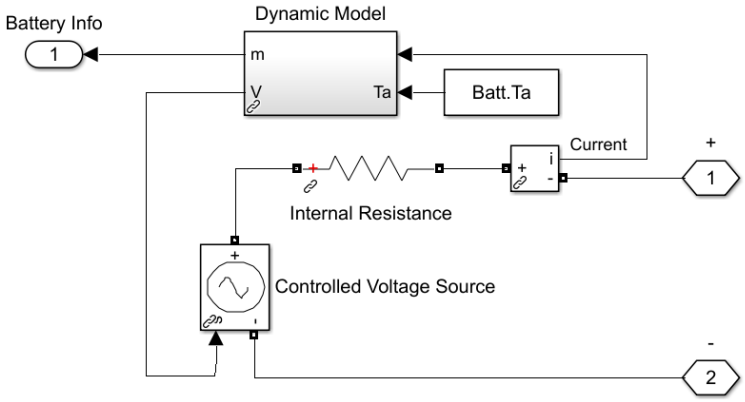

Figure 3.18: Model configuration of the Li-ion battery

Dynamic relations to find the charge and discharge curves are as follow, (Zhu and Li, 2013).

- **Battery voltage,** V_{Bat}

$$V_{Bat} = E_{Bat} - R_{int} I_{Bat} \tag{3.35}$$

- **Open circuit voltage for charge and discharge,** E_{Bat}

$$E_{Bat} = \begin{cases} E_0 - K\dfrac{Q}{Q-it}i^* - K\dfrac{Q}{Q-it}it + Ae^{-Bit} & \text{when} \quad i^* > 0, discharge \\ E_0 - K\dfrac{Q}{0.1Q+it}i^* - K\dfrac{Q}{Q-it}it + Ae^{-Bit} & \text{when} \quad i^* < 0, charge \end{cases} \tag{3.36}$$

- **State of charge**

$$SOC(\%) = 100(1 - \frac{1}{Q}\int_0^t I_{Bat}(t)dt) \tag{3.37}$$

Discharge curve under nominal conditions of the modelled battery have been given in Figure 3.19. An exponential voltage drop occurs when the battery is in the charge saturation limits whereas the middle region painted in gray represents the region when battery provides robust performance till the battery nominal voltage. The total discharge of the battery results with the sudden voltage drop occurring after the nominal discharge voltage. In the second plot, relation between discharge current and battery responses have been demonstrated. As expected, the larger loads resulting with larger current withdraws causes the battery to last less. Since the empirical data for discharge at a certain current was not available, the model could not be validated. On the other hand, the behaviour of the model is in the plausible intervals and matches with similar applications.

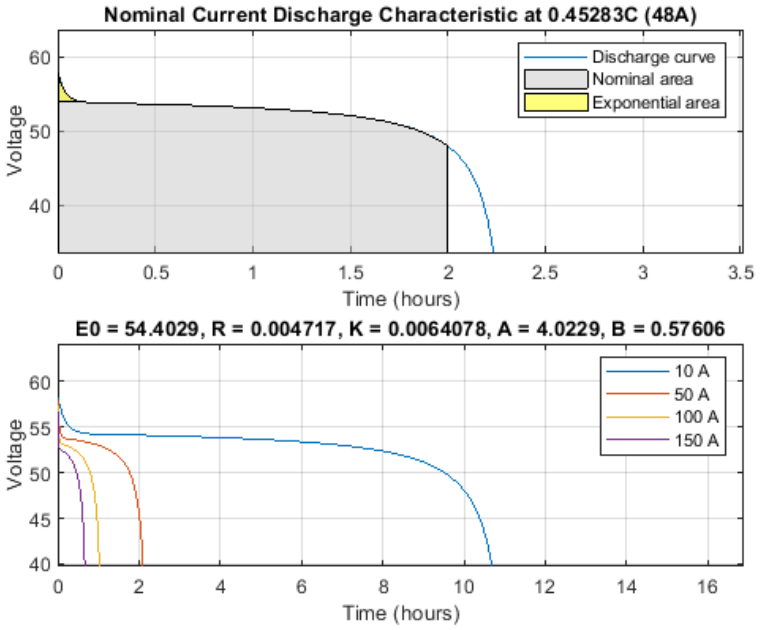

Figure 3.19: Discharge curve of modelled battery for nominal current (up) and various currents (down)

Battery charge and discharge limit characterization based on empirical data has been provided by the supplier. The curves have been embodied in the energy management system to ensure safe operation of the power-train. The limiting currents for certain depth of discharges have been drawn in Figure E.2.

3.3.4 Electric Motor

Attention has priorly been drawn on the efficiency and clean operation of the electric motors in the literature review. The modern diesel engines reach up to 50% efficiency which is still significantly under-performing in comparison to the electric motors reaching 95% with very efficient energy converters. Moreover, the maximal

torque can still be produced at the still state which makes the application less demanding on the nominal power. For the FCHEP application, brushless permanent magnet motor (BLDC) has been preferred.
BLDC motors does not directly operate from a DC voltage source, however basic principles of working are similar to a DC motor. BLDC is constructed like any other motor with a stator and a rotor. Rotor has permanent magnets, whereas the stator has coil windings, essentially like a DC motor turned inside out. The main physical phenomena is the interaction of magnetic field between coils and the magnets create the torque and hence the rotation. The magnets rotate around a fixed armature which eliminates the need for the brushes and commutator to connect the current to a moving armature. The current in the armature is electronically commutated through external circuit to control the rotation, as shown in Figure 3.20. The motor controller has generally three pairs of coil and at an instant two pairs of coil are powered which repels the rotor magnets and position of the magnet have been measured by Hall effect sensors to be processed by the controller. The controller provides triggering pulses to the electronic switches which magnetizes the stator and the rotor magnets rotates accordingly.

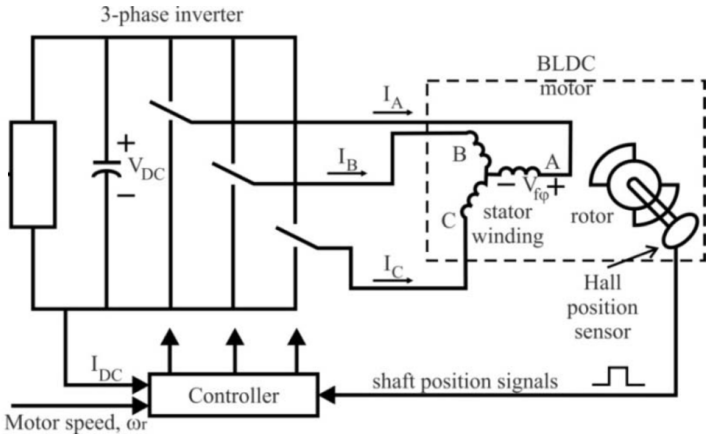

Figure 3.20: Outlook of a BLDC, (Gamazo-Real et al., 2010)

Despite the complexity of the electronic control, BLDC provides very long maintenance-free life, a smooth and silent operation, improved safety with spark-free operation, reduced electromagnetic interference and much smaller size, up to one third. Specifically for this power-train application of the pleasure boat, the reduced size and silent operations benefits were main driving force for the decision. Electric motor of the power-train is a 3 kW Golden Motor with nominal 4000 rpm. The motor performance data has been provided by the manufacturer, shown in Figure F.1 in a detailed fashion to map the whole performance interval with the complementary assumptions. In such a lucky case for a modeller, black-box modelling can be applied under the condition that performance limits and safety measures are taken without getting involved with the differential equations which always bring a margin of error even for the best modelling performances. Moreover, models embedding the explanation of the physical phenomena requires specific and detailed information, such as copper resistance, inverter circuit elements, static inertia coefficient and many

others. Since neither of those specifications has been provided nor testing of the component to extract these parameters was possible, the most appropriate decision was relying on the manufacturer performance data. Electric motor mapping has been developed as shown in Figure 3.21.

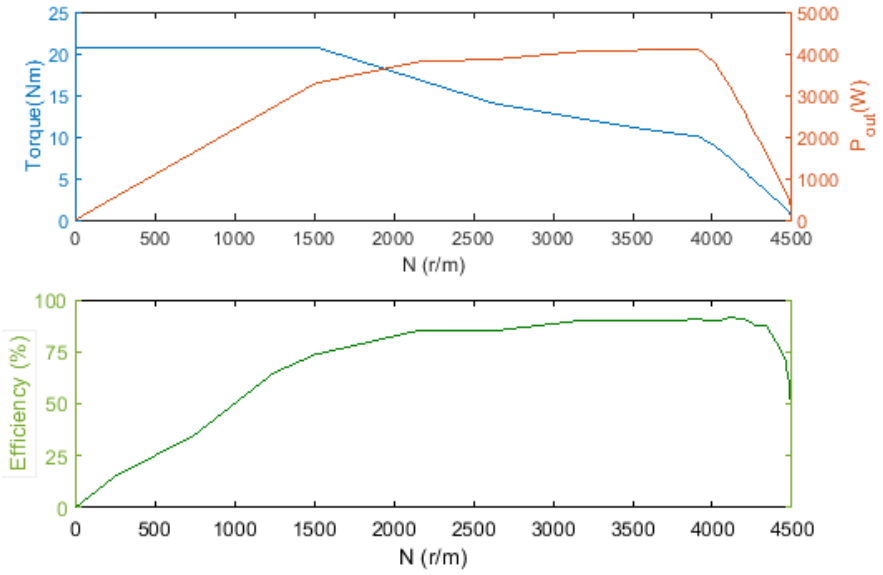

Figure 3.21: Performance map of the BLDC motor

As it can be noticed from the map as well, a BLDC has a parabolic efficiency curve suggesting that there are two torque-rotational speed couples for a single efficiency. Hence, the corresponding speed or torque should be known to find the efficiency under a certain load. For that reason propeller power curve needed to be embedded in the simulation to find the rotation of the shaft.

Propeller Power Curve

Boat speed is a function of the angular speed of the propeller, size of the propeller and the blade arrangement. It is intuitive that a propeller with larger and more blades requires more power for rotation. An undersized propeller cannot use all the energy produced by the motor, whereas an oversized propeller requires more power than what engine can provide. Hence, sizing and design of the propeller for the specific motor are important and require detailed calculations. An initial step for such a design problem is to plan the cruise performance. Feasible combination of the cruise speed and motor mechanical load have been based on the empirical curves relating vessel type, displacement and speed. Gunkan Curve and design optimization curves developed by Japanese navy for power boats are shown in Figure F.2.

It is necessary to relate the required output power for the transmission system to the propeller rotation speed. The output power from the motor is absorbed by the transmission system load and the boat speed corresponds to the thrust created by the propeller rotation. The rotating shaft transmits the power and the rotation speed. The torque of the motor and the end of the propeller shaft should be same, yet both of these

components have their own torque-rotational speed characteristics. For a constant torque, the output power at the motor side is proportional to the rotational speed. Besides, torque at the propeller side changes with respect to density of the fluid, rotational speed and diameter of the propeller. For a propeller of a given size, on a particular boat, the relationship between the power needed to turn the propeller at a certain angular speed has been modelled by Crouch speed prediction formula, given in (3.38) (Gerr, 1989), (Umeda and Shimizu, 2015).

$$P_{mload} = \gamma N^n \tag{3.38}$$

Propeller power curve describes the relation between required motor power output for the transmission system and rotation of the shaft. So that, with the information of the load on the transmission system, the angular speed of the shaft can be approximated through the propeller curve. The exact value of constant n can be found through analysis of the hull and propeller, however it is beyond the scope of this thesis. *Gerr* has concluded upon many experiments that n falls in between 2.2-3 and for an average performing boat. *Umeda* has suggested 3 for power boat applications. Using coefficient γ, propeller power curve can be driven. γ is a specific constant for a specific hull and propeller combination. Designation of the operation point for finding an appropriate combination of the motor and propeller is essential. The rated and maximum power and torque of the motor sets the limits for the propeller and motor coupling. However, it is desired to match them at an optimal zone of the motor efficiency map given in Figure 3.21. High efficiency zone should match with the rated power level, hence the maximum efficiency yielding rotation speed has been used to estimate γ. Driven propeller power curve is given in Figure 3.22. Upon market search, Yamaha three-blade with 11-in pitch and 9-in diameter has been spot as a candidate which can yield a similar power curve.

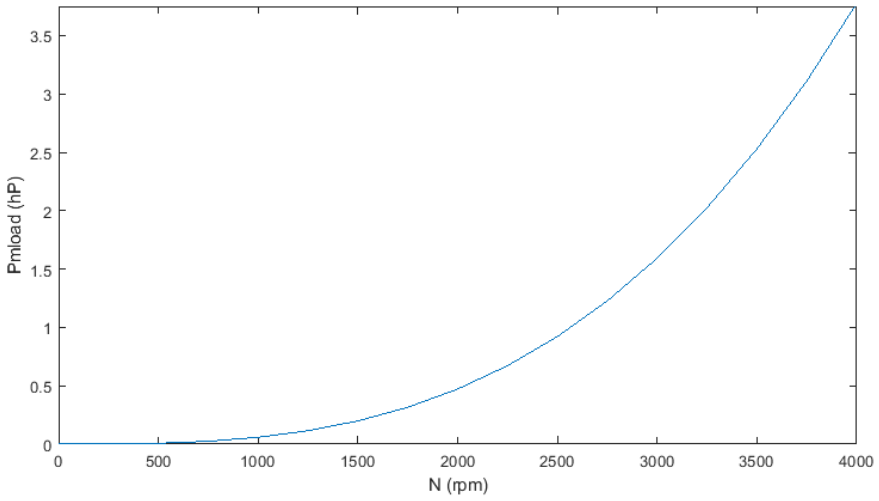

Figure 3.22: Propeller power curve

The motor model serves for two purposes; firstly calculating the available torque that motor can deliver based

on transmission system load and subsequently finding the efficiency for the respective performance demand and secondly using mechanical load on the motor to calculate the electrical load on the energy supply system. With the information of the required rotation rate for the corresponding load on the transmission system according to the drive cycle, the motor model calculates the motor performance and required electrical energy and specific current load based on dynamically measured voltage of the bus.

- **Mechanical load**

$$P_{mload} = \tau\omega \tag{3.39}$$

- **Electrical load on the bus**

$$P_{eload} = \frac{P_{mload}}{\eta_{BLDC}} \tag{3.40}$$

- **Power loss of the motor**

$$P_{BLDC,loss} = P_{eload} - P_{mload} \tag{3.41}$$

- **Current load on the bus**

$$I_{load} = \frac{P_{eload}}{V_{bus}} \tag{3.42}$$

The black box model configuration of the electric motor was given in Figure 3.23. A memory block with a unit delay for measured bus voltage has been utilized to avoid algebraic loops. After the mechanical load has been processed by the model, it is more convenient to call the electrical load, P_{eload} simply as P_{load}, since it is the main load managed by the EMS. The simulation indexing has been done in that manner as well.

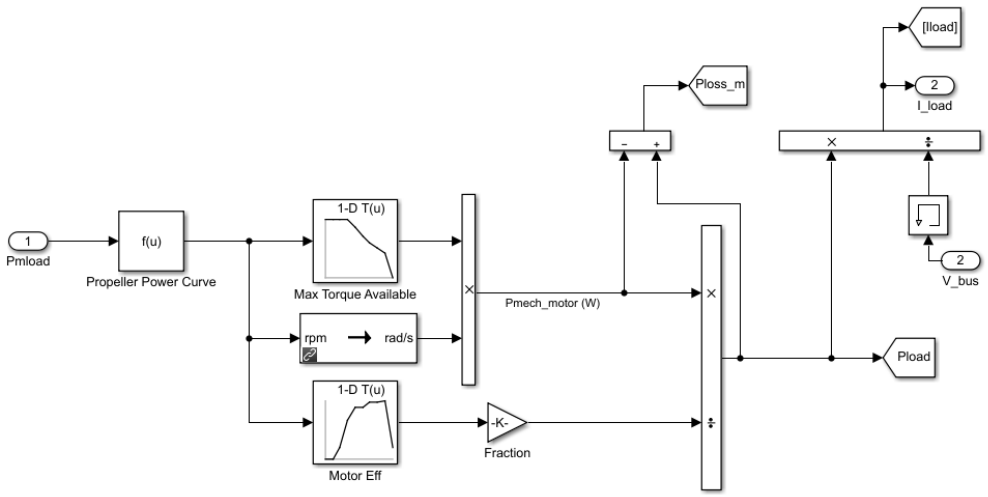

Figure 3.23: Electric motor modelling

When the black-box model has been compared with the white-box model given in Figure 3.21, the clear question emerging is how the energy supply system modelled through equivalent electric circuits could be connected to the algebraic calculations yielding the load on the bus. The connection has been made through

utilizing a controlled current source which has been implemented to the physical modelling as a sink whose modulation is controlled by the black-box modelling of the electric motor.

The electrical load to be managed by the hybrid energy supply system for the interested drive cycle is given in Figure 3.24. When the electrical load has been compared with the mechanical load on the power-train, it can easily be said that the low loads due to drive cycle causes inefficient performance of the electric motor.

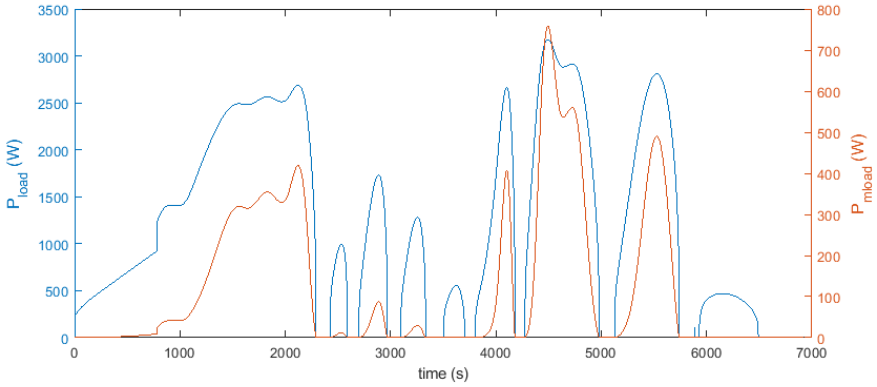

Figure 3.24: Electric load (P_{load}) and mechanical load (P_{mload}) on the bus

Chapter 4

Energy Management Strategy Algorithm

In this chapter, the high level control which determines the reference current of the fuel cell to operate the fuel cell in the most efficient region and meet the performance criteria of the power-supply, will be explained. There are two control systems designed for the power-train. The low-level control for the maintenance of the fuel cell voltage output for the bus voltage suitability and tracking the reference with a minimal error. It rejects the disturbances in the dynamic load under a single degree of freedom: control of the duty cycle, which has been explained in detail in section 3.3.2. Both control systems are compatible with digital control and integrated circuits, such as micro-controller, programmable logic controller or digital signal processors. Updating the control algorithms simply means updating the software and hence both of the strategies are designed to bear in mind the benefits of the digital control.

Hybridization of the fuel cell power-train enables downsizing which improves (i) the fuel economy since the high efficiency operation of the fuel cell can be better matched with the power requirements of the load cycle, (ii) the efficiency of the fuel cell system which requires smaller compressor and causes less parasitic loss, (iii) the propulsion due to the reduced overall weight. Hybridization solves two short-comings of the fuel cell as mentioned earlier: (i) poor dynamic response due to lag in the auxiliary components and (ii) oxygen starvation due to abrupt increase in the current demand which might cause short circuit and dead spots. Moreover, integration of a storage component enables recovery of the regenerative energy, which will not be concerned for this thesis. The need of hybridization arises the need of energy management system to distribute the load between the fuel cell and the battery.

The possibility to store the excess power in an electric hybrid power-train configuration enables an efficient operation. For fuel cell-battery hybridization, an efficient EMS is to allocate the average power delivery to the fuel cell and transient load balancing to the battery. In an ideal case, the average load delivered by the fuel cell corresponds to an efficient operation interval of the fuel cell as well. The design of the power-train

directly affects the design of the EMS. When the fuel cell is the main energy source, the battery is used for the load levelling: the battery is charged when the load is lower than the average, and discharged when higher power is needed than the average. On the other hand, when the fuel cell is placed for range extension, in other words the battery is the main energy source, the fuel cell generally is not capable of delivering the average load. In this case, the fuel cell serves the purpose of providing power and energy to be stored when the battery leaves the confident operation limits to deliver the load.

The modelled application of the fuel cell in the power-train is an range extender, as it can be understood from small ratio of the deliverable power. The target power of the fuel cell is determined with respect to the power requirement of the load and state of charge of the battery. The control of the fuel via fuel delivery system based on the reference fuel cell current, controls the actual power output of the fuel cell. The battery makes up the power difference between the load and delivered power by the fuel cell system and consequently power distribution is attained. The control algorithm should be able to safely start, monitor and shut down the fuel cell under all operating conditions.

The developed EMS has four objectives listed priority-wise as follows:

1. Safe operation of the power supplies: the maximum and minimum current limits of the components should be respected

2. Performance delivery: the load should be met

3. Efficient fuel cell operation: minimization of fuel consumption

4. Longevity of the fuel cell: smooth power allocation to the fuel cell to avoid switch on and off or frequent load changes

The high level controller needs to monitor several dynamic parameters of the power-train and know how the system is behaving in its entirety, to serve a load as shown in Figure 3.24. The high level controller uses a single degree of freedom, $I_{fc,ref}$, to achieve the desired power-train performance. At the low level control, the closed loop controller will focus on its sub-task without any direct correlation with overall supervision. The high level control of the energy management system configuration of the simulation is given in Figure 4.1.

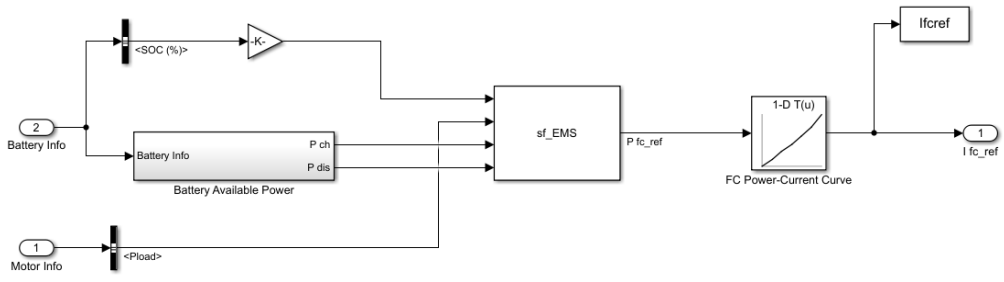

Figure 4.1: Simulation configuration of EMS

The EMS algorithm developed in C environment (see section G.1), was interfaced with a legacy code (see section G.3)in Simulink environment as a s-function block named as sf_EMS in the configuration. The high level control firstly collects the information on the state of charge, availability of the battery for charge and discharge according to battery safety limits, given in Figure E.2, dependent on the instantaneous voltage level and the instantaneous load from the power-train. This information is then assessed according to the power assist-map defined by the EMS algorithm. Since the first priority of the EMS is safety, the algorithm first seeks for the most efficient point of operation and the operation point reference is given after evaluation of the compatibility of that point with respect to the availability of the battery for safe operation. If the operation point is not eligible, the reference is incrementally increased or decreased until it fulfils the criteria. The power distribution reference always ensures safe operation and maximization of the efficiency for the required performance. The fuel cell does not run on the "thermostatic control" mode which simply turns the fuel cell on and off in case of need for the back-up power, because it is significantly inefficient and considerably reduces the life time of fuel-cell. The EMS is capable of switching the device on and off, in case of need, e.g. a violation of the safety margin for operation, otherwise the fuel cell keeps operating as efficient as possible. Matrix of the operation with respect to the fuel cell load is described in Figure 4.2.

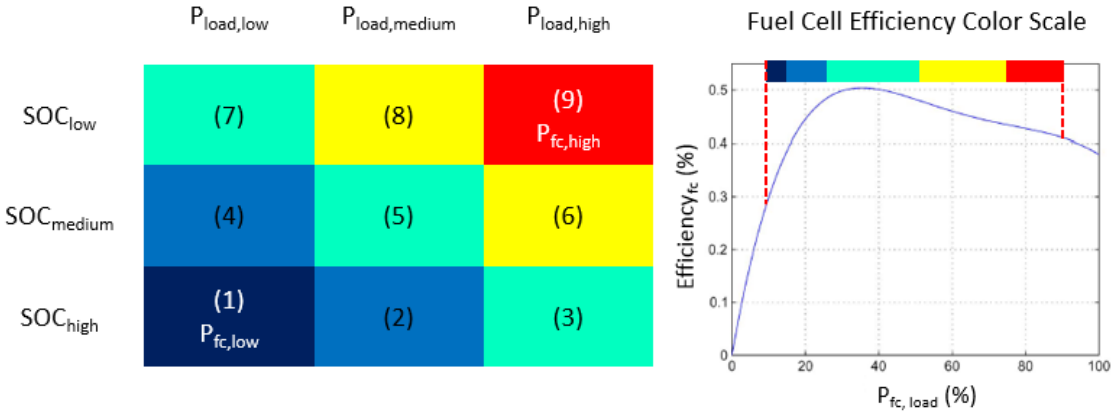

Figure 4.2: Energy management strategy from efficiency point of view

As seen in Figure 4.2, the optimum condition for the fuel cell operation is around 40% of the maximum power generation, which corresponds to 200 W for SuSy500. The maximum and minimum efficient working interval of the fuel cell set as 465 W and 50 W, corresponding to 27% and 40% fuel cell efficiencies respectively. The fuel cell may operate outside of this efficiency limits, if it is necessary for safety or performance delivery. The low and high bounds of the SOC for changing the operating condition can be set according to respective drive cycle and the power-train design. In this study, the limits were set to maintain energy storage meanwhile ensuring the prioritization of the EMS. The battery accepts charge or stores energy to be discharged according to load distribution. However the battery current does not exceed the defined thresholds for safety reasons. To achieve the performance criterion, four variables have been monitored, SOC, P_{dis}, P_{ch} and P_{load} to be compared with the defined battery and load limits and set the operation mode of the fuel cell. The load limits

have been defined in consideration of the load profile and battery capacity. The fuel cell starts operating at minimum level when the SOC is high and the load is low which has been decided in accordance with the longest low load interval and battery capacity. In parallel, the high load limit has been defined in the same manner and the fuel cell operates at maximum operation point if the SOC is low. The load distribution of the power-train under supervision of the EMS is given in Figure 4.3

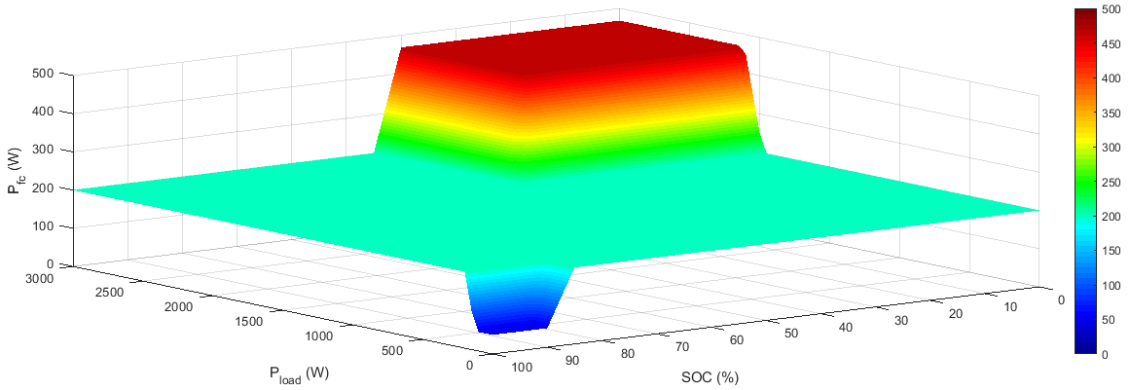

Figure 4.3: Energy Management Strategy

After the P_{fc} has been designated by the EMS, the $I_{fc,ref}$ signal for the fuel system delivery model to control the fuel flow, is calculated in consideration of the safe fuel cell operation conditions defined in a look-up table as *"FC Power-Current Curve"* in the simulation configuration. The safe operation conditions were provided by the manufacturer.

Chapter 5

Simulation and Analysis of FCHEP with Power Assisting EMS

The analysis of the power-train performance is presented in two sections. Since the drive cycle of interest does not necessarily test the performance of the power management under hard conditions. The first section is focused on performance of the EMS and power supply under transient load at extreme conditions. The second section presents the response of the complete power-train under the dynamic load modelled through the drive cycle.

5.1 Performance of FCHEP under Strong Transient Load

The power-train has been subjected to two different tests. Firstly, the power-train went under a sudden change from low load to high load and to medium load when SOC is below 5% to test the agility of the response of the power-train. In the second case, a low-transient pulse is given as a load to the power-train when the battery was approaching saturation.

5.1.1 High Load Transient with Low Battery Discharge Capacity

When the initial state of charge of the battery was 5%, the electric load managed by the power supply is shown in the first graph of Figure 5.1. The power supply was perfectly capable of catching the demand in the first second. The following graphs do not include the first second of the response, because the scaling would hinder the elaborate response analysis in the following seconds. The reference current of the fuel cell has been determined after available discharge capacity of the power-train according to the EMS algorithm. Discharge safety of the battery was controlled with respect to the load and candidate fuel cell reference power. Since, $P_{fc} < P_{load} \quad and \quad P_{dis} > P_{load} - P_{fc}$, fuel cell power has been deployed in it's efficient working region. Under the high load of 2500 W, fuel cell performed at 465 W, whereas in the other regions, fuel cell was

contributing with 200 W at its most efficient operating point since, the battery is capable of balancing the load. Trend decrease in the high load region of the $SOC(\%)$ indicates the high contribution of the fuel cell. Moreover, the bus voltage has been successfully balanced with only 0.2% error with respect to the nominal bus voltage by the low-level control system of the closed loop PI control.

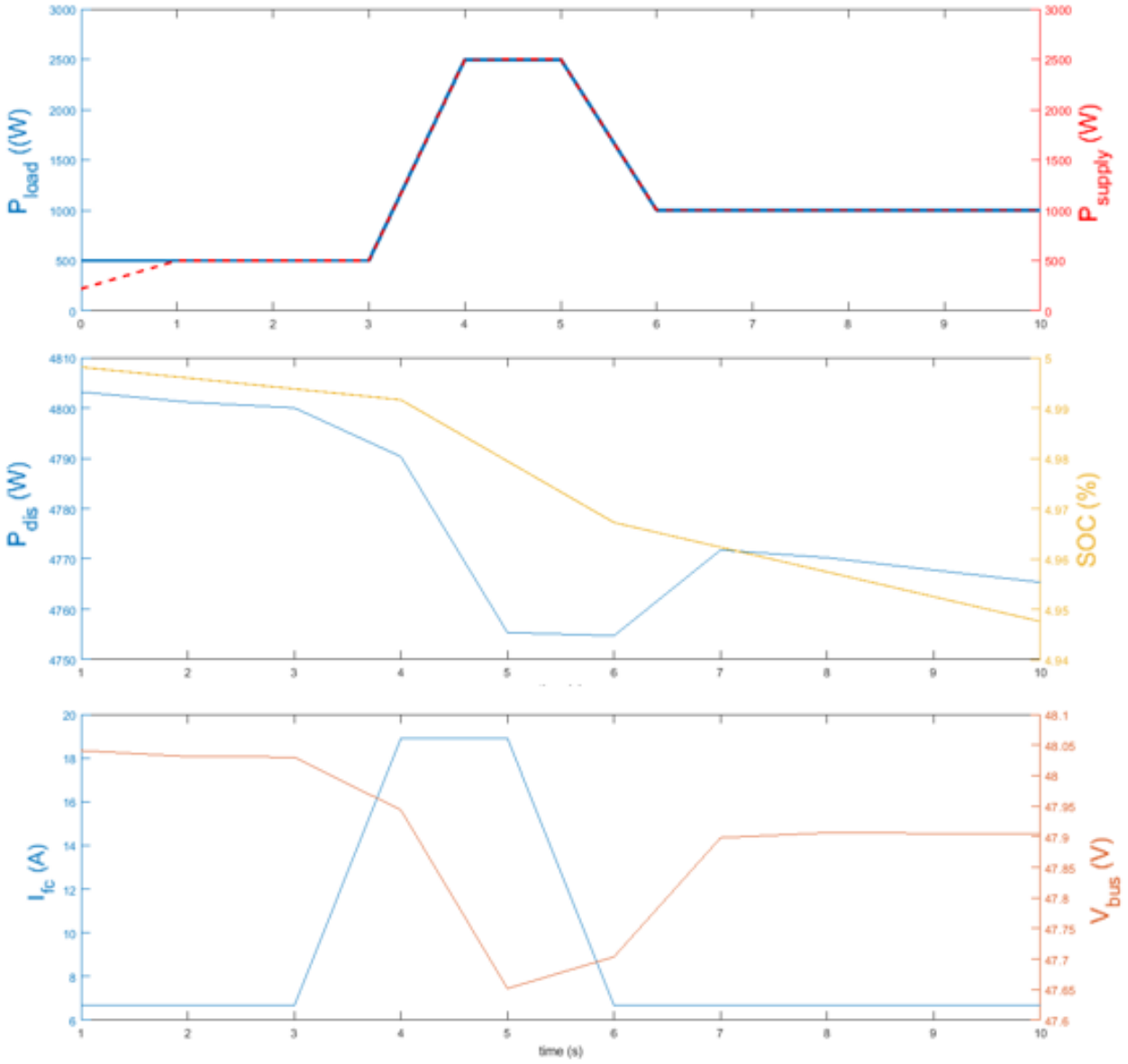

Figure 5.1: Power-train performance with high load transient

5.1.2 Low Load Transient with High Battery Discharge Capacity

Power distribution of the EMS could efficiently be handled by the power supply devices when initial state of charge was 95% and the load was suddenly minimized. The load pulse given to the system can be examined in Figure 5.2. In this case, the power-train was challenged with an excess of power generation. Hence, the power

production of the fuel cell should have decreased. The fuel cell reference current has been determined to be kept in minimum efficient working region, rather than being turned off according to the safety calculation conducted by EMS, $P_{fc} > P_{load} \quad and \quad P_{ch} > P_{fc} - P_{load}$ for charging mode of the battery. In the minimum load section, the only power delivery is by the fuel cell operating at minimum condition, hence $SOC(\%)$ stabilizes. The bus voltage is slightly higher, 49.16 V in average, than the nominal voltage, since the load of the power-train is much lower than the nominal load.

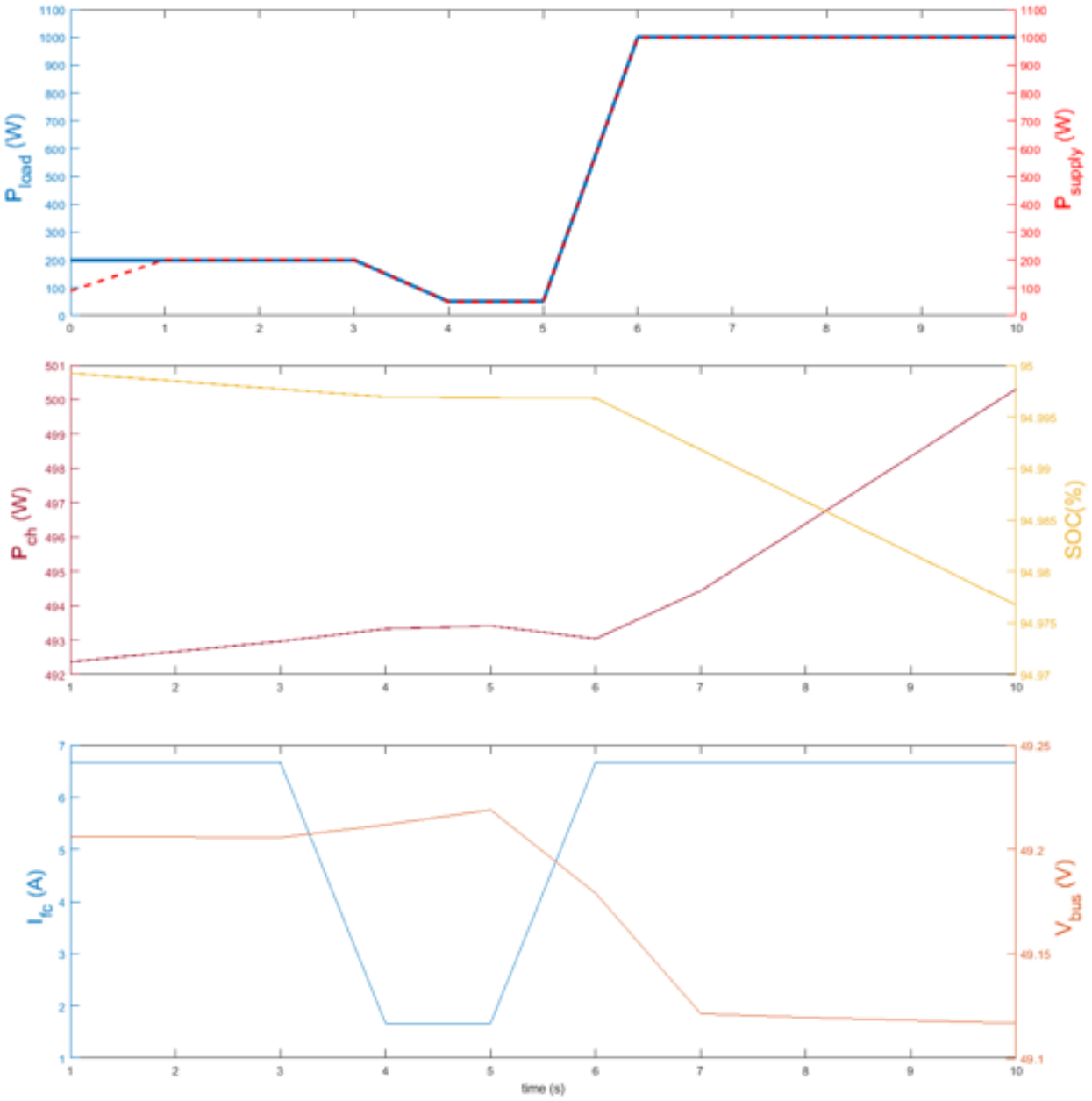

Figure 5.2: Power-train performance with low load transient

It has been proved that the designed power-train under management of the developed EMS performs well,

is precisely responding and ensuring safe and efficient performance delivery under the strong transient load even the conditions of the power-supplies are not the ideal. In both of the extreme cases, a need for leaving the efficient fuel cell operation interval has not arisen, since the charge and discharge capacity of the battery is significantly high in comparison to the fuel cell. In the following chapter, the power-train will not be under such sudden changes, although the maximum and minimum load limits will be broader than what subjected in this section.

5.2 Performance of FCHEP under In-Land Cruise Drive Cycle

The mechanical load mapped in Figure 3.7 is distributed along approximately 2 hours. The choice of 0.5% resolution for the accuracy in the results which accompanies DC-DC converter with 10 kHz PWM analysis. The computational effort is significantly high which takes more than 26 hours for 64-bit operating system with 2.40 GHz CPU. Hence, the drive cycle has been decided to down-sample by 1/10 which allows to preserve the load changes in a compressed amount of time. The obligatory decision puts the power-train under more challenging conditions, since the load changes happen in much tighter intervals. The shortcoming of this decision is not being able to project the energy expenditure of the power-train in long term performance. The compressed drive cycle with corresponding load on the bus is presented in Figure 5.3. As it can be seen, the peaks and the trends of the drive cycle has been preserved. The load on the bus dives to zero, when the boat starts deceleration and it starts tending up when the boat accelerates.

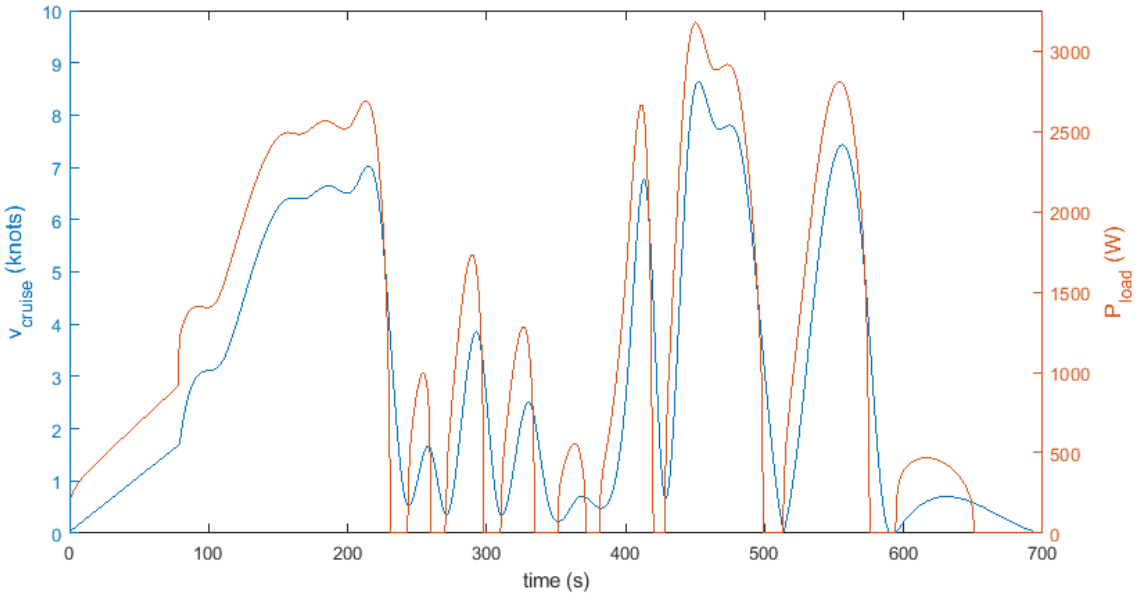

Figure 5.3: Down-sampled drive cycle and load on the DC-bus

The initial state of charge of the battery has been set as 50% for this simulation. The delivery of the

power-train is precisely matching with the power demand as shown in Figure 5.4.

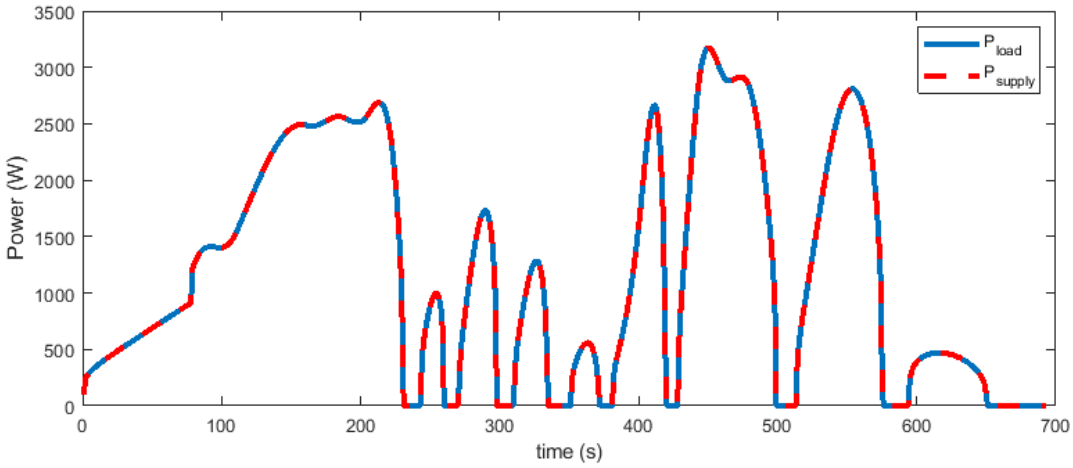

Figure 5.4: Power supply and demand match

Performance of Low-level Control

The performance of the low-level control was satisfactory, fluctuation of the bus voltage was restrained with $\pm 0.15V$ and the bus voltage average is 48.7 V, as shown in Figure 5.5. The voltage has been successfully boosted from the fuel cell to the DC-bus without causing disturbance on the bus. The bus voltage decreases with increasing load and increases with decreasing load, as expected.

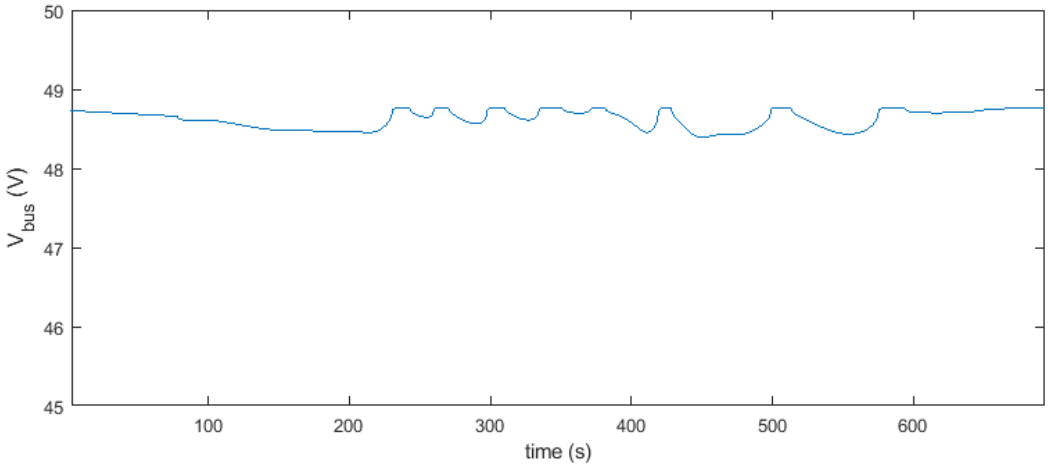

Figure 5.5: DC-bus voltage fluctuation

Performance of High-level Control

The power distribution allocated by the EMS after monitoring of the power-train system parameters was shown to be effective to be match the demand as shown in Figure 5.4. The power profiles of the fuel cell, the

battery and the load given by the electric motor are presented in Figure 5.6. The fuel cell generally operates at stable output other other than few disturbances whereas the battery floats to meet the load and store the excess power.

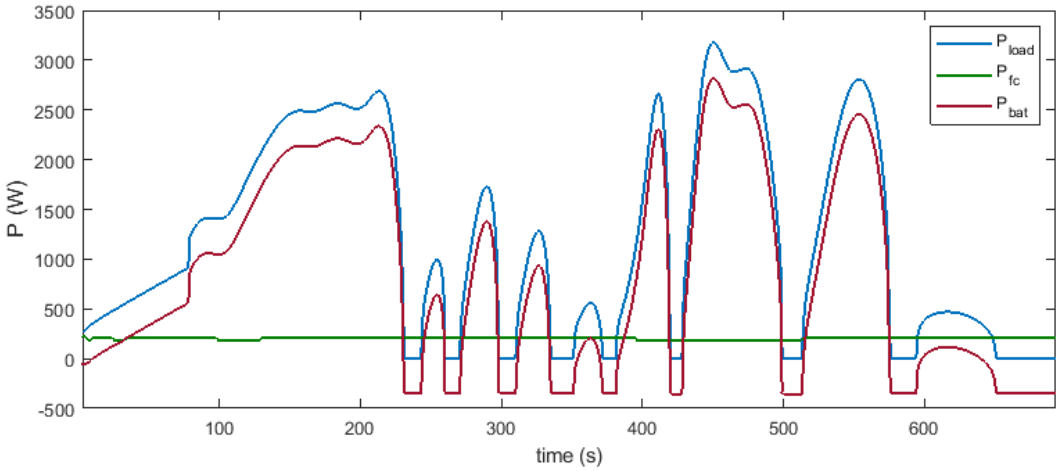

Figure 5.6: Power distribution in the power-train

Battery Performance

Fluctuation of the state of charge of the battery with respect to time and battery current is given in Figure 5.7. $SOC(\%)$ stabilizes when I_{bat} is below zero indicating the charging status of the battery. $SOC(\%)$ could never increase due to two reasons, first the characteristic of the drive cycle did not enable the conditions and the capacity of the battery is much higher than that of the fuel cell, the fuel cell generation could not summed up to noticeable charge of the battery.

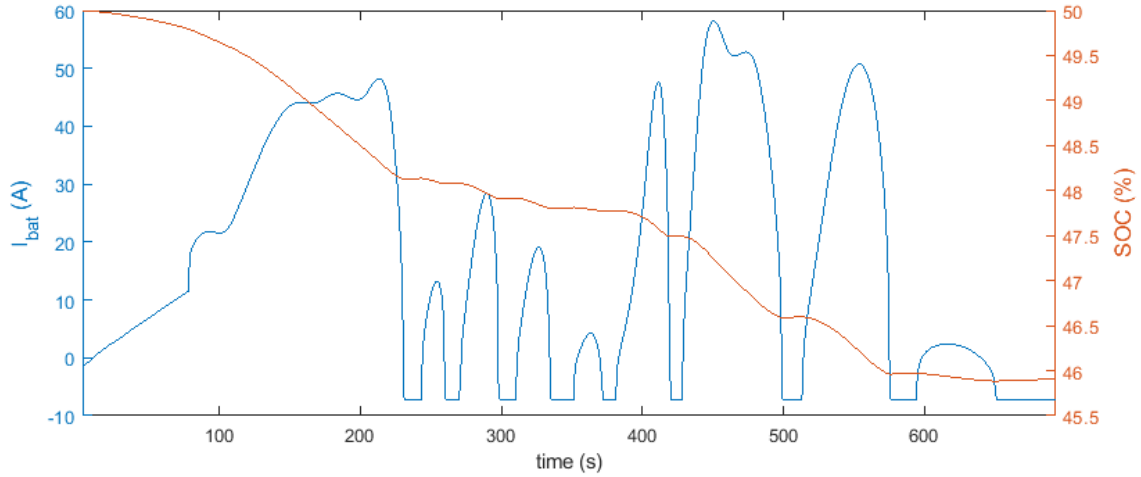

Figure 5.7: Response of the battery

Fuel Cell Performance

Figure 5.8 shows that the efficiency of the fuel cell reaches almost 50% in average which is the maximum efficiency the system can achieve, thanks to high $SOC(\%)$ during the cycle enabling efficient performance of the fuel. Hence, it can be concluded that the fuel cell management was highly efficient. The fuel cell deviates from the maximum efficient operation point slightly, due to variation in the DC-bus voltage which has been propagated to the fuel cell.

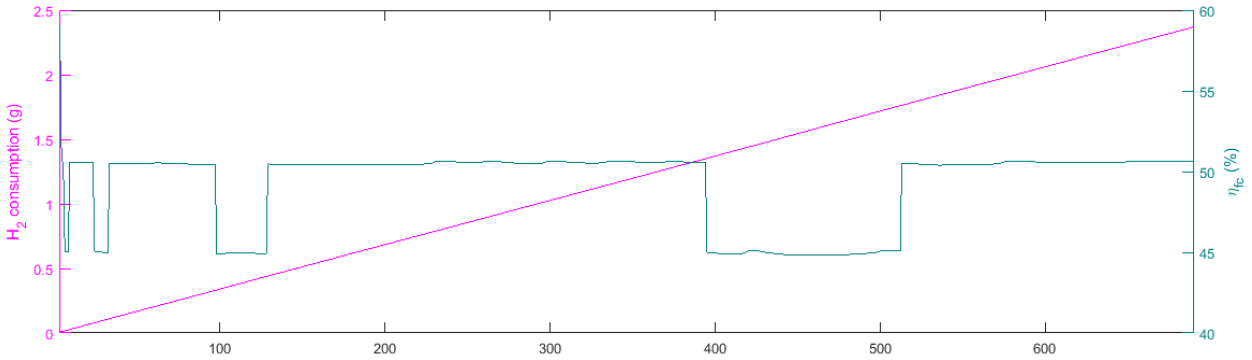

Figure 5.8: Fuel cell efficiency and fuel expenditure

Total fuel consumption, which has been set as pure H_2 at 2 bar in the model, is 2.38 gram for 1/10 reduced cycle of 2 hour in-land cruise.

Overlook of Power-train Performance

In the figure below, Figure 5.9, the variation of the voltage of the fuel cell and battery have been demonstrated in the upper figure. When the load of the electric motor and balancing currents of the fuel cell and battery shown in the figure below are considered, both battery and fuel cell changes their voltages to level the power. The ripple of the fuel cell voltage has been successfully limited by 2V thanks to efficient design of the DC-DC converter, whereas the battery voltage fluctuates much less due to powerful charge and discharge capacity. The fluctuation of the battery voltage is appreciably low, since the battery has no converter connected in between itself and the DC-bus, the fluctuations of the battery directly affects the other components. Moreover, the battery has a stable discharge profile until very deep discharge, beyond 95%, the boost converter never encounters with low voltage end.

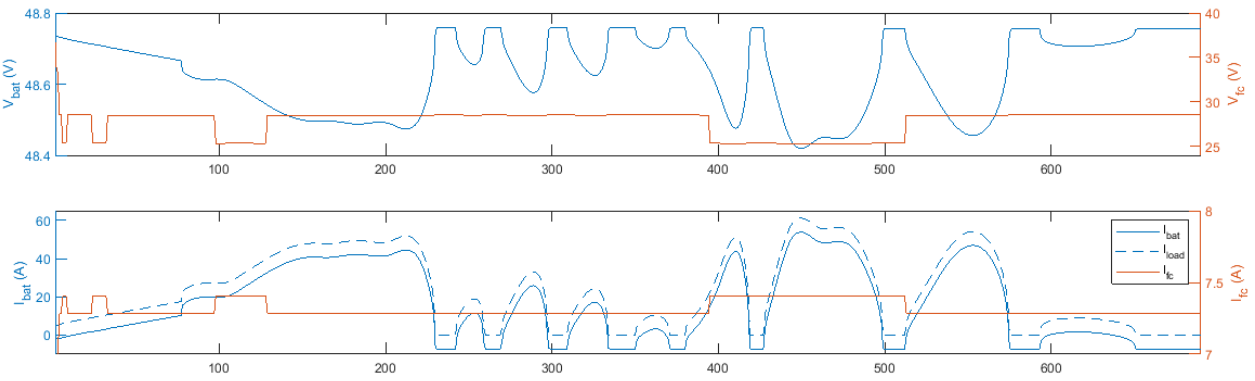

Figure 5.9: Voltage and current fluctuation of the power-train

The fuel cell current deviates slightly from the ideal due to the internal dynamic mechanisms of the fuel cell and voltage ripple by the DC-DC converter to maintain the outlet voltage. From Figure 5.10, it can be observed that the discharging energy is much higher than the charging energy of the battery, since the fuel cell integration in this particular FCHEP is for range extension. Nearly all of the energy for the cruise has been provided by the battery. Average fuel cell efficiency is 49.3% which indicates a highly efficient performance. The energy provided by the fuel cell has been calculated using the Lower Heating Value of hydrogen, 33.3 kWh/kg in consideration of the hydrogen consumption of 2.38 g corresponding to 285 kJ. The power-train hydrogen expenditure for the reduced drive cycle is 0.24 nmiles/g.

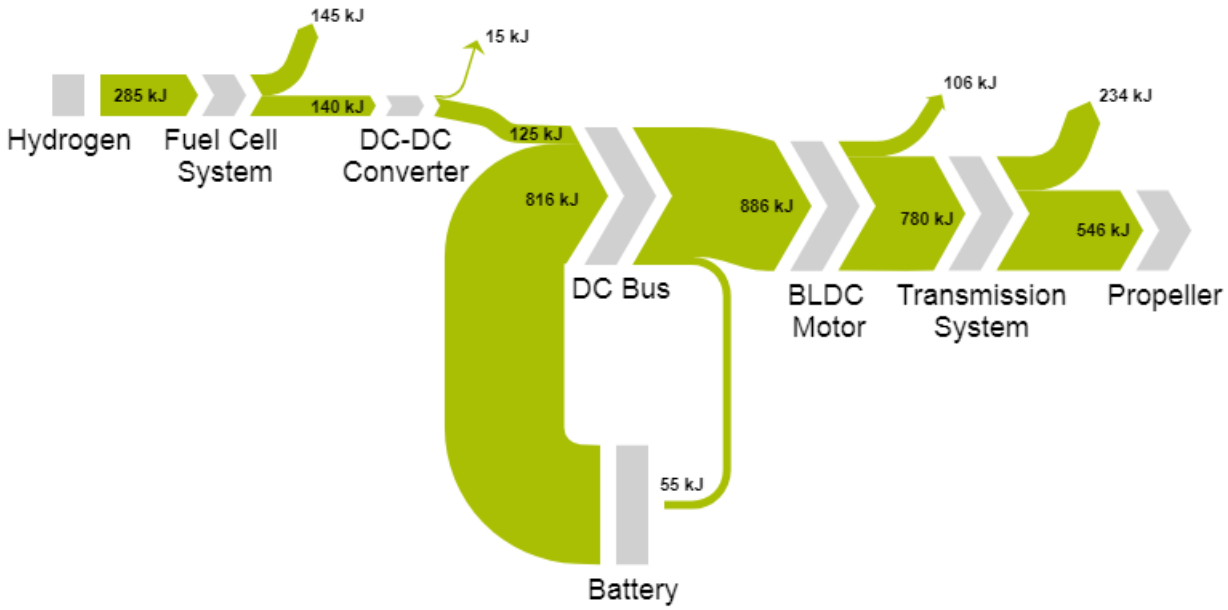

Figure 5.10: Sankey energy diagram of the drive-train

Designed DC-DC converter reaches 89% efficiency, which can be improved with high technology power

electronics. And it should be noted that the design of the DC-DC converter is totally based on theoretical calculations which contains error margin. 86% of the energy is provided by the battery which receives tiny amount of energy from the fuel cell. The electric motor performs with 88% efficiency, which is significantly higher than any other conventional motor for the maritime application. The BLDC motor is also capable of receiving regenerative energy which would improve the contribution of the motor and the efficiency of the complete power-train. The histogram of the drive cycle, shown in Figure 3.6, has shown that for in-land cruise applications, there is a significant potential for the regenerative energy saving. Finally the transmission system losses have assumed to be 30% to find out the mechanical energy on the propellers for creating the thrust. The over-all power-train efficiency is 74.6%, whereas the drive-train efficiency is 52.3%. Note that the energy analysis performed above is based on backward looking model of the complete boat and the respective dynamics. The modelling contains rough assumptions regarding naval engineering point of view. Moreover, the auxiliaries of the fuel cell system has not been considered for the modelling which would create additional energy expenditure. Thermal and degradation modellings of the battery and the fuel cell have not been conducted as well, which might lead to deviation from the ideal performance presented in this analysis.

Chapter 6

Genetic Algorithm Based Multi-Disciplinary Optimization

This chapter presents multi-objective genetic algorithm across disciplines to optimize hybridization of the power supplies of the FCHEP for cost minimization and downsizing the power-train meanwhile meeting performance criteria. The main target is to find the trade-off solutions, known as Pareto-optimal set satisfying objectives which will be explained in detail.

Classical optimization techniques might get 'stuck' in the local minima, whereas the genetic algorithms enable the global space search thoroughly. Genetic algorithm (GA), as its name suggests, is inspired by the natural selection which runs by survival of the fittest among individuals over consecutive generations for solving a problem. GA is applicable for both continuous and discrete functions, since it is derivative free optimization technique. The algorithm evolves the objective function through starting with randomly allocating the variables within the search region which makes the algorithm to be less vulnerable for the local minima. The generated variables are named as "individuals", a binary encoding applies for each of them and those binary string of digits are known as "genes" which carries collection of genetic traits. The individuals are evaluated with respect to objective functions and the results give the fitness of the individuals. Genetic operators; selection, cross-over and mutation, are then applied to the population of individuals.

- **Selection:** Fittest individuals have higher chances to be selected and produce more offspring in the succeeding generation.
- **Cross-over:** The selected individuals exchanges equivalent length of their genes for cross-over.
- **Mutation:** Finally, mutation is performed by flipping a gene randomly to ensure genetic diversity in the population.

In essence, the cross-over exploits the potential of the local search region, whereas random mutations explores the global space. The population of parents are then replaced with the off-spring population to be evaluated

for the objective functions. This process is repeated till the fittest candidates are obtained.

Most real world engineering problems involve simultaneous optimization of multiple incommensurable and contradicting objectives. For a power-train, cost minimization objective is likely to be contradict with performance maximization, yet none of them to be sacrificed to acquire a high quality solution. Hence, multi-objective optimization should be benefited. Success of GA in terms of global space exploration makes the methodology suitable for the multi-objective optimization problems. With the single objective problems, GA stores a single fitness value for every solution in the population. However, with multi-objective problems, every individual has a number of fitness values, one for each objective. This creates a problem for judging the overall fitness of the solutions. A common way of tackling the multi-criterion decision making is converting multi-objective optimization into a single objective optimization by creating a weighted solution. However, combining separate fitnesses in this way is akin to comparing completely different criteria; the question of whether a good apple is better than a good orange is meaningless. The concept of Pareto-optimal solution can be a solution with multiple fitness values. A Pareto-optimal solution exists in a solution set, if it is not dominated by any other solution with respect to all objectives involved. The individuals are evaluated according to their rank which indicates the convergence to the optimal Pareto set and the crowding distance that reflects the solution diversification.

Aim of the conducted multi-objective genetic algorithm based optimization is to minimize the cost of the power-supplies of the power-train and achieve lean hybridization while ensuring the delivery of the performance for the desired drive cycle of interest, in-land cruise cycle. From backward modelling point of view, for a certain acceleration profile, minimization of the weight enables downsizing of the power-train. On the other hand, for a forward looking model, minimized weight of the power-train results with improved acceleration performance, through direct correlation with Newton's second law. The optimization problem is formulated as following:

$$
\begin{aligned}
&Minimize \quad J(X_D, U(X_D)) \quad w.r.t. \quad X_D \\
&\qquad where \quad variables \quad X_D = [x_1, x_2] \quad and \quad x_1 \in [250, 3000], x_2 \in [250, 3000] \\
&\qquad where \quad objectives \quad U_1(X_D) = \alpha_1 x_1 + \alpha_2 x_2 \quad and \quad U_2(X_D) = \beta_1 x_1 + \beta_2 x_2 \\
&\qquad Subjected \quad to \quad c(X_D) \\
&\qquad where \quad constrain \quad c_1(X_D) : P_{peak} < x_1 + x_2 \\
&\qquad where \quad constrain \quad c_2(X_D) : 1.1(E_{cycle}) < Q_{b,sc} V_{b,sc} + \phi_{fc} x_2 \Delta t_{cycle}
\end{aligned}
$$

Table 6.1: **Optimization problem variables and constants**

Battery rated power, x_1	[250 W, 3000 W]
Fuel cell rated power, x_2	[250 W, 3000 W]
Unit battery cost, α_1	0.814 €/W
Unit fuel cell cost, α_2	3.8 €/W
Unit battery weight, β_1	0.012 kg/W
Unit fuel cell weight, β_2	0.006 kg/W
Scaled nominal battery capacity, $Q_{b,sc}$	0.019 Ah/W
Scaled nominal battery voltage, $V_{b,sc}$	0.009 V/W
Load factor of fuel cell, ϕ_{fc}	0.4

The variables are the rated power of the battery and the fuel cell, respectively. The objective function $U_1(X_D)$ minimizes the cost of the power-train, with the constants α_1 and α_2 standing for unit cost of the supplies per W. The second objective function seeks for minimization of the weight of the power supplies which is the main reason for hybridization, since the battery systems are much heavier than the fuel cell systems despite being significantly cheaper. The unit weight constants β_1 and β_2 are given with in the Table 6.1. The constraints of the optimization are delivery of peak power and ensuring that the range of the boat is capable of delivering 10% more than required. It should be noted that this optimization does not embody con-current optimization of the energy management strategy and does not give insight about the dynamic behaviour of the power-train as well. The level of abstraction in the modelling of the power-supplies is rough and solely based on scaling of the existing components. The charge and discharge dynamics of the battery is much sophisticated than the scaling with respect to constant nominal voltage. The fuel cell energy contribution is also relying on the experience that it will be generally operated at high efficiency region, which corresponds to load factor, ϕ_{fc} of 0.4. Hence, this optimization can only be an initial design optimization which needs to be supported with third discipline of energy management system directly relates with dynamic operation of the power-train. Computational expense of the con-current optimization of EMS and third evaluation of the fitness of the individuals on the equivalent circuit based model of the power-supply is quite high and requires high performing CPU.

The modelling and simulation of this optimization study was implemented in MATLAB/Simulink environment, where the boat, transmission system and electric motor modules described in chapter 3, were created in Simulink and the simulation results are brought to Matlab environment with m-files. The flow of the optimization is described in Figure 6.1. The backward model of the boat firstly assesses the load profile on the hybrid power-supply indicating the peak power demand to set the first constrain. The chosen genetic algorithm is *gamultiobj* which executes to find fit candidates fulfilling both objectives. The constrain of the optimization is determined through energy mapping for desired performance of the power-supply. The second

non-linear constrain ensures the range of the boat. The fittest individuals take place in the Pareto-optima set if they can satisfy range and peak power delivery criteria.

There are two scripts for the non-linear mix integer optimization procedure, the main script and the constraint script. The main script is used to define the upper and lower bounds of the design variables and the definition of the objective functions as well to execute the optimization, whereas the constraint script communicates with the Simulink model for the power profile and energy map.

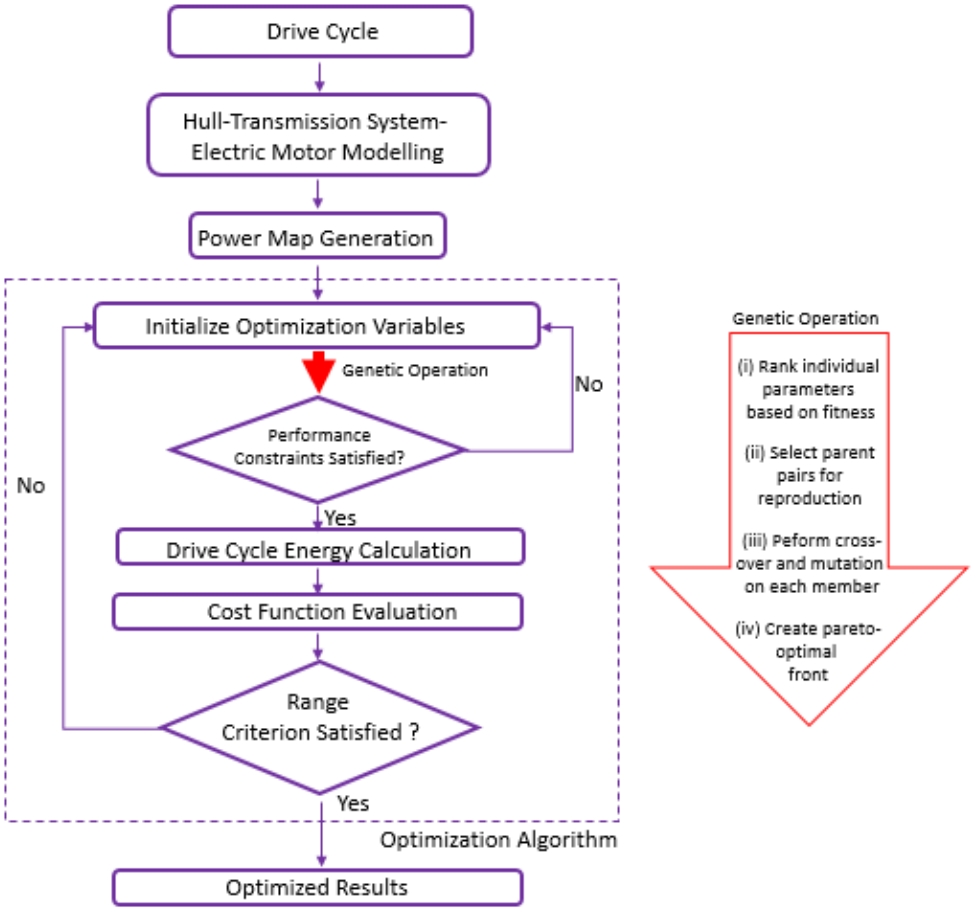

Figure 6.1: Optimization flowchart

Summary of the parameters of the devised multi-objective algorithm is listed in Table 6.2. The population size causes higher number of generations, which in turn, results in improved accuracy of solutions.

Table 6.2: **Multi-objective genetic algorithm parameters**

Population size	200
Fitness tolerance	0.001
Cross-over probability	0.85
Mutation probability	0.1

Results of the optimization are shown in Figure 6.2. The Pareto-optimal set details have been listed in section G.1. The Pareto-optimal set provides more degrees of freedom to the designers during selection of variables of interest, since none of the solutions is superior to the other, designer can choose among the solutions. The score diagram shows the range of the Pareto-optimal set, the cost minimization objective converged with the fittest individuals in between 5334€ - 11052€ interval, whereas the weight of the power-supply has been minimized in 20.5 kg - 40.3 kg range. Many of the Pareto-optimal solutions are above 10000€, since after significantly lean power-train can be achieved.

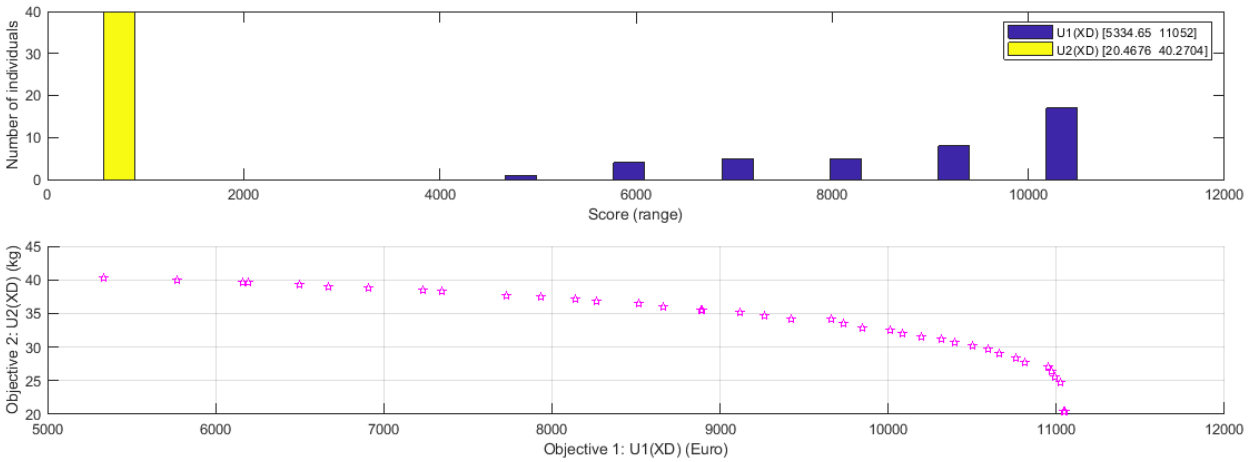

Figure 6.2: Optimization results: Score histogram (up), Pareto-optimal front (down)

Optimization results have been analysed based on hybridization ratio of the power-supply as well, as shown in Figure 6.3. Hybridization ratio is the ratio of the fuel cell rated power to the power-supply grant rated power, since the analysed FCHEP is a range extender. Current design of the power-train deploys 500 W fuel cell and 5000 W battery, corresponding to 0.1 hybridization ratio. In parallel with the detailed analysis of the performance presented in chapter 5, the power supply with 0.1 hybridization ratio meets the load. However, the fitness value of the design is 5970€ for 63 kg, which clearly could not take place in the Pareto-set due to over-sizing, hence suggests poor accelerative performance due to bulky design. Ideal hybridization ratios have been optimized in between 0.2 - 0.9, although the variable constraints were enabling much higher and lower results.

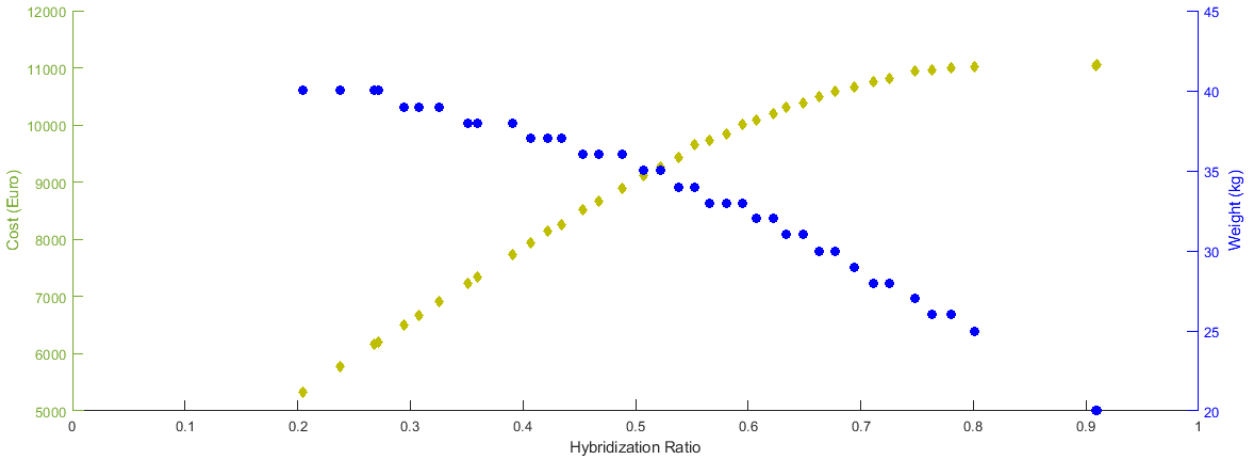

Figure 6.3: Effect of degree of hybridization on cost and down-sizing

Even with a prior objective of achieving minimum cost, a power-train could have fulfil the load for in-land cruise with much less weight. For instance, with the hybridization ratio 0.2, the power-train could have built for 10% less cost and 37% reduced weight.

Chapter 7

Conclusion and Future Work

The key contributions of the research are three fold. Firstly, the development of a simulation of a fuel cell hybrid electric power-train through combining different modelling techniques for the components to acquire a performance coherent with the reality was achieved. Secondly, an energy management system exploiting the full potential of the integration of a fuel cell to an electric power-train for range extension purposes while ensuring safe and efficient performance delivery was developed. Thirdly, the optimal hybridization options for the power-supplies of the power-train through multi-objective genetic algorithm seeking for the multi-disciplinary objectives: cost minimization and lean hybridisation was explored.

For the modelling of the power-train which has been compromised of commercially available products, different levels of mathematical framework have been utilized for the four main components: fuel cell, battery, DC-DC converter and BLDC motor. The framework developed for the fuel cell modelling based on differential equations reflects the intrinsic dynamics and successfully matched with the experimental recordings. Moreover, a fuel delivery system modelling was used to correlate the supervisory energy management system with the fuel cell. It is important that the delay in the fuel cell response is mainly constrained by the fuel delivery system rather the internal dynamics and it is important to consider the lag due to mechanic and fluid system control. For connecting the fuel cell to the main bus, its voltage should be controlled. Instead of modelling a full bridge SMPS which only utilized as a boost converter by design, a novel boost converter and control have been designed for the simulation. The methodology for designing of the converter has been satisfactory, since the converter performed precise and accurate under high amplitude impulses. However, the boat power-trains are usually under transient loads and through open loop control of the converter, the bus could not achieve a resilient performance. Hence, a system identification study, based on an under damped pair of complex-conjugate poles, has been conducted to derive transfer function of the designed DC-DC converter. The closed loop PI control, based on the transfer function was much better than of Ziegler-Nichols ultimate gain method applied on the system itself that proves the reliability of Simulink environment for dynamic adjust required for the system identification. For modelling of the Li-ion battery, an

equivalent circuit model has been used and to ensure obligation to the battery limits, limits provided by the manufacturer have been implemented into the supervisory system management. For this type of power-train architecture, the size of the battery is crucial to balance the transient load and buffer the current ripples to acquire longevity and efficient performance of the fuel cell. Although for lean power-train design purposes, choice of a low hybridization ratio, is not preferable. The 5 kW battery has proven a comfortable management of the load. The electric motor modelling has been coupled with a propeller curve derivation to utilize the full performance map provided by the motor manufacturer. The propeller curve was driven based on an empirical study. This approach was found to be weak, hence utilization of a real propeller curve should be preferred for more reliable results in case of availability. Finally, for efficient computation purposes a comparative analysis for powergui solver options have been evaluated. Tustin discretized method embodied in a discrete solver at 0.5% resolution achieved almost identical results with continuous solver in 1/20 computing duration. For simulation purposes, as much as the data provided by the manufacturer has been utilized to obtain a simulation with high fidelity, and for this, three levels of modelling needed to be executed harmoniously. The key approach is to start modelling piece by piece while trying to avoid over-complicating the system with the white-box modellings, although the basic instinct of a model developer is to describe the underlying physical phenomena.

The designed power-train for a low-power boat application was found to be the most commercially preferable and have the potential to fulfil performance expectations with a successful EMS after the extensive literature review on EMS of the architecture T2 type. It provides the necessary flexibility and energy density in the power-train through battery and the single converter can be enough for the load balancing. State based power-assisting EMS has been developed based on the load profile driven according to an in-land cruise cycle, hence the algorithm had the advantage of the backward looking model. To demonstrate the capability of the proposed high and low level power management systems, the designed power-train has been subjected to high and low load transients under extreme conditions. The power-train has shown immediate and precise response to the load with only 0.2% deviation from nominal bus voltage, as shown in 5.1 and 5.2. In order to evaluate the performance of the power-train under usual conditions of cruise cycle, down-sampling was applied to preserve transient trends of the load. The dynamic performance of the power-train and capability of the developed EMS have been highly precise. The EMS has managed to acquire a performance that the battery was following the load whilst the fuel cell operating at optimal efficiency. The current load on the components were optimized and a safe performance was ensured. The bus voltage ripple has been restricted to only $\pm 0.15V$ as shown in 5.5 and the overall power-train efficiency has almost reached 75%. The power-train hydrogen expenditure is 0.24 nmi/g which can be a reference for further studies.

A multi-objective genetic algorithm has been developed to minimize the capital cost of the power supplies and acquire a lean hybridisation which are the two main challenges in front of this technology and the most undeveloped topic of the interested field in the literature as well. Instead of a con-current optimization

embodying the detailed physical modelling of the components, system level modelling abstraction has been applied to get an outline for the performance criteria in terms of the transient load and range. From both scientific and commercial point of view, the multi-objective optimization of the power-train design is promising. Nowadays, it is quite easy to develop a driving profile of a user and customizing the design yields much efficient designs as proved with the optimization results. For the required drive cycle, the power-train could have been produced with 35% reduced weight for 90% cost of it. Backward modelling utilizing an estimated drive cycle offers a one step ahead intuition for the design of a power-train and provides an overall understanding of its performance. Moreover, the EMS design benefits from the load profile prediction as well, as in the case of this study.

Hybridization of a battery electric power-train with a fuel cell for range extension purposes for a zero-emission boat has proved to be a powerful alternative to substitute the pollutant internal combustion deployed low-power boats in the same segment. The developed power-train has a highly agile and efficient performance under usual and extreme cruise conditions. The simulations of the boost converter implemented power-train and optimization studies have shown that there is still plenty of room for cost reduction and performance improvement. Still, the diffusion of the technology in the market is weighed down in the short-term by the classic chicken and egg problem of the infrastructure. Hopefully, the possibilities deployed in this thesis will provide strategic advantages and innovation for the zero-emission maritime transportation in the future.

Future Work

There are still many opportunities for augmentation of the developed simulation, yet it can serve as a foundation for further research and improvement. Implementation of the auxiliary systems for the fuel cell and the hydrogen storage will provide much accurate understanding of the dynamics and the energy expenditure of the power-train, since specifically the compressor has a considerable power load. Moreover, the current modelling does not encompass the long-term behaviour of the power-train which has effect on the performance and the operational costs as well. Hence, upgrading the models of the battery and the fuel cell for ageing and degradation is beneficial. Furthermore, the individual component performance within the system and overall system performance experiments are important for validating the simulation. Once coherence of the simulation is proven, hardware-in-loop simulations can provide significant improvement possibilities.
The foremost importance should be given to development of a more reliable and accurate load profile through detailed transmission system modelling.
Since the simulation has been constructed modularly, a change in the EMS is easily applicable and interfacing the simulation for other computer languages, such as C and Java, is possible. Therefore, study on the new generation EMSs, such as machine learning or optimization based strategies can be promising.
The genetic algorithm based optimization can be extended with inclusion of the variables of the EMS for con-current optimization which requires a high computational power. Alternatively, the initial hybridization estimation can be validated with a detailed dynamic model which has been already developed, yet necessary

scaling of the components should be handled as a next step.

Finally, exploration of the single stage power conversion for the power-train architecture and possibilities for exploiting the regenerative power can be favourable research topics.

References

AirClim and European Environmental Bureau. Air pollution from ships. Technical report, Laholm, 2011.

AIS Marine Traffic. Global Ship Tracking Intelligence. URL https://www.marinetraffic.com/.

I. Aschilean and M. Varlam. Hybrid electric powertrain with fuel cells for a series vehicle. *Energies*, 11(1294), 2018.

F. Assadian, G. Mohan, and S. Longo. Comparative analysis of forward-facing models vs backward-facing models in powertrain component sizing. In *Hybrid and Electric Vehicles Conference 2013 (HEVC 2013)*, 2013. ISBN 978-1-84919-776-2. doi: 10.1049/cp.2013.1920.

T. Azib, O. Bethoux, G. Remy, C. Marchand, and E. Berthelot. An innovative control strategy of a single converter for hybrid fuel cell/supercapacitor power source. *IEEE Transactions on Industrial Electronics*, 2010. ISSN 02780046. doi: 10.1109/TIE.2010.2044123.

J. Bell. *Design and Control of a Hydrogen Fuel Cell Vehicle*. Master of science thesis, UNIVERSITY OF CALIFORNIA, 2016.

J. Bernard and S. Delprat. Fuel-Cell Hybrid Powertrain: Toward Minimization of Hydrogen Consumption. *IEEE Transactions on Vehicular Technology*, 58(7), 2010.

K. Billings and T. Morey. *Switchmode power supply handbook*. McGraw-Hill, third edition, 2011.

Bloomberg. Toyota, Shell Among Giants Betting $10.7 Billion on Hydrogen, 2017. URL https://www.bloomberg.com/news/articles/2017-01-17/toyota-shell-among-auto-and-oil-giants-forming-hydrogen-council.

Brian Su-Ming Fan. *Multidisciplinary Optimization of Hybrid Electric Vehicles: Component Sizing and Power Management Logic*. Doctor of philosophy, University of Waterloo, 2011.

P. Bubna, S. G. Advani, and A. K. Prasad. Integration of batteries with ultracapacitors for a fuel cell hybrid transit bus. *Journal of Power Sources*, 2012. ISSN 03787753. doi: 10.1016/j.jpowsour.2011.09.097.

G. Ceballos, P. R. Ehrlich, A. D. Barnosky, A. García, R. M. Pringle, and T. M. Palmer. Accelerated modern human-induced species losses: Entering the sixth mass extinction. *Science Advances*, 2015. ISSN 23752548. doi: 10.1126/sciadv.1400253.

S. Chanda and A. Snyder. NoElectric Drivetrain Testing Using Smart Green Technology. *SAE International*, 1, 2012.

J.-C. Ciscar, A. Iglesias, L. Feyen, L. Szabó, D. V. Regemorter, B. Amelung, R. Nicholls, P. Watkiss, O. B. Christensen, R. Dankers, L. Garrote, C. M. Goodess, A. Hunt, A. Moreno, J. Richards, and A. Soria. Physical and economic consequences of climate change in Europe. *Proceedings of the National Academy of Sciences*, 2011. ISSN 1091-6490. doi: 10.1073/pnas.1011612108/-/DCSupplemental.www.pnas.org/cgi/doi/10.1073/pnas.1011612108.

A. Codina. *System Level Modelling of Fuel Cell Driven Electric Vehicle*. Msc, Chalmers University of Technology, 2017.

J. Cook, N. Oreskes, P. T. Doran, W. R. Anderegg, B. Verheggen, E. W. Maibach, J. S. Carlton, S. Lewandowsky, A. G. Skuce, S. A. Green, D. Nuccitelli, P. Jacobs, M. Richardson, B. Winkler, R. Painting, and K. Rice. Consensus on consensus: A synthesis of consensus estimates on human-caused global warming. *Environmental Research Letters*, 2016. ISSN 17489326. doi: 10.1088/1748-9326/11/4/048002.

M. Copisarow. Marine fouling and its prevention, 1945. ISSN 00368075.

CORDIS. Final Report - HYMAR. Technical report, INTERNATIONAL COUNCIL OF MARINE INDUSTRY ASSOCIATIONS, 2013. URL https://cordis.europa.eu/result/rcn/57677{_}en.html.

H. S. Das, C. W. Tan, and A. H. Yatim. Fuel cell hybrid electric vehicles: A review on power conditioning units and topologies, 2017. ISSN 18790690.

P. K. Das, X. Li, and Z.-S. Liu. Analysis of liquid water transport in cathode catalyst layer of PEM fuel cells. *International Journal of Hydrogen Energy*, 2010. ISSN 03603199. doi: 10.1016/j.ijhydene.2009.12.160.

C. Desai. Optimal Design of a Parallel Hybrid Electric Vehicle using Multi-Objective Genetic Algorithms. In *IEEE Vehicle Power and Propulsion Conference*, Dearborn, 2009.

B. Douglas. *The Fundamentals of Control Theory*. 2017. URL https://www.patreon.com/posts/fundamentals-of-13367470.

M. Dresselhaus and G. Crabtree. Basic research needs for the hydrogen economy. Technical report, US Department of Energy, 2004.

M. Elhogary and I. Seediek. Overview of alternative fuels with emphasis on the potential of liquefied natural gas as future marine fuel. *Engineering for the Maritime Environment*, 229(4):365–375, 2015.

European Commission. Directive 2013/53/EU, 2017. URL https://ec.europa.eu/growth/single-market/european-standards/harmonised-standards/recreational-craft{_}en{#}(1)ESO.

European Commission. Energy Flow Diagrams, 2018. URL https://ec.europa.eu/eurostat/web/energy/energy-flow-diagrams.

H. Fathabadi. Fuel cell hybrid electric vehicle (FCHEV): Novel fuel cell\SC hybrid power generation system. *Energy Conversion and Management*, 156:192–201, 2018.

T. Fletcher. *Optimal energy management strategy for a fuel cell hybrid electric vehicle*. Doctoral thesis, Loughborough University Institutional Repository, 2017.

Frauscher. 740 Mirage Air, 2018. URL https://www.frauscherboats.com/en/Electric-Yachts/740-Mirage-Air.

S. Fuchs and B. Reuter. An Overview of Costs for Vehicle Components, Fuels and Greenhouse Gas Emissions, 2017.

J. C. Gamazo-Real, E. Vázquez-Sánchez, and J. Gómez-Gil. Position and speed control of brushless dc motors using sensorless techniques and application trends, 2010. ISSN 14248220.

D. Gao and J. Zhenhua. Development and performance analysis of a hybrid fuel cell/battery bus with an axle integrated electric motor drive system. *i n t e r n a t i o n a l journal o f hydrogen energy*, 41:1161–1169, 2016.

D. Gao, Z. Jin, J. Zhang, J. Li, and M. Ouyang. Comparative study of two different powertrains for a fuel cell hybrid bus. *Journal of Power Sources*, 2016. ISSN 03787753. doi: 10.1016/j.jpowsour.2016.04.046.

P. Garcia, J. P. Torreglosa, L. M. Fernandez, and F. Jurado. Control strategies for high-power electric vehicles powered by hydrogen fuel cell, battery and supercapacitor. *Expert Systems with Applications*, 2013. ISSN 09574174. doi: 10.1016/j.eswa.2013.02.028.

D. Gerr. *The Propeller Handbook*. International Marine Publishing, 1989.

G. Goyal. *Model Based Automotive System Integration: Fuel Cell Vehicle Hardware-In-The-Loop*. Master of science in technology, ARIZONA STATE UNIVERSITY, 2014.

M. Grapentin. *Marktanalyse und Entwicklung eines Geschäftsmodells für ein Sportboot mit PEM-Brennstoffzellen-Antriebstechnologie*. Msc thesis, Technische Universität Berlin, 2017.

G. Gunnarsson and J. B. Skúlason. Regenerative electric/hybrid drive train for ships. Technical report, Nordic Innovation, 2016.

Y. N. Harari. *Sapiens: A brief History of Humankind*. 1989. ISBN 9788578110796. doi: 10.1017/CBO9781107415324.004.

O. Hegazy and J. Van Mierlo. Particle swarm optimization for optimal powertrain component sizing and design of fuel cell hybrid electric vehicle. In *Proceedings of the International Conference on Optimisation of Electrical and Electronic Equipment, OPTIM*, 2010. ISBN 9781424470198. doi: 10.1109/OPTIM.2010.5510447.

Honda. GM and Honda to Establish Industry-First Joint Fuel Cell System Manufacturing Operation in Michigan, 2017.

G. Hoogers. *Fuel Cell Technology Handbook*. 2003. ISBN 0849308771.

E. Hosseinzadeh. *Modeling and Design of Hybrid PEM Fuel Cell Systems for Lift Trucks*. Phd, Technical University of Denmark, 2012.

J. Hou. *Control and Optimization of Electric Ship Propulsion Systems with Hybrid Energy Storage*. Doctor of philosophy, University of Michigan, 2017.

K. W. Hu, P. H. Yi, and C. M. Liaw. An EV SRM Drive Powered by Battery/Supercapacitor with G2V and V2H/V2G Capabilities. *IEEE Transactions on Industrial Electronics*, 2015. ISSN 02780046. doi: 10.1109/TIE.2015.2396873.

T. k. Ibrahim, M. Kamil, O. I. Awad, M. M. Rahman, G. Najafi, F. Basrawi, A. N. Abd Alla, and R. Mamat. The optimum performance of the combined cycle power plant: A comprehensive review, 2017. ISSN 18790690.

IMO. UN body adopts climate change strategy for shipping, 2018a. URL http://www.imo.org/en/MediaCentre/PressBriefings/Pages/06GHGinitialstrategy.aspx.

IMO. Prevention of Air Pollution from Ships, 2018b. URL http://www.imo.org/en/ourwork/environment/pollutionprevention/airpollution/pages/air-pollution.aspx.

International Organization for Standardization. ISO 8178-1:2017.

M. Jain. Genetic algorithm based optimal powertrain component sizing and control strategy design for a fuel cell hybrid electric bus. In *2009 IEEE Vehicle Power and Propulsion Conference*, 2009.

B. James. Mass Production Cost Estimation of Direct H2 PEM Fuel Cell Systems for Transportation Applications: 2016 Update. Technical report, Strategic Analysis, 2017.

M. Jang and V. G. Agelidis. A minimum power-processing-stage fuel-cell energy system based on a boost-inverter with a bidirectional backup battery storage. *IEEE Transactions on Power Electronics*, 2011. ISSN 08858993. doi: 10.1109/TPEL.2010.2086490.

H. Jingang and J.-F. Charpentier. An Energy Management System of a Fuel Cell/Battery Hybrid Boat. *Energies*, 7, 2014.

M.-J. Kim. Power management and design optimization of fuel cell/battery hybrid vehicles. *Journal of Power Sources*, 165:819–832, 2007.

I. Leikarnes. *Modelling and Simulating a Hybrid Electric Vehicle*. PhD thesis, The Arctic University of Norway, 2017.

Q. Li, W. Chen, Y. Li, S. Liu, and J. Huang. Energy management strategy for fuel cell/battery/ultracapacitor hybrid vehicle based on fuzzy logic. *International Journal of Electrical Power & Energy Systems*, 2012. ISSN 01420615. doi: 10.1016/j.ijepes.2012.06.026.

M. Mattsson and J. Thordsson. *Marine Hybrid Electric Powertrain*. Msc, Chalmers University, 2010.

D. McDonald. Electric Vehicle Drive Simulation with MATLAB/Simulink. In *Proceedings of the 2012 North-Central Section Conference*. American Society for Engineering Education, 2012.

A. Melero-Pérez and W. Gao. Fuzzy Logic energy management strategy for Fuel Cell/Ultracapacitor/Battery hybrid vehicle with multiple-input DC/DC converter. In *Vehicle power and propulsion conference*, pages 199–206, 2009.

A. F. Molland. *The maritime Engineering Reference Book*. 2008. ISBN 9780750689878. doi: 10.1016/B978-0-7506-8987-8.X0001-7.

NASA. Climate Change: Vital Signs of the Planet: Evidence, 2016.

NSBA. Review of All-Electric and Hybrid-Electric Propulsion Technology for Small Vessels. Technical report, Nova Scotia Boatbuilders Association, 2015.

F. Odeim and J. Roes. Power management optimization of an experimental fuel cell/battery/supercapacitor hybrid system. *Energies*, 8, 2015.

G. Offer and D. Howey. Comparative analysis of battery electric, hydrogen fuel cell and hybrid vehicles in a future sustainable road transport system. *Energy Policy*, 38(1), 2010.

M. J. Ogburn. *Systems Integration, Modeling, and Validation of a Fuel Cell Hybrid Electric Vehicle*. Master of science thesis, Virginia Polytechnic Institute and State University, 2000.

D. F. Opila, X. Wang, R. McGee, R. B. Gillespie, J. A. Cook, and J. W. Grizzle. An energy management controller to optimally trade off fuel economy and drivability for hybrid vehicles. *IEEE Transactions on Control Systems Technology*, 2012. ISSN 10636536. doi: 10.1109/TCST.2011.2168820.

S. Pacala and R. Socolow. Stabilization wedges: Solving the climate problem for the next 50 years with current technologies, 2004. ISSN 00368075.

A. Rousseau and P. Sharer. Energy storage requirements for fuel cell vehicles. Technical report, SAE, 2004.

L. Shaftesbury, A. Ashley, E. Shaftesbury, and A. A. Cooper. Stanford Encyclopedia of Philosophy. *The Stanford Encyclopedia of Philosophy*, 2011. ISSN 00261068. doi: 10.1111/1467-9973.00225.

V. Shagar. Effect of Load Changes on Hybrid Shipboard Power Systems and Energy Storage as a Potential Solution: A Review. *Inventions*, 2(21), 2017.

C. Shulock and E. Pike. Vehicle electrification policy study-Technology Status. Technical report, ICCT: The International Council on Clean Transportation, 2011.

D. Skender. *Modelling of Test Bench for Road Load Simulation*. Msc, Linköping University, 2017.

R. C. Smith. *DESIGN OF A CONTROL STRATEGY FOR A FUEL CELL / BATTERY HYBRID POWER SUPPLY*. Master of science, Texas A&M University, 2009.

N. M. Souleman, O. Tremblay, and L. A. Dessaint. A generic fuel cell model for the simulation of fuel cell vehicles. In *5th IEEE Vehicle Power and Propulsion Conference, VPPC '09*, 2009. ISBN 9781424426003. doi: 10.1109/VPPC.2009.5289692.

I. Staffell. Results from the Microcab fuel cell vehicle demonstration at the University of Birmingham. *International Journal of Electric and Hybrid Vehicles*, 2011. ISSN 1751-4088. doi: 10.1504/IJEHV.2011.040473.

N. Sulaiman, M. A. Hannan, A. Mohamed, E. H. Majlan, and W. R. Wan Daud. A review on energy management system for fuel cell hybrid electric vehicle: Issues and challenges, 2015. ISSN 18790690.

K. Targoński. DC/DC Boost converter for fuel cells. Technical report, INSTITUTE OF ENERGY TECHNOLOGY AALBORG UNIVERSITY, 2006.

E. Tazelaar and B. Veenhuizen. Energy Management Strategies for Fuel Cell Hybrid Vehicles; an Overview. In *EVS27*, Barcelona, 2013.

Transparency Market Research. Logistics Market- Global Industry Analysis, Size, Share, Growth, Trends, and Forecast 2016 - 2024. Technical report, 2015.

A. Umeda and E. Shimizu. Design strategy of Battery Powered Boat and its evaluation. In *Proceedings of the Twenty-fifth (2015) International Ocean and Polar Engineering Conference*, Hawaii, 2015.

US Naval Academy. *RESISTANCE AND POWERING OF SHIPS*.

A. Wilson and G. Kleen. Fuel Cell System Cost - 2017. Technical report, Department of Energy, USA, 2017.

B. Wu. *Fuel Cell Hybrid Electric Vehicle Powertrain Modelling and Testing*. Phd thesis, Imperial College London, 2014.

Xcellsis and Ballard. Hydrogen fuel cell engines and related technologies. Technical report, College of the Desert, 2001.

L. Xiaofen. A Review of Concurrent Optimization Methods. *International Journal of Bio-Inspired Computation*, 6(1):22–31, 2014.

C. Xie and S. Quan. Multiple model control for hybrid power system of fuel cell electric vehicle. In *IEEE vehicle power and propulsion conference*, 2008.

S.-b. Yang. A Electric Vehicle Powertrain Simulation and Test of Driving Cycle Based on AC Electric Dynamometer Test Bench. In *Proceedings of International Conference on Mechanical Engineering and Material Science*. Atlantis Press, 2012.

H. Zhao and A. Burke. Effects of Different Powertrain Configurations and Control Strategies on Fuel Economy of Fuel Cell Vehicles. In *The 25th World Battery, Hybrid and Fuel Cell Electric Vehcle Symposium*, Shenzhen, 2010.

C. H. Zheng, C. E. Oh, Y. I. Park, and S. W. Cha. Fuel economy evaluation of fuel cell hybrid vehicles based on equivalent fuel consumption. *International Journal of Hydrogen Energy*, 2012. ISSN 03603199. doi: 10.1016/j.ijhydene.2011.09.147.

C. Zhu and X. Li. Development of a theoretically based thermal model for lithium ion battery pack. *Journal of Power Sources*, 223:155–164, 2013.

Appendices

Appendix A

Zero-Emission Boat Market Survey

Table A.1: **Zero-Emission boat and yacht manufacturers**

	Manufacturer	**Nationality**	**Involved Players**	**Link**
Sailing Boats	African Cat	NL	Green Motion Propulsion	africancats.com
	Elco Electric Launch	US	Elco Motors, Delka	elcomotoryachts.com
Commercial Motor Boats	Grove boats	CH	-	grove-boats.com
Leisure Motor Boats	Frauscher	AUT	-	frauscherboats.com
	Boesch Boats	CH	Kräutler, Erun	boesch-boats.ch
	Whisper Boats Builder Academy	S AFR	Vetus	wbba.co.za
	Nimbus	SWE	ElectroEngine	nimbus.se
	Elco Electric Launch	US	Elco Motors, Delka	elcomotoryachts.com
	Austrian Marian boat	AUT	Piktronik, Erun	boote-marian.at
	Excellent Yachts	NL	Bellman, Victron	excellent-yachts.com
	Aquawatt	AUT	-	aquawatt.at
	Polar boats	NOR	Vetus, Ladac Haze	polarboat.no
	Patterson Boatwork	UK	-	pattersonboatworks.co.uk
	Lear Electric Boats	US	-	lear-electric-boats.com
	Feller Yachting	GER	Dymax	felleryachting.de
	Knierim Yachtbau	GER	PlanetSolar	knierim-yachtbau.de
	Duffy	US	-	duffyboats.com
	Torqeedo	GER	-	torqeedo.com

Appendix B

Hull Resistance Calculation Parameters

TABLE 1. William Froude's Plank Friction Experiments

Nature of Surface	*Length, L*			
	2 feet	*8 feet*	*20 feet*	*50 feet*
*Values for f**				
Varnish	0.0117	0.0121	0.0104	0.0097
Paraffin	0.0119	0.0100	0.0088	.....
Calico	0.0281	0.0196	0.0184	0.0170
Fine Sand	0.0231	0.0166	0.0137	0.0104
Medium Sand	0.0257	0.0178	0.0152	0.0139
Coarse Sand	0.0314	0.0204	0.0168	.....
Values for n				
Varnish	2.00	1.85	1.85	1.83
Paraffin	1.95	1.94	1.93	....
Calico	1.93	1.92	1.89	1.87
Fine Sand	2.00	2.00	2.00	2.06
Medium Sand	2.00	2.00	2.00	2.00
Coarse Sand	2.00	2.00	2.00	....

* The *f* values are for fresh water. For sea water multiply by 64/62.4.

Figure B.1: Viscous force parameters for hull resistance calculation, (Copisarow, 1945)

Appendix C

Battery Information

Table C.1: **Fuel cell simulation specifications**

Fuel Cell Nominal Parameters	
Stack Nominal Power	468 W
Stack Maximal Power	500 W
Resistance	0.76 Ohms
Nernst Voltage of One Cell (En)	1.1715 V
Hydrogen Utilization	0.976
Oxidant Utilization	0.7332
Nominal Fuel Consumption	5.645 slpm
Nominal Air Consumption	13.43 slpm
Exchange Current (i_0)	4.86 A
Exchange Coefficient (alpha)	-1.09
Fuel Cell Signal Variation Parameters	
Fuel Composition	99.95 %
Oxidant Composition	21 %
System Temperature	298 K
Fuel Supply Pressure	2 bar
Air Supply Pressure	1 bar

Produkt	**SuSy500**
Leistungsdaten	20 – 40 ... 46
Spannung	16 - 21 V DC
Leistung	500 W nominal
Stromstärke	18 A bei Nennleistung
Effizienz	~45 % bei 500 W
Wasserstoffverbrauch	ca. 4,5 Nl/ min bei 500 W
Wasserstoffqualität	3.0
Standzeit/ Lebensdauer	2000 h bei 200 Start/ Stopp-Zyklen
Optimale Arbeitstemperatur	55 °C (Stacktemperatur)
Schnittstellen & Elektrik	
Wasserstoff-Eingang	G 1/8" Innengewinde
Wasserstoff-Eingangsdruck	2 – 20 bar
Stromabnahme	4 mm² Schraubklemme
Steuerung	SUB-D9
Überstromschutz	22 A (flink)
Allgemeine Daten	
Abmessungen (L x B x H)	244 mm x 159 mm x 180 mm
Gewicht	~ 3,9 kg
Geräuschentwicklung	~45 dBA in 7 m Abstand (bei Volllast)
Emissionen	Wasser (feuchte Luft), Wärme
Einbaubedingungen & Lagerung	
Einbauraum (L x B x H)	≥ 244 mm x 160 mm x 200 mm
Neigung um Querachse	20° für 60 Sekunden, 10° dauerhaft
Neigung um Längsachse	20° für 60 Sekunden, 10° dauerhaft
Betriebshöhe	bis max. 1.500 m über NN
Starttemperatur	5 – 35 °C
Betriebstemperatur	5 – 35 °C
Lagertemperatur	-10 – 55 °C

Figure C.1: Data-sheet of Susy500 by Baltic Fuel Cell

Appendix D

DC-DC Converter Information

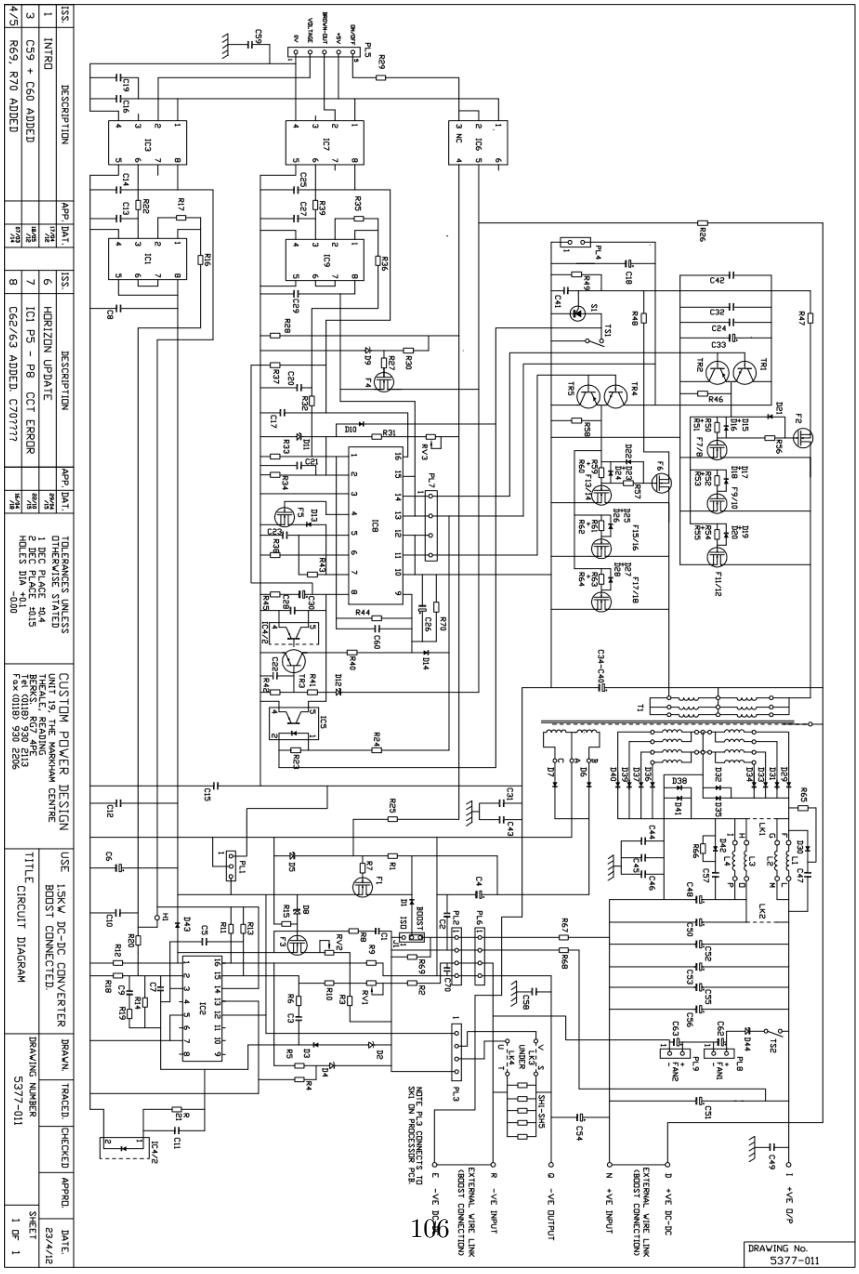

Figure D.1: Circuit diagram of full bridge SMPS, SM5567

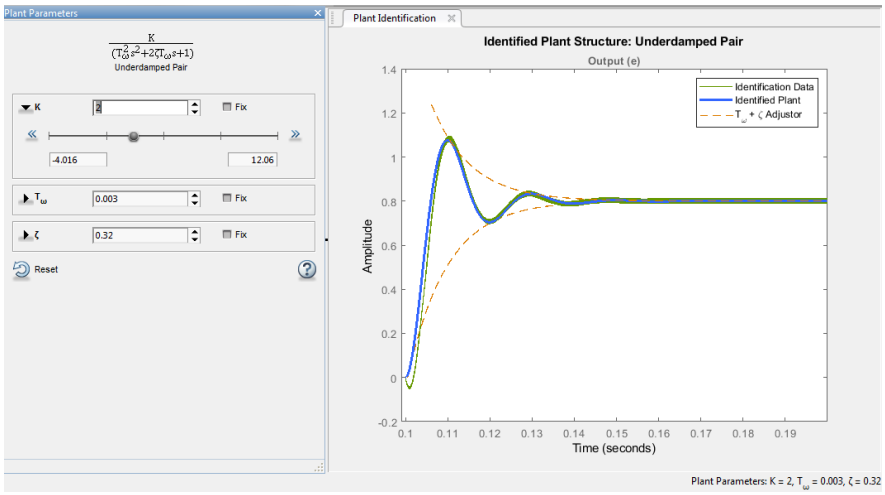

Figure D.2: System identification for closed loop DC-DC converter under step pulse

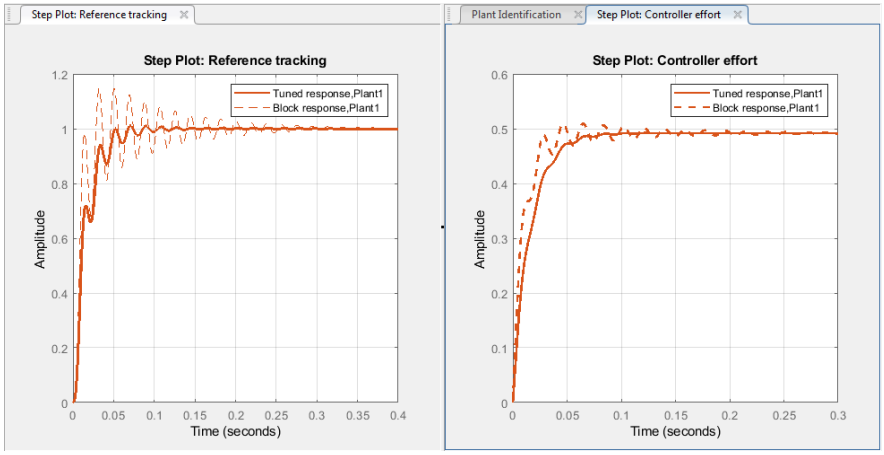

Figure D.3: Comparative results of tuned and untuned PI control of DC-DC converter

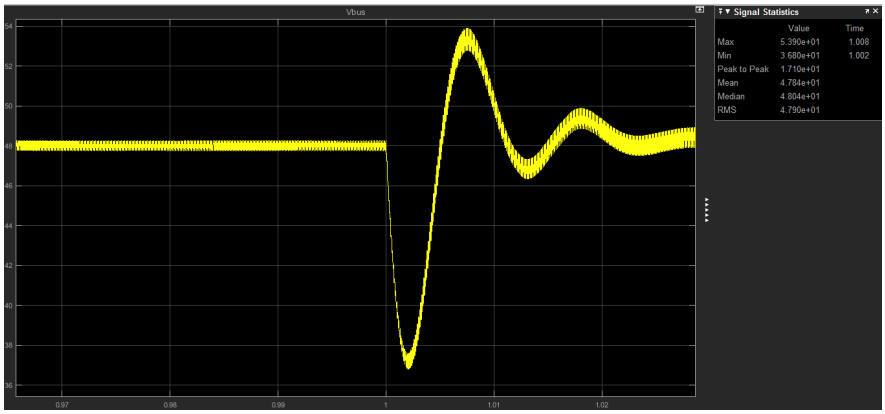

Figure D.4: Step response measurement of the bus voltage with closed loop PI control

Appendix E

Fuel Cell Information

14 TECHNISCHE DATEN

TECHNISCHE DATEN	
Nennspannung	48 V
Kapazität	106 Ah
Energie	5,5 kWh
Leistung nom.	5 kW
Leistung max.(10 s)	15 kW
Ladeverfahren	CC-CV
Zyklen (bei 90% DOD und 1C)	7000
Eigenverbrauch (abgeschaltet)	< 7 W (0 W)
Zulässige Zelltemperatur bei Entladung	-20 °C bis +50 °C
Zulässige Zelltemperatur bei Ladung	2 °C bis 45 °C
Ladeschlussspannung (dynamisch)	58,8 V
Entladeschlussspannung (dynamisch)	37,8 V
Maximaler Ladestrom (kurzzeitig)	212 A
Maximaler Entladestrom (kurzzeitig)	318 A
SCHNITTSTELLEN	
Kommunikation	CAN 2.0A nicht galvanisch getrennt, 500 kbit/s
Stromanschluss	Hochstromsteckverbinder
Indikator-Ring	Rot, Gelb, Grün
4 Taster	ESC, UP, DOWN, ENTER
MECHANISCHE GRÖSSEN	
Breite x Höhe x Tiefe **neeo**Rack	483 mm x 266 mm x 487 mm
Breite x Höhe x Tiefe **neeo**Qube	456 mm x 456 mm x 280 mm
Gewicht (**neeo**Qube / **neeo**Rack)	62 kg / 58 kg
UMGEBUNGSBEDINGUNGEN	
Max. Luftfeuchtigkeit	85%, nicht kondensierend
Zulässige Umgebungstemperatur im Betrieb	0 °C bis 40 °C
Empfohlene Umgebungstemperatur	20 °C
Lagerung	20 °C empfohlen, s. Hinweise zur Lagerung
SONSTIGES	
Gewährleistung (EU)	2 Jahre*
Garantie	10 Jahre **
GERÄTESCHUTZART	
Nach DIN 60529	IP50
ZUBEHÖR	
Feinsicherung mit Halter	1A
Ethernet RJ45-Kabel CAN-Costumer	3 m
DC-Leistungskabel	50mm² mit Hochstromsteckverbinder

* gemäß unseren Geschäftsbedingungen ** gemäß unseren Garantiebedingungen

Figure E.1: Data-sheet of neeoRack Li-ion battery

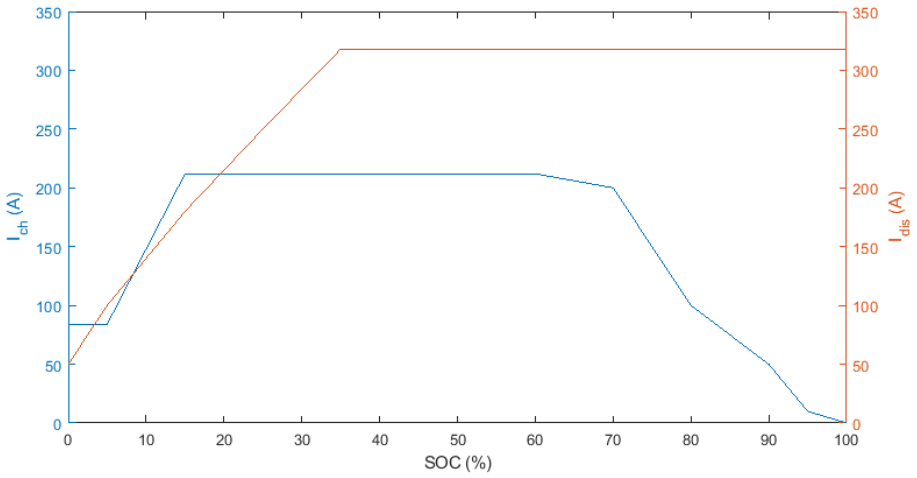

Figure E.2: Charge and Discharge Limits of neeoRack

Appendix F

Electric Motor Information

Golden Motor电机测试数据报表								
电机型号	3KW			额定电压			48(V)	
单位名称	GOLDEN MOTOR			额定电流			85(A)	
测试人	1			额定功率			3000(W)	
测试日期	2014-12-31			额定转速			4000(r/m)	
No.	U(V)	I(A)	Pin(W)	T(N.m)	N(r/s)	N(r/m)	Pout(W)	n(%)
1	48.0	14.87	715.3	0.7	74.8	4489	371.0	51.9
2	48.0	15.30	735.7	0.9	74.8	4487	433.0	58.9
3	48.0	16.07	773.0	0.9	74.7	4484	432.0	55.9
4	48.0	16.82	809.2	1.0	74.7	4480	494.0	61.0
5	48.0	18.10	870.5	1.1	74.5	4472	554.0	63.6
6	48.0	19.91	957.6	1.4	74.4	4461	676.0	70.6
7	48.0	22.67	1090	1.7	74.1	4445	796.0	73.0
8	48.0	26.16	1258	2.1	73.7	4421	975.0	77.5
9	48.0	30.02	1443	2.5	73.3	4396	1152	79.8
10	48.0	34.17	1643	3.0	72.8	4366	1384	84.2
11	48.0	38.39	1845	3.5	72.3	4339	1615	87.5
12	48.0	43.64	2097	4.0	71.8	4308	1841	87.8
13	48.0	49.07	2358	4.6	71.1	4267	2061	87.4
14	48.0	54.37	2613	5.2	70.6	4234	2338	89.5
15	48.0	59.81	2874	5.9	70.0	4200	2610	90.8
16	48.0	65.69	3157	6.5	69.3	4159	2866	90.8
17	48.0	71.96	3458	7.3	68.7	4119	3180	92.0
18	48.0	78.72	3783	8.0	67.9	4073	3425	90.5
19	48.0	87.20	4186	8.9	67.0	4017	3773	90.1
20	48.0	94.31	4527	10.0	65.2	3914	4098	90.5
21	48.0	94.55	4538	10.9	59.6	3578	4084	90.0
22	48.0	94.83	4551	12.2	52.8	3170	4050	90.0
23	48.0	94.60	4540	14.0	43.9	2632	3859	85.1
24	48.0	93.03	4465	16.8	36.1	2167	3812	85.4
25	48.0	92.81	4455	20.8	25.1	1508	3284	73.7

Figure F.1: Performance recording of Golden Motor 3 kW

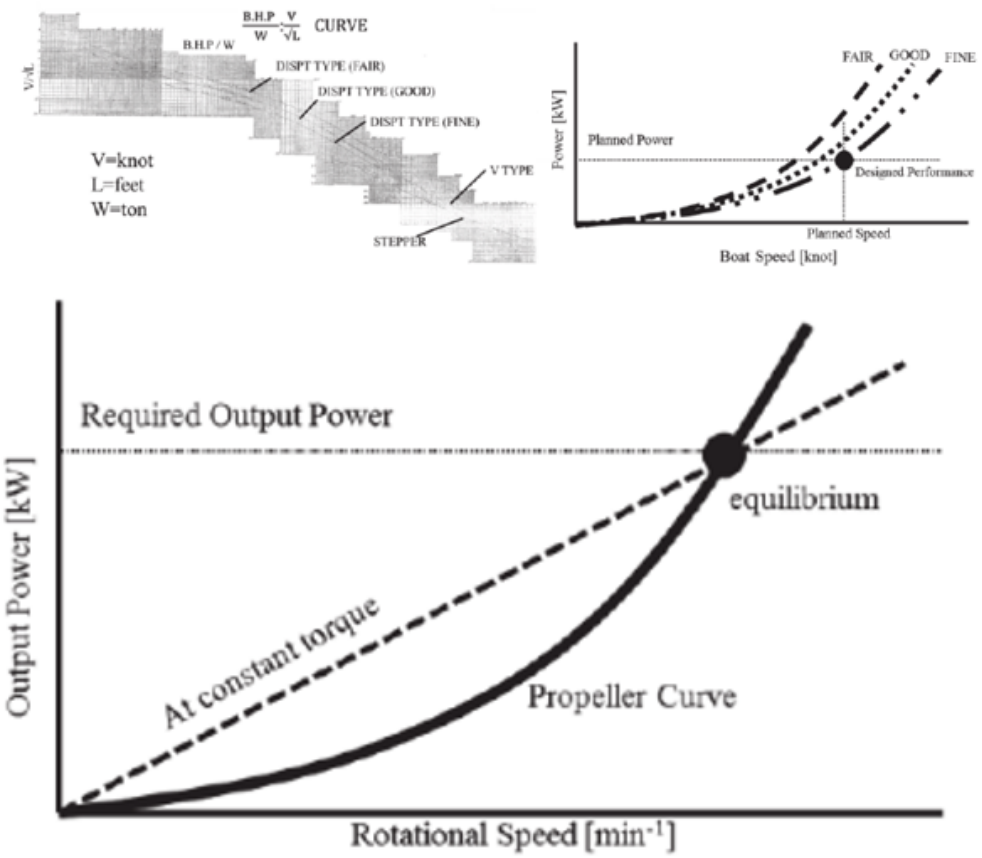

Figure F.2: Evolution of Gunkan curve (upper left) to power-speed curve (upper right) and propeller power curve (lower), (Umeda and Shimizu, 2015)

Appendix G

EMS Algorithms

G.1 Source Code of EMS algorithm in C environment

```
#include "EMSm_lib.h"
#define Pfcmax 465
#define Pfcmin 50
#define Pfcopt 200
#define Ploadhigh 2000
#define Ploadlow 100
double EMSm(double SOC,double Pload, double Pch, double Pdis)
{
double Pfc;
  if (SOC<0.4)
        {if (Pload>Ploadhigh)
            Pfc=Pfcmax;
        else if (Pload<=Ploadhigh)
            Pfc=Pfcopt;}
```

```
15
16    else if (SOC>0.4&&SOC<0.9)
17          {Pfc=Pfcopt;}
18
19    else if (SOC>0.9)
20          {if (Pload<=Ploadlow)
21              Pfc=Pfcmin;
22          else if (Pload>Ploadlow)
23              Pfc=Pfcopt;}
24
25 /*Charging mode safety*/
26  if (Pfc>Pload&&Pch<Pfc-Pload)
27     {do {
28        Pfc=Pfc-10;}
29        while( Pch>Pfc-Pload);}
30
31 /*Discharge mode safety*/
32  else if (Pfc<Pload&&Pdis<Pload-Pfc)
33     {do {
34        Pfc=Pfc+10;}
35        while( Pdis>Pload-Pfc);}
36
37 return Pfc;
38 }
```

G.2 Header of EMS algorithm in C environment

```
#ifndef EMSm_LIB_H_INCLUDED
#define EMSm_LIB_H_INCLUDED

double EMSm(double SOC,double Pload, double Pch, double Pdis);

#endif // ADD_LIB_H_INCLUDED
```

G.3 Legacy code of EMS algorithm

```
        %%%-MATLAB_Construction_Commands_Start
        def = legacy_code('initialize');
        def.SFunctionName = 'sf_EMS';
        def.OutputFcnSpec = 'double y1 = EMSm(double u1, double u2,
        def.HeaderFiles = {'EMSm_lib.h'};
        def.SourceFiles = {'EMSm.c'};
        legacy_code('sfcn_cmex_generate', def);
        legacy_code('compile', def);
        %%%-MATLAB_Construction_Commands_End
%Must specify the S_FUNCTION_NAME as the name of the S-function
#define S_FUNCTION_NAME  sf_EMS
#define S_FUNCTION_LEVEL 2
#include "simstruc.h"
%Specific header file(s) required by the legacy code function
```

```
15 #include "EMSm_lib.h"
16 static void mdlInitializeSizes(SimStruct *S)
17 {
18     ssSetNumSFcnParams(S, 0);
19     if (!ssSetNumDWork(S, 0)) return;
20     ssSetNumPWork(S, 0)
21     if (!ssSetNumInputPorts(S, 4)) return;
22 %Configure the input port 1
23     ssSetInputPortDataType(S, 0, SS_DOUBLE);
24     {
25         int_T u1Width = 1;
26         ssSetInputPortWidth(S, 0, u1Width);
27     }
28     ssSetInputPortComplexSignal(S, 0, COMPLEX_NO);
29     ssSetInputPortDirectFeedThrough(S, 0, 1);
30     ssSetInputPortAcceptExprInRTW(S, 0, 1);
31     ssSetInputPortOverWritable(S, 0, 1);
32     ssSetInputPortOptimOpts(S, 0, SS_REUSABLE_AND_LOCAL);
33     ssSetInputPortRequiredContiguous(S, 0, 1);
34 %Configure the input port 2
35     ssSetInputPortDataType(S, 1, SS_DOUBLE);
36     {
37         int_T u2Width = 1;
38         ssSetInputPortWidth(S, 1, u2Width);
```

```
39      }
40      ssSetInputPortComplexSignal(S, 1, COMPLEX_NO);
41      ssSetInputPortDirectFeedThrough(S, 1, 1);
42      ssSetInputPortAcceptExprInRTW(S, 1, 1);
43      ssSetInputPortOverWritable(S, 1, 1);
44      ssSetInputPortOptimOpts(S, 1, SS_REUSABLE_AND_LOCAL);
45      ssSetInputPortRequiredContiguous(S, 1, 1);
46  %Configure the input port 3
47      ssSetInputPortDataType(S, 2, SS_DOUBLE);
48      {
49          int_T u3Width = 1;
50          ssSetInputPortWidth(S, 2, u3Width);
51      }
52      ssSetInputPortComplexSignal(S, 2, COMPLEX_NO);
53      ssSetInputPortDirectFeedThrough(S, 2, 1);
54      ssSetInputPortAcceptExprInRTW(S, 2, 1);
55      ssSetInputPortOverWritable(S, 2, 1);
56      ssSetInputPortOptimOpts(S, 2, SS_REUSABLE_AND_LOCAL);
57      ssSetInputPortRequiredContiguous(S, 2, 1);
58  %Configure the input port 4
59      ssSetInputPortDataType(S, 3, SS_DOUBLE);
60      {
61          int_T u4Width = 1;
62          ssSetInputPortWidth(S, 3, u4Width);
```

```
63      }
64      ssSetInputPortComplexSignal(S, 3, COMPLEX_NO);
65      ssSetInputPortDirectFeedThrough(S, 3, 1);
66      ssSetInputPortAcceptExprInRTW(S, 3, 1);
67      ssSetInputPortOverWritable(S, 3, 1);
68      ssSetInputPortOptimOpts(S, 3, SS_REUSABLE_AND_LOCAL);
69      ssSetInputPortRequiredContiguous(S, 3, 1);
70  %Set the number of output ports
71      if (!ssSetNumOutputPorts(S, 1)) return;
72
73      ssSetOutputPortDataType(S, 0, SS_DOUBLE);
74      {
75          int_T y1Width = 1;
76          ssSetOutputPortWidth(S, 0, y1Width);
77      }
78      ssSetOutputPortComplexSignal(S, 0, COMPLEX_NO);
79      ssSetOutputPortOptimOpts(S, 0, SS_REUSABLE_AND_LOCAL);
80      ssSetOutputPortOutputExprInRTW(S, 0, 1);
81  %Register reserved identifiers to avoid name conflict
82      if (ssRTWGenIsCodeGen(S) || ssGetSimMode(S)==SS_SIMMODE_EXTER
83          ssRegMdlInfo(S, "EMSm", MDL_INFO_ID_RESERVED, 0, 0, ssGe
84      }
85      ssSetModelReferenceNormalModeSupport(S, MDL_START_AND_MDL_PR
86  %Set the number of sample time
```

```
87      ssSetNumSampleTimes(S, 1);
88  %Set the compliance with the SimState feature
89      ssSetSimStateCompliance(S, USE_DEFAULT_SIM_STATE);
90      ssSetSupportedForRowMajorCodeGen(S, true);
91      ssSetArrayLayoutForCodeGen(S, SS_COLUMN_MAJOR);
92  %Set the Simulink version this S-Function has been generated in
93      ssSetSimulinkVersionGeneratedIn(S, "9.1");
94
95      ssSetOptions(S,
96          SS_OPTION_USE_TLC_WITH_ACCELERATOR |
97          SS_OPTION_CAN_BE_CALLED_CONDITIONALLY |
98          SS_OPTION_EXCEPTION_FREE_CODE |
99          SS_OPTION_WORKS_WITH_CODE_REUSE |
100         SS_OPTION_SFUNCTION_INLINED_FOR_RTW |
101         SS_OPTION_DISALLOW_CONSTANT_SAMPLE_TIME
102     );
103 }
104 static void mdlInitializeSampleTimes(SimStruct *S)
105 {
106     ssSetSampleTime(S, 0, INHERITED_SAMPLE_TIME);
107     ssSetOffsetTime(S, 0, FIXED_IN_MINOR_STEP_OFFSET);
108
109     #if defined(ssSetModelReferenceSampleTimeDefaultInheritance)
110     ssSetModelReferenceSampleTimeDefaultInheritance(S);
```

```
111     #endif
112 }
113 static void mdlOutputs(SimStruct *S, int_T tid)
114 {
115     real_T* y1 = (real_T*) ssGetOutputPortSignal(S, 0);
116     real_T* u1 = (real_T*) ssGetInputPortSignal(S, 0);
117     real_T* u2 = (real_T*) ssGetInputPortSignal(S, 1);
118     real_T* u3 = (real_T*) ssGetInputPortSignal(S, 2);
119     real_T* u4 = (real_T*) ssGetInputPortSignal(S, 3);
120 %Call the legacy code function
121     *y1 = EMSm(*u1, *u2, *u3, *u4);
122 }
123 %Required S-function trailer
124 #ifdef     MATLAB_MEX_FILE
125 # include "simulink.c"
126 #else
127 # include "cg_sfun.h"
128 #endif
```

Appendix H

Pareto Optimal Set of Optimization

Table H.1: **Pareto-front solution set**

Index	$U_1(X_D)$ **(€)**	$U_2(X_D)$ **(kg)**	x_1 **(W)**	x_2 **(W)**
1	7732	38	2374	1526
2	11023	25	686	2754
3	11047	20	284	2846
4	9122	35	1934	1986
5	10084	32	1508	2331
6	11052	20	282	2848
7	8890	36	2005	1910
8	5335	40	2972	767
9	10593	30	1205	2529
10	8265	37	2221	1699
11	10948	27	904	2687
12	6911	39	2604	1261
13	8890	36	2005	1910
14	7346	38	2485	1401
15	10195	32	1445	2373
16	9662	34	1758	2166
17	6195	40	2777	1035
18	9425	34	1801	2094
19	10662	29	1130	2564
20	6162	40	2792	1024
21	10994	26	772	2728
22	10812	28	999	2631
23	10502	30	1266	2492
24	10759	28	1057	2605
25	10317	31	1396	2416
26	9734	33	1686	2201
27	5769	40	2884	900
28	8665	36	2088	1833
29	7234	38	2525	1363
30	7937	37	2323	1591
31	8137	37	2266	1656
32	11052	20	282	2848
33	10973	26	840	2708
34	10393	31	1325	2451
35	8514	36	2151	1780
36	6673	39	2660	1186
37	9263	35	1867	2038
38	10010	33	1564	2299